WATER RESOURCES ASSESSMENT OF NORTHERN CYPRUS FOR A SUSTAINABLE MANAGEMENT

A THESIS SUBMITTED TO
THE BOARD OF GRADUATE PROGRAMS
OF
MIDDLE EAST TECHNICAL UNIVERSITY, NORTHERN CYPRUS CAMPUS

BY

ADNAN YASER ADNAN HILAL

IN PARTIAL FULFILLMENT OF THE REQUIREMENTS
FOR
THE DEGREE OF MASTER OF SCIENCE
IN SUSTAINABLE ENVIRONMENT AND ENERGY SYSTEMS PROGRAM

February 2021

Approval of the Board of Graduate Programs

Prof. Dr. Oğuz Solyalı
Chairperson

I certify that this thesis satisfies all the requirements as a thesis for the degree of Master of Science

Assoc. Prof. Dr. Ceren İnce Derogar
Program Coordinator

This is to certify that we have read this thesis and that in our opinion it is fully adequate, in scope and quality, as a thesis for the degree of Master of Science.

Asst. Prof. Dr. Bertuğ Akıntuğ
Co-Supervisor

Asst. Prof. Dr. Bengü Bozkaya Schrotter
Supervisor

Examining Committee Members

Asst. Prof. Dr. Aykut Argönül
METU NCC Chemical Engineering

Asst. Prof. Dr. Bengü Bozkaya Schrotter
METU NCC Chemical Engineering

Asst. Prof. Dr. Bertuğ Akıntuğ
METU NCC Civil Engineering

Asst. Prof. Dr. Hasan Zaifoğlu
METU NCC Civil Engineering

Asst. Prof. Dr. Saltuk Pirgalıoğlu
EUL Department of Environmental Sciences

I hereby declare that all information in this document has been obtained and presented in accordance with academic rules and ethical conduct. I also declare that, as required by these rules and conduct, I have fully cited and referenced all material and results that are not original to this work.

Name, Last name: Adnan Yaser Adnan, Hilal

Signature :

ABSTRACT

WATER RESOURCES ASSESSMENT OF NORTHERN CYPRUS FOR A SUSTAINABLE MANAGEMENT

Hilal, Adnan Yaser Adnan
Master of Science, Sustainable Environment and Energy Systems Program
Supervisor: Asst. Prof. Dr. Bengü Bozkaya Schrotter
Co-Supervisor: Asst. Prof. Dr. Bertuğ Akıntuğ

February 2021, 153 pages

Increasing world population and industrialisation lead to a rapid rise in water consumption and demand. As a result, both surface and sub-surface water resources were overexploited in most parts of the world, including Northern Cyprus in the Eastern Mediterranean region over the past years. In this study, the spatial distribution and temporal variation of daily, monthly, seasonal and yearly rainfall patterns in Northern Cyprus are analysed using Concentration Index, Precipitation Concentration Index, Seasonality Index and gamma distribution, respectively. A significant variation of daily and annual rainfall patterns are observed in the majority of the stations. Additionally, monthly water balance components, including potential evapotranspiration, actual evapotranspiration, soil storage capacity, water surplus, and runoff, are estimated in the study area. Thirty-six years of daily rainfall and monthly average temperature data collected in thirty-three stations across the study region is used in the mentioned parts of the study. Moreover, the available runoff water for harvesting in the main water streams and the main cities are evaluated. A substantial amount, around 12% of the rainfall, is found to be available for harvesting

in the main cities and from the main streams. Furthermore, the possibility of introducing reverse osmosis seawater desalination as a sustainable and climate-independent source of potable water is investigated. Additionally, this study aims to deliver reliable and scientific data to fill the literature gap to improve the sustainable management of water resources in Northern Cyprus.

Keywords: Water balance, Rainfall patterns, Seawater desalination, Water harvesting, Northern Cyprus

ÖZ

SÜRDÜRÜLEBİLİR BİR YÖNETİM İÇİN KUZEY KIBRIS'TA SU KAYNAKLARI DEĞERLENDİRMESİ

Hilal, Adnan Yaser Adnan
Yüksek Lisans, Sürdürülebilir Çevre ve Enerji Sistemleri
Supervisor: Asst. Prof. Dr. Bengü Bozkaya Schrotter
Co-Supervisor: Asst. Prof. Dr. Bertuğ Akıntuğ

Şubat 2021, 153 sayfa

Artan dünya nüfusu ve sanayileşme, su tüketiminde ve talebinde hızlı bir artışa neden olmaktadır. Sonuç olarak, Doğu Akdeniz bölgesindeki Kuzey Kıbrıs dahil olmak üzere dünyanın birçok yerinde hem yüzey hem de yeraltı su kaynakları aşırı istismar edilmiştir. Bu çalışmada, Kuzey Kıbrıs'ta günlük, aylık, mevsimsel ve yıllık yağış modellerinin mekansal dağılımı ve zamansal değişimi sırasıyla Konsantrasyon İndeksi, Yağış Konsantrasyon İndeksi, Mevsimsellik İndeksi ve gama dağılımı kullanılarak analiz edilmiştir. Ek olarak, çalışma alanında potansiyel evapotranspirasyon, fiili evapotranspirasyon, toprak depolama kapasitesi, su fazlası ve akış dahil olmak üzere aylık su dengesi bileşenleri tahmin edilmiştir. Çalışmanın belirtilen bölümlerinde bölgedeki otuz üç istasyonda toplanan otuz altı yıllık günlük yağış ve aylık sıcaklık değerleri kullanılmıştır. Ayrıca, ana akarsularda ve büyük şehirlerde hasat için mevcut akış suyu değerlendirilmiştir. Yağışın yaklaşık yüzde 12'sini oluşturan önemli bir miktarın, ana şehirlerde ve ana akarsulardan hasat için uygun olduğu bulunmuştur. Ayrıca, sürdürülebilir ve iklimden bağımsız bir içme suyu kaynağı olarak ters ozmoz ile deniz suyunun tuzdan arındırma olasılığı

araştırılmıştır. Bu çalışma, Kuzey Kıbrıs'ta su kaynaklarının sürdürülebilir yönetimini iyileştirmek için literatür boşluğunu dolduracak güvenilir ve bilimsel veriler sunmayı amaçlamaktadır.

Anahtar Kelimeler: Su dengesi, Yağış modelleri, Deniz suyu arıtımı, Su hasadı, Kuzey Kıbrıs Türk Cumhuriyeti

Dedicated to My Parents; Yaser and Nehayah

ACKNOWLEDGMENTS

I wish to express my deepest gratitude to my supervisor Asst. Prof. Dr. Bengü Bozkaya Schrotter and co-supervisor Asst. Prof. Dr. Bertuğ Akıntuğ for their guidance, advice, criticism, support and insight throughout the research. Also, I would like to thank Dr. Jean-Christophe Schrotter for sharing his valuable expertise and insight into the thesis.

I would also like to extend my gratitude towards my jury members, Asst. Prof. Dr. Hasan Zaifoğlu, Asst. Prof. Dr. Saltuk Pirgalıoğlu and Asst. Prof. Dr. Aykut Argönül for their time and valuable feedback.

Additionally, I wish to convey my gratitude to Assoc. Prof. Dr. Julian Saurin, for the time he spared for the conversations we had, which all gave me a deeper insight into my surroundings.

Words can't express how grateful I am to my dear parents, Nehayah and Yaser Hilal for their genuine love and help; I couldn't ask for more. This endeavour wouldn't be possible without your ultimate support.

Furthermore, I would like to thank my family, my sweet sister May, my brothers Mohammed and Taher, my sister-in-law Waad and my brother-in-law Bassam for their support; they have always been there for me. Also, I would like to thank my nephews and nieces, Moath, Lian, Alma and Hisham for all the joy they brought to my life.

Moreover, I wish to convey my deepest gratitude to my friends Abood Nassar, Moutaz Sweileh and Yusef Theeb for their support during the hard challenges.

I thought of many ways to thank Nuray Vakitbilir for her ultimate and continuous support and help, but there are no words to show how glad, thankful and blessed to have her during this journey.

Additionally, I would like to extend my gratitude to Asst. Prof. Dr. Mustafa Ozser and chemistry group for their support and for giving me the opportunity to experience the academic career.

TABLE OF CONTENTS

APPENDICES

LIST OF TABLES

TABLES

LIST OF FIGURES

FIGURES

LIST OF ABBREVIATIONS

ABBREVIATIONS

AET	Actual Evapotranspiration
CI	Concentration Index
DAF	Dissolved Air Flotation
DEM	Digital Elevation Map
ED	Electrodialysis
ERDs	Energy Recovery Devices
GIS	Geografic Information System
LSI	Langelier Saturation Index
MED	Multi-Effect Distillation
MK	Mann-Kendall
MP	Monthly Total Precipitation
MSF	Multi-Stage Flash
MT	Monthly Average Temperature
PCI	Precipitation Concentration Index
PDT	Positive Displacement Type
PET	Potential Evapotranspiration
P_{total}	Total Precipitation
PV	Pressure Vessel
RO	Reverse Osmosis
S	Water Surplus
SEC	Specific Energy Consumption
SI	Seasonality Index
STC	Soil Moisture Storage Capacity
TDS	Total Dissolved Solids
TM	Thornthwaite and Mather
TMP	Transmembrane Pressure

TRO	Total of Runoff
UF	Ultrafiltration
UV	Ultraviolet Light
VC	Vapour Compression
WHO	World Health Organization
$(1/\beta)$	Scale Parameter
(α)	Shape Parameter

CHAPTER 1

INTRODUCTION

Faith and existence of societies are directly linked to freshwater availability. However, many factors, including climate change, population growth, and lifestyles, create stress on the available water resources. The water balance assessment is the primary key for sustainable water resources management (Axelsson & Stefánsson, 2003; Loucks, 2000; Salvati et al., 2008; UNESCO, 2020).

Various researchers have reported changes in rainfall patterns leading to an increase in the frequency of extreme events, including floods and droughts (Coscarelli & Caloiero, 2012; Deng et al., 2018; Michiels, Gabriels, & Hartmann, 1992; Suhaila & Jemain, 2012). In addition to risking lives and damaging properties, water availability, groundwater recharging, river regimes, and hydroelectric potential could be altered by the changes in the extreme event frequency. Thus, analysing the spatial and temporal characteristics of precipitation is essential.

World Resources Institutes estimated that up to 20% of the world population would suffer from water scarcity by 2050 (Ngongondo, Xu, Tallaksen, & Alemaw, 2015). However, the future of water availability is dependant on human activities, water management and planning. Defining a suitable and sustainable water resources management approach is case dependant as each region is considered a unique case. The need for water resources assessment and planning have a high priority in islands and areas with low and irregular rainfall patterns. Additionally, a noticeable regional difference in climate change effects emphasises the need for a different analysis of the water balance components in each region (Jasrotia, Majhi, & Singh, 2009; Leta, El-Kadi, Dulai, & Ghazal, 2016; Ngongondo et al., 2015).

Various researchers have studied the components of the hydrological cycle. Spatial and temporal rainfall patterns are the most studied part of the water balance (Coscarelli & Caloiero, 2012; Ngongondo et al., 2015; Tao et al., 2018; Zhang, Xu, Gemmer, Chen, & Liu, 2009).

Water scarcity is one of the main challenges of this century. The water scarcity could be presented as a physical lack of drinkable water as happening in many countries, including Cyprus, Egypt, Syria, India, Pakistan, Australia and many more countries as shown in Figure 1.1. Another possibility could be economic water scarcity where economical or political limitations restrict the access to existing water resources, as happening in many African countries and other countries in South Asia and America, as illustrated in Figure 1.1.

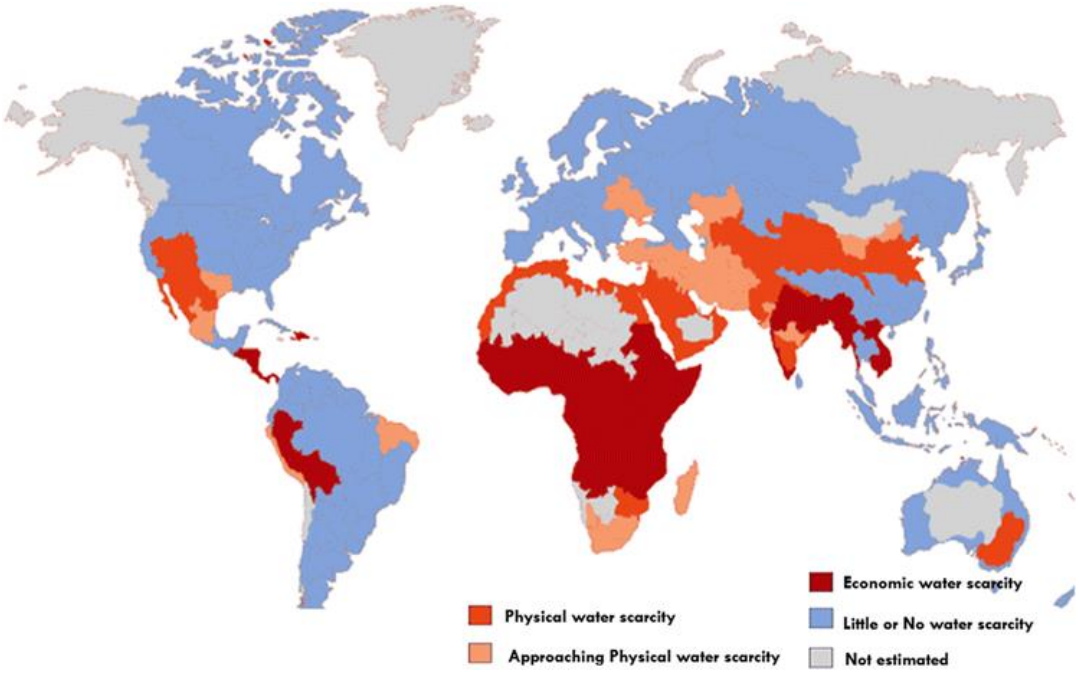

Figure 1.1. Worldwide water scarcity map (Gude, 2017)

The increase in water demand created higher stress on surface and sub-surface water resources in many countries, including America and Middle East countries. Northern Cyprus is a case in point, where the most significant sub-surface water reservoirs (aquifers) were exposed to intensive water withdrawal resulting in an increase of its

salinity to the unusable level due to the seawater intrusion (Arslan & Akün, 2019; Ergil, 2000; Gude, 2017). Additionally, a limited number of irrigation dams are available in Northern Cyprus. However, most of these dams serve only for a limited period in summer before drying out (Phillips Agboola & Egelioglu, 2012). Therefore, an unconventional water source became essential. Currently, 75 million m^3/year of drinking water could be imported from Turkey using a suspended pipeline through the Mediterranian Sea. However, this is the first project of this type in the world; hence it includes uncertainties and many challenges in maintenance. Moreover, as can be noted in Figure 1.1, Turkey is also approaching physical water scarcity. Thus, a prolonged drought in the Eastern Mediterranean region would significantly impact the amount of water imported from Turkey (Oner, 2019).

Therefore, another unconventional and sustainable source of potable water as an emergency plan in case of long-term maintenance, or as a supplementary source to compensate the water deficit due to the increase in water demand or drought events in the region is necessary. The most common unconventional source of potable water is seawater desalination. Besides, it is a well known and reliable method, and it is a climate-independent source of water. Therefore, it could be considered and studied as a sustainable drinking water source in water-scarce regions (Jones, Qadir, van Vliet, Smakhtin, & Kang, 2019).

1.1 Motivation and Objectives

The importance of water is evident in humans' daily practices and needs, from consumption to industrial and economic development, including agricultural activities. However, water resources management has been a challenge for various societies in human history. In the present, global warming, human population increase, change in living standards, and industrial development all add to the challenge of sustaining the water resources. In water resources management, each case is unique, which means that applying a region's solution or plan does not necessarily work for another case. The first step for sustainable water resources

management is evaluating the water balance components and measuring their temporal changes. Water balance analysis is the centrepiece in water resources assessment. Two main variables that have a direct effect on the water balance, are temperature and precipitation. The former has been studied in (Koyuncu, 2019), and the latter has not been analysed enough in the literature, hence it is analysed thoroughly in the first part of this study to give a better understanding to the water balance analysis.

For this purpose, this study aims to:

1- Provide a better understanding of the spatial distribution of rainfall patterns across Northern Cyprus.
2- Evaluate the temporal changes of the rainfall patterns.
3- Analyse the main components of water balance in the study area.
4- Estimate the amount of rainfall water available for harvesting.
5- Provide a technical design of low-energy consumption seawater desalination plant for Northern Cyprus as a sustainable, climate-independent, and reliable solution together with the water supply project from Turkey.

The results of this study should provide decision-makers with more data to reassess and plan future designs of water structures and choose the optimum water harvesting system for each location. Furthermore, it provides a technical design of seawater desalination plant as unconventional sources of potable water for Northern Cyprus.

1.2 Thesis Organisation

This thesis is made of six main chapters. Following the introduction, a literature review and background information are provided in Chapter 2, where both simple concept explanation of the used methodologies and a review of the used methods in the literature are given. In Chapter 3, the region of concern and the used dataset are dispensed. Chapter 4 presents the methodology where a more detailed demonstration of the path of this research, methods, and assumptions are stated. In Chapter 5, the

results are illustrated and discussed. The summary of the thesis and the highlights are given in Chapter 6.

CHAPTER 2

BACKGROUND AND LITERATURE REVIEW

This chapter is divided into two main sections. The first section will give background information on rainfall patterns, water balance and seawater desalination. In the second section, the related studies in the literature have been reviewed.

2.1 Background

2.1.1 Water Pipeline from Turkey

A submerged pipeline connecting Turkey with Northern Cyprus across the Mediterranean Sea has been built between 2011 and 2015, with an annual capacity of 75 million m^3. The source of water in the project is from Alakopru Dam in Anamur, Turkey, with 80 km length of the pipeline transferring the water to the coast of Güzelyalı and then to Gecitkoy Dagdere Dam. The project is designed to serve water to Northern Cyprus until 2045, and it is one of a kind, as there are no similar projects (Oner, 2019).

The project is completed with pipelines networks connecting the Gecitkoy Dagdere dam with the rest of the main districts of Northern Cyprus. Additionally, pumping stations and water treatment plants has been built as part of the project (Oner, 2019). The project path and pipelines networks are shown in Figure 2.1.

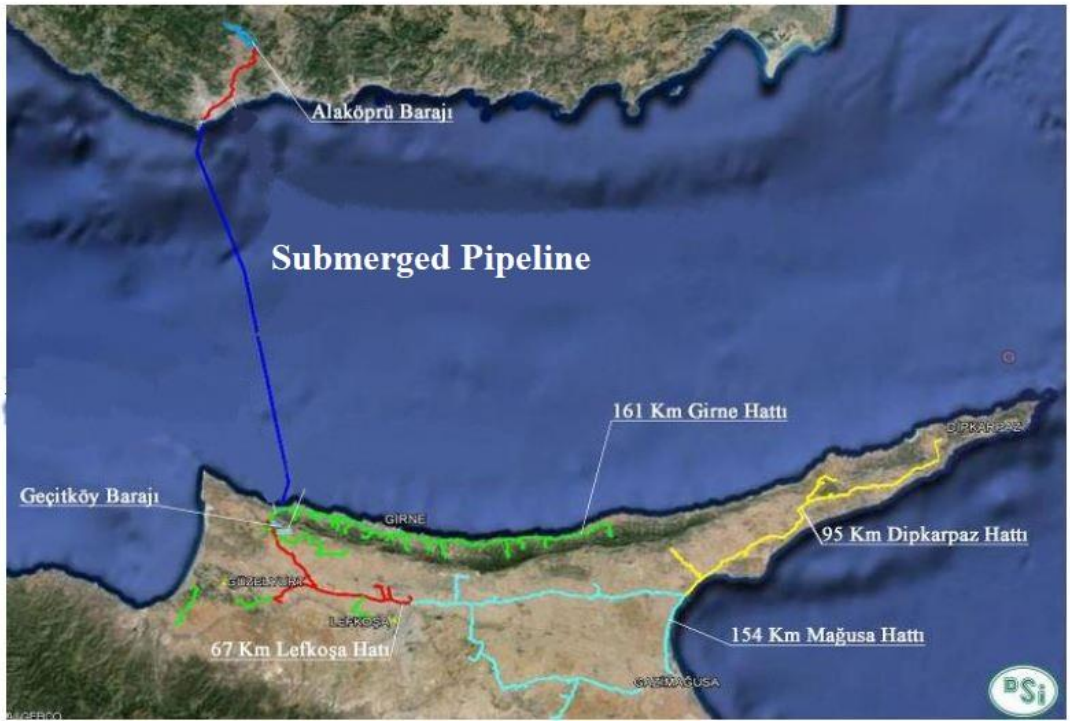

Figure 2.1. The pipeline project between Turkey and Northern Cyprus (Oner, 2019)

2.1.2 Water Balance and Rainfall Patterns

The effects of change in rainfall characteristics could be avoided by analysing the statistical structure of rainfall characteristics for the concerned region (Coscarelli & Caloiero, 2012). Indices such as Concentration Index (CI), Precipitation Concentration Index (PCI), and Seasonality Index (SI) are appropriate tools to define rainfall characteristics. CI is analysed to understand the changing weight of daily precipitation. On the other hand, PCI gives patterns of the relative distribution of the rain over a year, where SI is estimated to understand the seasonal variation of rainfall patterns. In general, CI, PCI, and SI are used to analyse the spatial and temporal distribution of daily, monthly and seasonal rainfall patterns, respectively (De Luís, Raventós, González-Hidalgo, Sánchez, & Cortina, 2000; Martin-Vide, 2004; Michiels et al., 1992; Zhang et al., 2008). To evaluate the trend type and magnitude in the temporal change of these indices, various types of trend tests are available.

However, in the literature, the Mann-Kendall (MK) trend test is the dominant test in this field (Chowdhury & Beecham, 2009; Easterling et al., 2000; Kampata, Parida, & Moalafhi, 2008; Ngongondo, Xu, Gottschalk, & Alemaw, 2011; Tao et al., 2018; Zhang et al., 2009). Additionally, statistical distributions could be used in rainfall analysis (Katz & Brown, 1992). Gamma distribution is suggested to be used in climatological data analysis by many researchers, mainly due to its flexibility (Husak, Michaelsen, & Funk, 2007; Ison et al., 1971; Queluz & Klar, 2013; Stern & Coe, 1984; Wilks & Wilks, 1990).

Water balance can be generally described as the method to identify the flow in and out of a specific region. Identifying the water balance components could be achieved by using various water budget models that use energy balance, hydrochemical traces, isotopes and volume balance (Bhattarai, Dougherty, Marzen, & Kalin, 2012; Boulet et al., 2000; Nachiappan, Kumar, & Manickavasagam, 2002; Widén-Nilsson, Halldin, & Xu, 2007). However, water volume balance, specifically Thornthwaite and Mather (TM) proposed water balance, become the most used model in recent years. This model requires precipitation, temperature, the number of daytime hours, and soil storage capacity in the study area as inputs. The main components produced by the TM water balance are potential evapotranspiration (PET), actual evapotranspiration (AET), water surplus (S) and runoff. PET is the maximum capacity of vibration from both the surface of the ground and the flora known as evapotranspiration, and it is dependant on the temperature and location. On the other hand, AET is the real evapotranspiration, and it is affected both by the temperature and the precipitation. Runoff and S are the excess amounts of precipitation on the soil surface, as shown in Figure 2.2 (Ghandhari & Alavi Moghaddam, 2011; Jasrotia et al., 2009; Ngongondo et al., 2015; Nugroho, Tamagawa, Riandraswari, & Febrianti, 2019). The water balance components' temporal changes can be determined using the MK trend test (Ngongondo et al., 2015).

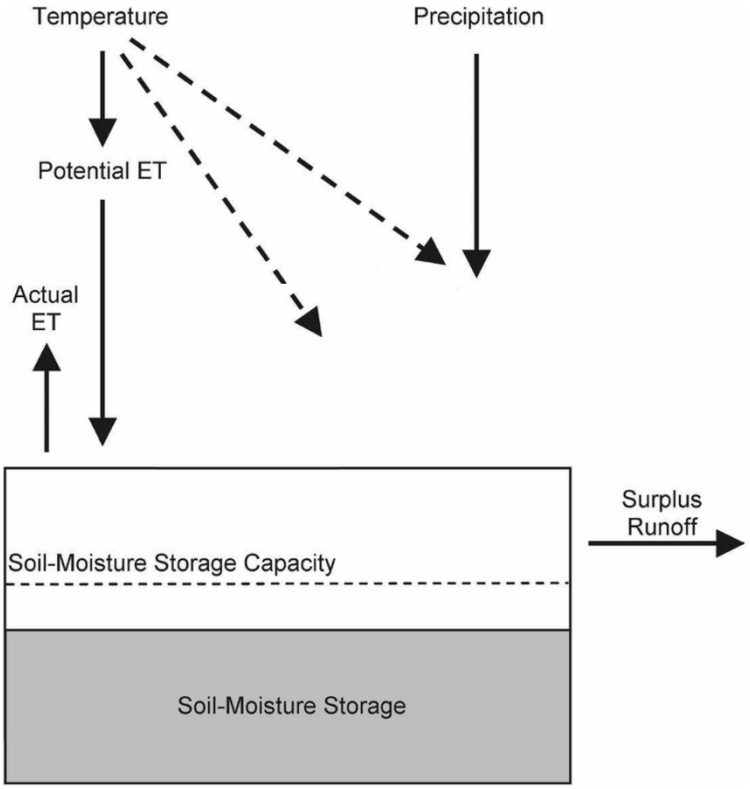

Figure 2.2. TM water balance main components (USGS, 2007)

Identifying water balance elements is the primary step for sustainable water resources management. Additionally, the results of the model could be further analysed using software like Google Earth and more commonly, Geographic Information System (GIS). By integrating the model findings with a digital elevation model (DEM), the analysis could give more valuable information regarding the water paths, the basins distribution and the discharging points. Such data could be vital in designing water-holding structures like dams and urban planning (Jasrotia et al., 2009; Leta et al., 2016).

2.1.3 Seawater Desalination

Conventionally, water reservoirs and surface water are the sources of potable water. However, in water-scarce regions like the Middle East and the Mediterranean,

unconventional potable water sources become vital in supporting the population growth and economic development. As most of the counties in these regions are coastal counties, many rely on seawater desalination as a sustainable and reliable source of potable water.

Water desalination processes are mainly divided into two types:

- Thermal Desalination
- Membrane Processes

Both processes are further divided into subcategories, as shown in Figure 2.3.

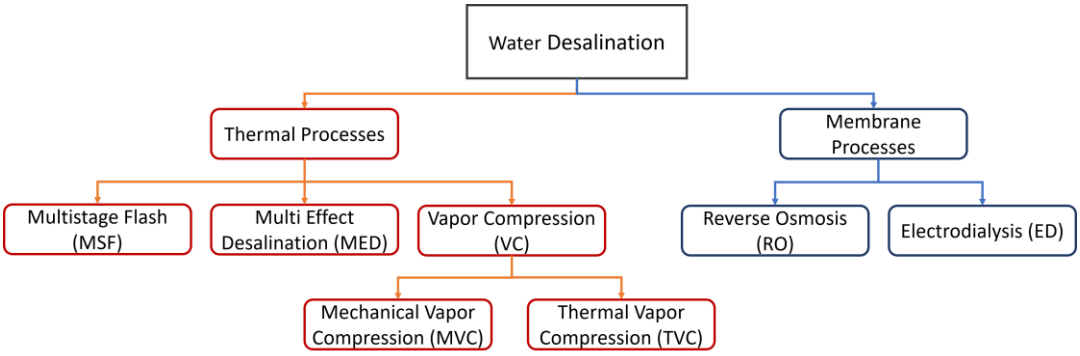

Figure 2.3. Categories of water desalination technologies

Thermal desalination, also known as Phase-Changing Desalination, is the conventional desalination processes, and it is categorised into four types based on the working principle, as shown in Figure 2.3 (Al-Karaghouli & Kazmerski, 2013).

In contrast to thermal water desalination, membrane process conventionally uses only electricity as a source of energy.

Historically, thermal desalination technologies were the dominant desalination technologies around the globe. However, in recent decades a noticeable increase in RO operational capacity can be observed, as illustrated in Figure 2.4. Due to this trend, the operational capacity of RO is the current dominant desalination technology, as it stands for almost 70% of the operational water desalination capacity in the world (Jones et al., 2019).

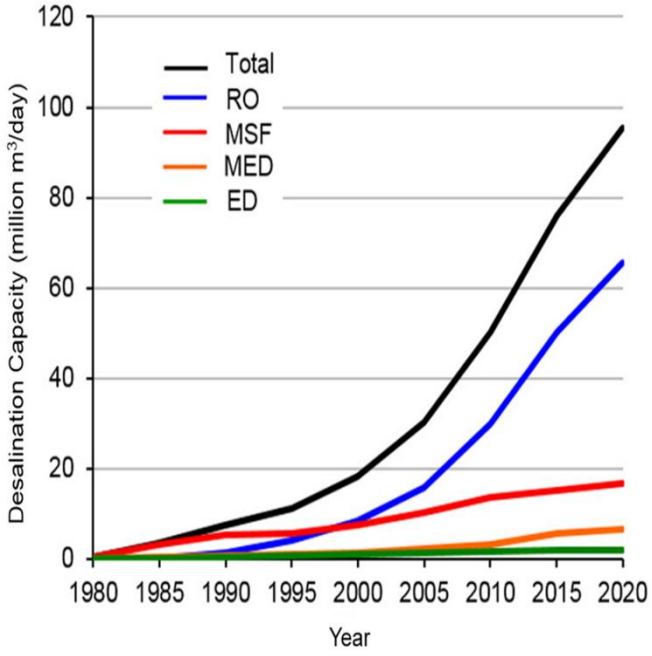

Figure 2.4. The operational capacity of water desalination by the technology around the world (Jones et al., 2019)

2.1.4 Seawater Desalination by Reverse Osmosis

Osmosis is the natural phenomenon that describes the movement of the water through a semi-permeable barrier from the low concentration side to the high concentration side. The created pressure due to this phenomenon is called osmotic pressure, and it is illustrated in Figure 2.5.

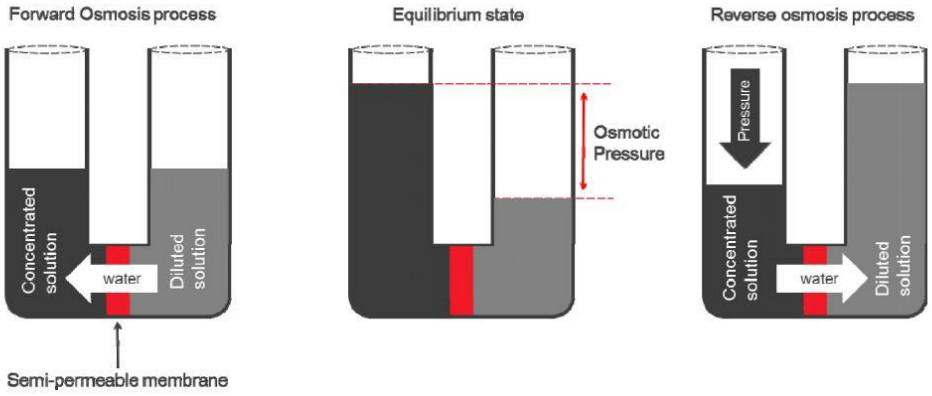

Figure 2.5. Demonstration of Osmosis phenomenon, osmotic pressure and reverse osmosis (Khalaf et al., 2013)

Reverse Osmosis (RO) is a high-pressure filtration system, where semi-permeable membranes are used to allow only the water to pass through it and block the salt as the applied pressure is higher than the osmotic pressure.

Two main types of water desalination systems are available, namely Brackish Water RO (BWRO) and Seawater RO (SWRO) systems. Each system works in a different range of pressure, which is 17 – 27 bars and 55 – 82 bars, respectively. The main difference between the two systems is the feedwater; BWRO the concentration of the ions, Namely Total Dissolved Solids (TDS) is less than 3000 mg/L. On the other hand, in seawater, the TDS concentration is higher than 3000 mg/L and up to 45000 mg/L. The TDS concentration in the water has a direct relation with the required energy for the desalination. As the TDS concentration increases, the solution's osmotic pressure rises, leading to higher energy consumption in the water desalination process.

Different RO configurations are used to achieve the system target. Single and multi-pass RO configurations are commonly used in water desalination plants where multi-pass systems are used to increase the quality of desalinated water, known as permeate. The permeate of the first pass is desalinated furthermore in the second pass, as shown in Figure 2.6, where concentrate refers to high salinity water produced

as a by-product of the desalination process. This type of is commonly used when a very high permeate quality is required. Also, two pass configuration is used to enhance boron removal. As the boron charge changes with the change in pH, i.e. in medium with pH higher than ten, most of the boron gets a negative charge which eas its rejection by the RO modules. Hence, the water pH is increased between the first and the second pass, allowing the membrane to reject a higher percentage of the boron in the water. The increase of the permeate quality using multi-pass configuration decreases the system recovery (Gude, 2018b).

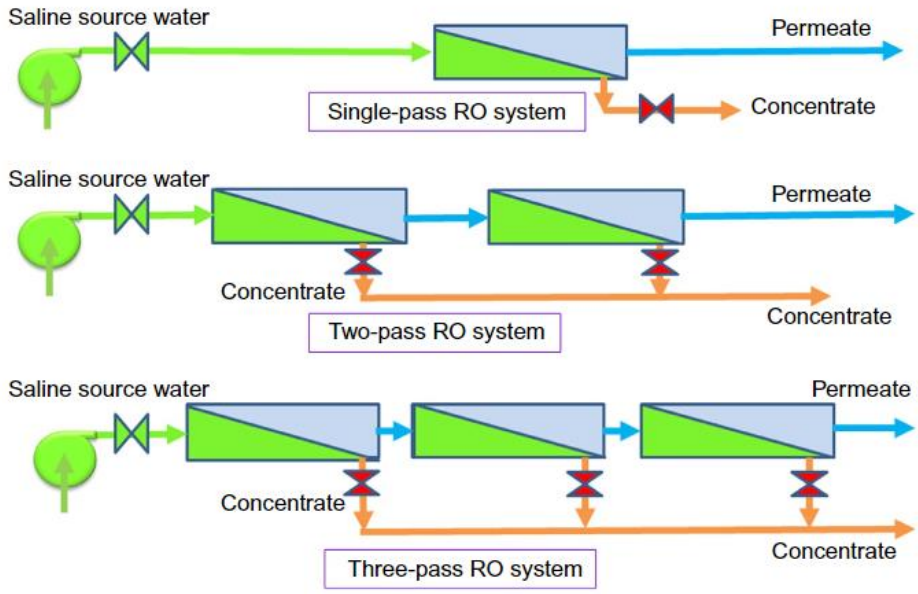

Figure 2.6. Single and multi-pass configuration (Gude, 2018b)

The second type of RO configuration is the number of stages. In multi-stage systems, the concentrate of a stage is desalinated in the following stage, as presented in Figure 2.7. The main aim is to increase recovery and decrease the overall concentrate volume (Gude, 2018a).

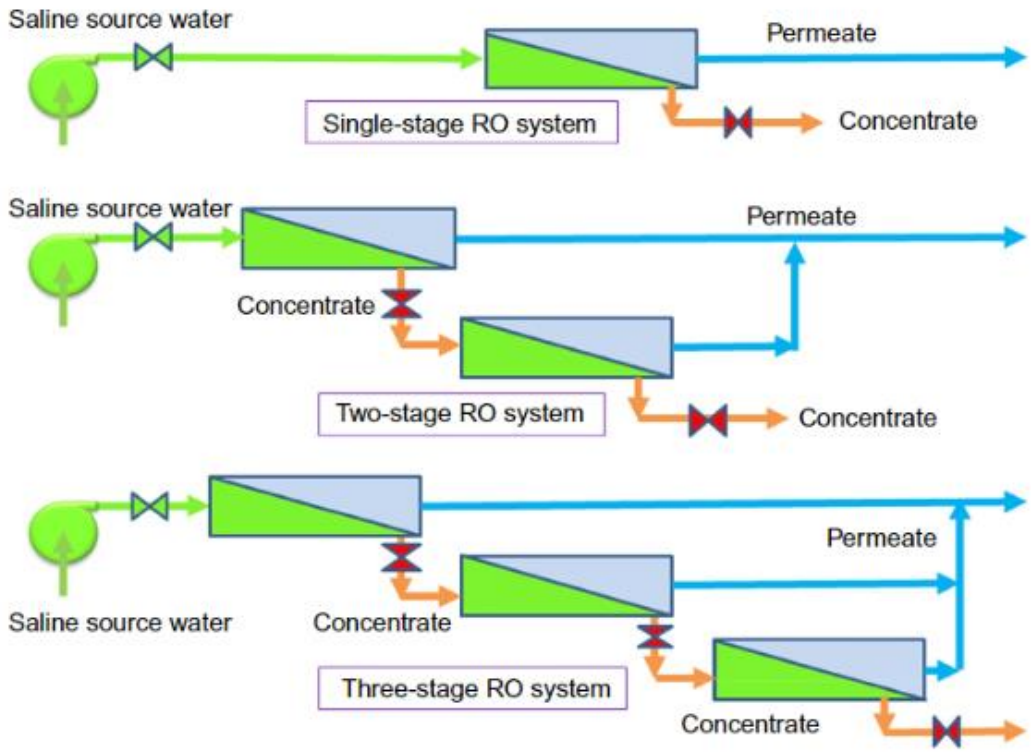

Figure 2.7. Single and multi-stage configuration (Gude, 2018b)

Based on the water source and the target quality, desalination plant configurations are specified. A combination of both multi-stage and multi-pass could be needed in some cases.

Sufficient flow of water in all stages could be ensured using two technologies. The simple one is called backpressure, which uses valves on the permeate side to control the flow rate and the pressure in each stage. This technology has a low capital cost; however, it results in energy loss. The second method is using booster pumps between the stages. This technology has a higher capital cost but improves the system's efficiency.

2.1.4.1 Pretreatment

Pretreatment is a vital step in water desalination. Stable and reliable water desalination production using RO is dependent on feedwater quality. Variation of the feedwater would affect the system's long-term performance and increase maintenance costs (Wolf, Siverns, & Monti, 2005). The two main types of seawater pretreatment are conventional pretreatment and ultrafiltration pretreatment.

2.1.4.1.1 Conventional Pretreatment

Generally, conventional pretreatment starts with open seawater intake and consist of mechanical screen filtration, breakpoint chlorination, coagulation and fluctuation, multi-media filtration and cartridge filter, as shown in Figure 2.8. In the coagulation process, a chemical substance like aluminium sulfate is added to the water. This addition would neutralise the particles' negative charge. In the fluctuation process, the neutralised particles accumulate together by mixing the water. This process results in higher quality water by removing the suspended particles (Wolf et al., 2005).

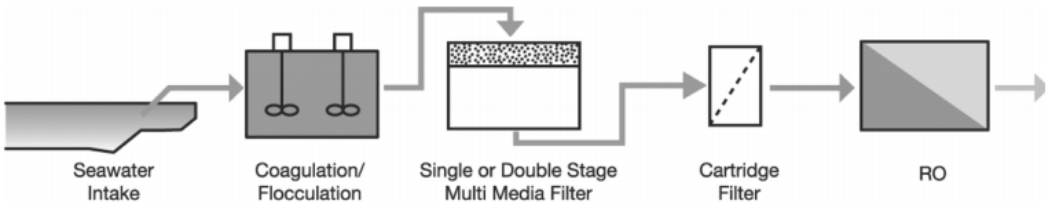

Figure 2.8. Conventional pretreatment process flow diagram (Wolf et al., 2005)

Moreover, a system named Dissolved Air Flotation (DAF) is commonly used after coagulation and flocculation. The DAF has two main chambers; the first one is called the contact zone. In this zone, air bubbles are introduced to feedwater producing a white water solution. Then the white water moves to the separation zone where the dissolved air pushes the majority of the suspended solids and organic matters to the upper area of the water where it gets concentrated and removed. This process is

demonstrated in Figure 2.9. The air is recovered from the product water and pressurised and used again in the process (Edzwald, 2010). This pretreatment's main disadvantages include a high land footprint and fluctuation of the feedwater quality throughout the year.

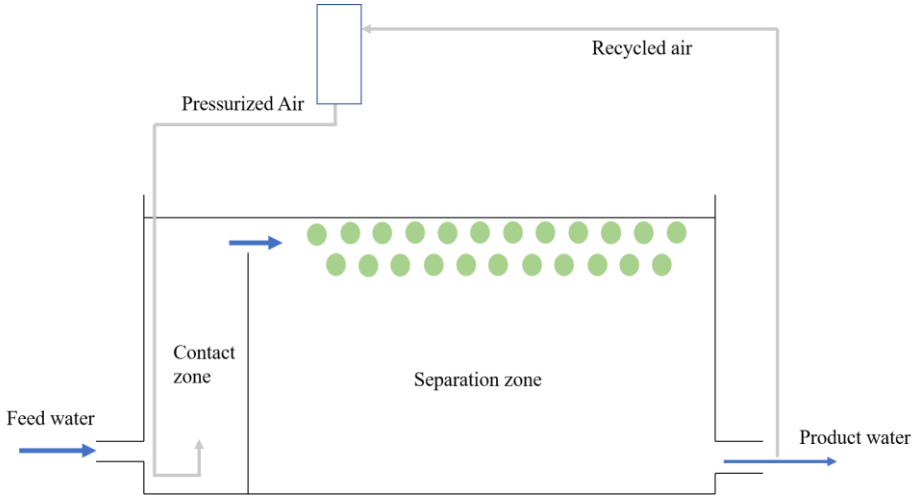

Figure 2.9. DAF schematic diagram (Edzwald, 2010)

2.1.4.1.2 Ultrafiltration Pretreatment

Ultrafiltration (UF) is considered as a new alternative to the conventional pretreatment in newly designed seawater desalination plants. The main reason for this trend is the independency between the raw water and the feedwater quality. In other words, the steady high-quality feedwater is produced throughout the year regardless of the change in the raw water quality. In UF pretreatment, mechanical screening is followed by UF modules that are used to treat the raw water before the RO processes, as shown in Figure 2.10 (Vedavyasan, 2007; Wolf et al., 2005). The slight increase in energy consumption by using a UF system could be compensated by the rise in the RO modules' recovery, and the decrease in chemical usage and the required maintenance (Vedavyasan, 2007). Detailed analysis considering several parameters will be required to undertake a complete comparison of the two technologies.

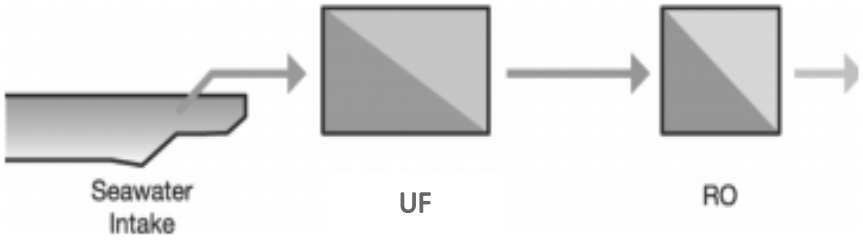

Figure 2.10. UF pretreatment process flow diagram (Wolf et al., 2005)

2.1.4.2 Energy Recovery Devices

One of the main components of RO plants is the high-pressure pumps. Therefore RO technology is an energy-intensive water desalination process. However, the concentrate leaves the system with high pressure. Harvesting the concentrate's energy is critical for reducing energy consumption which is possible via energy recovery devices (ERDs) (Huang, Pu, Wu, Wu, & Leng, 2020). ERDs are divided into two main categories based on the working principle, which are centrifugal type and positive displacement type.

2.1.4.2.1 Centrifugal Type

Centrifugal ERDs are considered as the old technology of energy recovery in RO plants. This type is more suitable for small scale desalination plants as it has relatively low efficiency, around 50% on average. Pelton turbine, turbochargers and hydraulic pressure boosters are examples of this type (Gude, 2018a; Huang et al., 2020)

2.1.4.2.2 Positive Displacement Type

Positive displacement type (PDT) ERDs are the new technology in water desalination energy recovery. It is a more attractive option for large scale water desalination plants as it operates on high efficiency, more than 90%. Isobaric ERDs, piston devices, and pressure exchangers are classified as PDT ERDs (Gude, 2018a).

In centrifugal ERDs, the hydraulic energy of the concentrated water is converted to other forms of intermediate energy, mainly mechanical energy. On the other hand, in PDTs, the brine's hydraulic energy is recovered directly as hydraulic energy, and it is provided to the feedwater, as shown in Figure 2.11 (Huang et al., 2020).

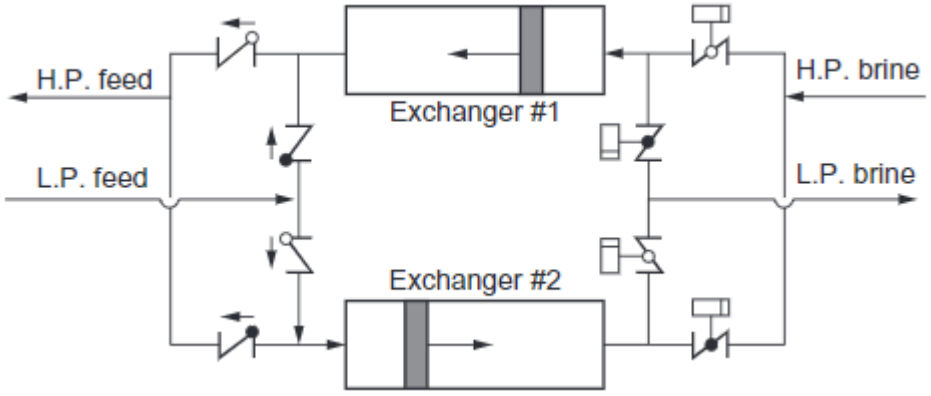

Figure 2.11. Simple PDT device scheme diagram (Gude, 2018a)

2.1.4.3 Posttreatment

In the water desalination process, most of the needed minerals for the human body are removed from the water, which would affect human health in long-term consumption. Therefore, meeting the drinking water guidelines is necessary. Besides the potential health effect, the produced water should neither be aggressive nor corrosive to allow safe distributed by pipelines. Aggressive water would attack the calcium carbonate in the concrete pipelines. On the other hand, corrosive water would affect the mild steel pipelines causing a higher corrosion rate. Hence, the permeate water should be further treated after the RO system to remineralise the

permeate and ensure its stability before the distribution. Also, this process ensures a balanced and safe water for human consumption (Withers, 2005). Various remineralisation methods are available as posttreatment for desalinated water.

The first and simplest method is the addition of carbon dioxide and hydrated lime. The lime storge and the dosing are the main challenges in this process. Another option for remineralisation is using carbon dioxide and limestone. However, this method has a higher level of complexity. Other methods, including hydrated lime and sodium carbonate, and sodium bicarbonate and calcium sulfate, are not suitable for large scale water desalination plant due to the high cost (Withers, 2005). The usage of treated seawater and blending it with the permeate is considered only in thermal desalinated water as it has a low TDS concentration.

Another important posttreatment step is disinfection. Water disinfection could be conducted using different practices, including ultraviolet light (UV), ozone, and chlorine. UV light is an effective and affordable disinfection method. However, ozone and UV do not produce disinfection residues that can stay in the water during the water distribution, limiting their use in large-scale water desalination plants (Withers, 2005). On the other hand, chlorine is suitable for large water desalination and distribution. Furthermore, chlorine is a cheaper more common alternative.

2.1.4.4 Concentrate Treatment

The concentrate volume of a desalination plant commonly ranges between 50% to 60% of the feedwater depending on the recovery rate. It is a significant amount of high salinity water with TDS ranges between 60000 to 80000 mg/L, which could cause environmental damage if it was discharged to the sea as it is (Xu et al., 2013).

Various concentrate management approaches are available in the literature, including deep-well injection, evaporation ponds, mixing with treated used water, and the water desalination plant integrated with salts extraction industry. However, it is commonly discharged to the sea (Xu et al., 2013).

The deep-well injection requires specific geological features and intense monitoring, making it unsuitable for most cases. Evaporation ponds are used to decrease the volume of the concentrate. Also, some thermal process could be utilised to achieve zero liquid discharge (ZLD). However, this method requires a large land footprint and results in a significant increase in cost (Xu et al., 2013). Mixing the treated water with the concentrate that is usually discharged to the sea could be used to decrease the concentrate salinity to a value close to the seawater salinity before releasing it to the sea.

In some cases, the concentrate water was processed and treated and used in a salt extraction industry. This solution could be a beneficial use of the concentrate. In Japan, grain salts are recovered and processed for use from the concentrate of an electrodialysis desalination plant. Using the concentrate water for salts-recovery could save up to 20% of the consumed energy in salt production processes (Davis, 2006; Xu et al., 2013).

2.2 Literature Review

2.2.1 Rainfall Patterns and Water Balance

Spatial and temporal characteristics of rainfall have been studied in many countries around the world. In Zhang et al. (2009), the annual rainfall concentration has been studied, and its pattern has been identified by using 45 years of data in the Pearl River basin in China using CI and MK test. This study found an upward trend in CI values after 1990, indicating an increase in the extreme events frequency.

In Tao et al. (2018), the spatial distribution of daily rainfall patterns has been evaluated using CI and SI. The study found that northern and south-western China have high CI values indicating that heavy daily rainfall events have a significant portion of the annual total rainfall in those regions.

Using CI, Peninsular Spain has been categorised into two areas. With high CI value, eastern Spain obtains 70% or more of its annual rainfall from 25% of the rainy days. The rest of the country reported receiving more regular daily rainfall with lower CI values (Martin-Vide, 2004).

A recent study used CI to evaluate the precipitation characteristics over the Mediterranean region with a focus on the Western Mediterranean region, where an increase in the CI values is observed (Mathbout, Lopez-Bustins, Royé, Martin-Vide, & Benhamrouche, 2020).

Both CI and PCI have been used to analyse the spatial rainfall patterns in the Calabria region of Italy. The results suggested that the western side has the lowest CI values in the study area, whereas the eastern side has heavy and short rainfall. Computed PCI results show a greater seasonality on the east side of the area where heavy and aggressive rain is received (Coscarelli & Caloiero, 2012).

To express the distribution of rainfall throughout the year, PCI has been utilised in Spain (Michiels et al., 1992). Another study has used the same index to evaluate the spatial and temporal rainfall patterns in east Spain (De Luís et al., 2000), where a significant variation in the monthly total precipitation across the study region is observed.

Additionally, SI has been used to analyse the spatial and temporal precipitation patterns in western India (Guhathakurta & Saji, 2013) and Greece (Livada & Asimakopoulos, 2005). In India, a decrease in total monthly rainfall between January and May over the last hundred years is observed. On the other hand, In Greece, a greatly seasonal rainfall pattern with long and dry summer is observed.

Furthermore, CI, PCI and SI have been used to analyse the spatial and temporal distribution of rainfall patterns in the Pearl River Basin in China. The study results showed a tendency to decrease in seasonal and annual rainfall events in the study region. A decrease in the wet season duration has also been noted, causing frequent irregularities in rainfall patterns (Deng et al., 2018).

Other indices like Standard Precipitation Index (SPI), Normalized Difference Vegetation Index (NDVI) and The Niño index are also used in the literature to analyse the change in rainfall patterns and its effect (Fustos, Abarca-Del-Rio, Moreno-Yaeger, & Somos-Valenzuela, 2020; S Khan, Gabriel, & Rana, 2008; Lana, Serra, & Burgueño, 2001; Nicholson, Davenport, & Malo, 1990).

Probability density functions are also common in analysing the rainfall patterns. Gamma distribution has been used to analyse the annual rainfall patterns in the southern part of Cyprus (Michaelides, Tymvios, & Michaelidou, 2009). The study found that the majority of the stations have a low probability of high yearly rainfall values. The same methodology has been applied to a wide range of climates in Africa (Husak et al., 2007). This study found that Gamma distribution is suitable for various climates.

Increase in frequency of extreme events as a result of climate change lead many researchers to focus on temporal change of intensity and frequency of precipitation events. MK trend test has been used by many researchers to analyse trends of precipitation indices such as CI, PCI etc. both on a regional and global scale. Karl (1998) concluded that the frequency of rainfall extremes has a significant upward trend over the previous few decades in the USA using MK. Tao et al. (2018) observed substantial positive trends of extreme rainfall indices in the northern part of China and scattered parts of southern China using the Mann-Kendall trend test.

A list including a highlight of references that used various methodologies in analysing the rainfall patterns is shown in Table 2.1. in this table, the used methodology, the research year, and country are presented.

Table 2.1. List of rainfall patterns studies in the literature, including the study methodology, region and year

Reference	*Index*	*Trend test*	*Country*
Zhang et al. (2009)	CI	MK	China
Coscarelli & Caloiero (2012)	CI, PCI	MK	Italy
Tao et al. (2018)	CI, SI	MK	China
Martin-Vide (2004)	CI	-	Spain
De Luís et al. (2000)	PCI	-	Spain
Guhathakurta & Saji (2013)	SI	-	India
Livada & Asimakopoulos (2005)	SI	-	Greece
Mathbout et al. (2020)	CI	MK	Mediterranean region
Deng et al. (2018)	CI, PCI, SI	MK	China
Michaelides et al. (2009)	Gamma	-	Sothern Cyprus
Husak et al. (2007)	Gamma	-	Africa

Water balance is essential for water resources management. The charging rate of lake Qinghai in west China has been estimated using the volumetric water balance (Li, Xu, Sun, Zhang, & Yang, 2007). It has also been used to analyse the water balance component of Tonle Sap Lake in Cambodia (Kummu et al., 2014). In (Kenway, Gregory, & McMahon, 2011), the volumetric balance has been used to study the main components in the urban cities in Australia.

The temporal changes in the discharging rate of the Lena River in Russia have been evaluated by analysing the water balance components, where an upward trend was noticed in the runoff values between 1936 and 2001 (Berezovskaya, Yang, & Hinzman, 2005).

In Spain, the water balance analysis has been studied to modify the irrigation system based on the water deficit values to conserve water (Isidoro, Quílez, & Aragüés, 2004). In (Leta et al., 2016), water budget analysis combined with GIS were used to evaluate the effect of climate change on the water balance components.

The water balance components have been analysed in Indonesia, using the TM model. The study found a potential for water harvesting of the runoff as the rainfall value is 1.9 times higher than the AET value of the same region (Nugroho et al., 2019). A general view of the water balance in Italy was presented in Salvati et al. (2008).

TM model was used to evaluate the temporal change on the water balance in Malawi between 1971 and 2000. The study results showed a decrease in precipitation, AET and runoff during the study period (Ngongondo et al., 2015).

TM model was used to determine the water balance components. The runoff value has been combined with ArcGIS and DEM to estimate the possible water harvesting strategies for the Himalaya region in India (Jasrotia et al., 2009).

There are many studies on variations of rainfall characteristics and water balance analysis around the world in the literature. However, minimal studies in the literature have been conducted on these topics for Cyprus.

The water reuse was investigated for Northern Cyprus in Elkiran, Aslanova, & Hiziroglu (2019). Also, the effect of tourism on the groundwater has been studied in Vehbi & Doratli (2010).

Additionally, the possibility for small scale water harvesting for university campus was analysed in Northern Cyprus by Harb (2015). The salinity problem of Guzelyurt aquifer, which is one of the main aquifers in Northern Cyprus, has been evaluated in Ergil (2000). This study showed the need for sustainable water management to avoid reaching the contamination level of Gazimagusa aquifer, one of the largest aquifers in Northern Cyprus. It is now ultimately out of service because of the high salinity due to the seawater intrusion.

Another study used seven indices to evaluate the frequency of extreme events in Northern Cyprus. A minor number of the stations showed any significant upward trend in the extreme precipitation frequency during the study period (Zaifoğlu, Akıntuğ, & Yanmaz, 2017). Using MK trend test, annual and monthly time series precipitation data have been evaluated. The study concluded no significant trend in the annual rainfall patterns. However, a shift in the monthly rainfall data has been observed (Seyhun & Akıntuğ, 2013).

The potential evapotranspiration of Northern Cyprus has been determined using various methodologies in Koyuncu (2019). Furthermore, temporal change has been investigated. In which a significant upward trend has been observed in the majority of the stations. In Cakal (2016), droughts severity and frequency in Northern Cyprus have been studied using the Palmer Index. More recently, drought events in Northern Cyprus have been further investigated using Standard Precipitation Index (SPI), Z-Score Index (ZSI), Rainfall Departure from Mean (RD), China Z- Index (CZI), and Rainfall Deciles based Drought Index (RDDI) in Khan (2019).

It is evident that more studies are needed to evaluate the spatial variation of rainfall patterns across Northern Cyprus. This type of research could be a key for sustainable water resources management and could provide a useful tool for infrastructure design. Additionally, the effects of climate change vary from place to place, evaluating these changes, and addressing them could be vital for future planning, especially for areas where water resources are minimal, like Northern Cyprus. More importantly, there is no study that has been conducted in Northern Cyprus to evaluate the water balance components.

2.2.2 Seawater Desalination

The leading technology in seawater desalination is RO as it is the most commonly used technology around the world, as shown in Figure 2.4. However, high capacity

MSF plants are still operating in energy-rich countries, especially in UAE (Ettouney & Wilf, 2009).

Seawater desalination became the main source of potable water in many countries, especially in the Middle East, as Saudi Arabia is the top desalinated water producer worldwide. In the first ten countries with the highest water desalination capacity, countries from the Middle East and the Mediterranean regions, as shown in Table 2.2, suffer from water scarcity.

Table 2.2. Country ranking based on water desalination capacity (Darre & Toor, 2018)

Country ranking based on desalinated water production	*Country*	*Total capacity (million Mm^3/d)*
1	Saudi Arabia	9.9
2	USA	8.4
3	UAE	7.5
4	Spain	5.3
5	Kuwait	2.5
6	China	2.4
7	Japan	1.6
8	Qatar	1.4
9	Algeria	1.4
10	Australia	1.2

Additionally, in Southern Cyprus, RO desalination plants are the primary unconventional potable water source, as presented in Table 2.3.

Table 2.3. RO desalination plants in southern Cyprus (Oner, 2019)

Plant name	*Capacity (m^3/day)*
Dhekelia Desalination Plant	60000
Larnaca Desalination Plant	64000
Limassol (Episkopi) Desalination Plant	60000
EAC Vassilikos Desalination Plant	60000
Paphos Desalination Plant	15000

Various studies tackled different aspects of water desalination in Cyprus. In (Fylaktos, Mitra, Tzamtzis, & Papanicolas, 2015) the economic element of a combined renewable energy system and RO desalination cogeneration unit for Southern Cyprus was investigated. Additionally, the integration of solar energy for water desalination application for Northern Cyprus was reviewed in (Phillips Agboola & Egelioglu, 2012). Utilising solar energy in desalination has been considered in experimental studies in Northern Cyprus (Ekin, 2016; O Aybar, Egelio-lu, & Atikol, 2005). In the southern part of the island, the economic aspect of solar desalination was the focus of many studies (S. Kalogirou, 1997, 1998; S. A. Kalogirou, 2001; Poullikkas, 2010). Furthermore, RO desalination plants' performance in southern Cyprus has been evaluated by (Gasia-Bruch et al., 2011; Tsiourtis, 2001). In Northern Cyprus, due to the high price of electricity, governmental subsidies are needed to achieve economically feasible seawater desalination. Additionally, it has been concluded in different studies that the RO plant capacity has an inverse relation with specific investment cost, which known as economy of scale, as shown in Figure 2.12 (Ghaffour, Missimer, & Amy, 2013; Mayor, 2020).

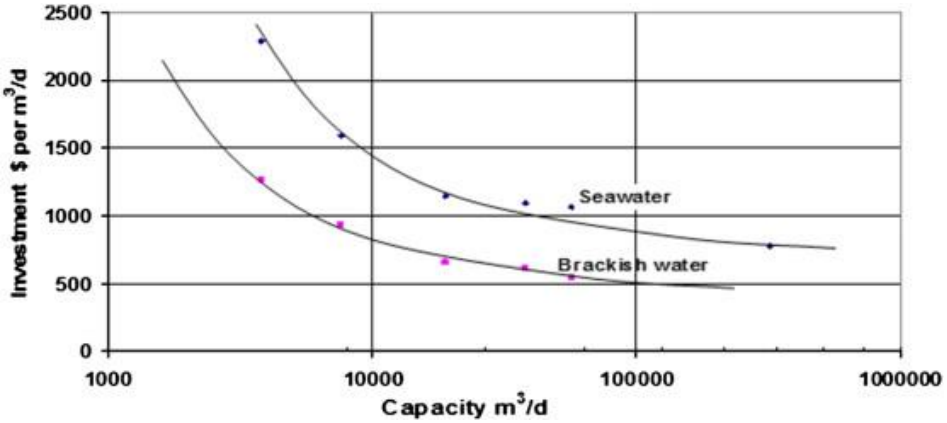

Figure 2.12. The relation between RO plant capacity and its specific investment cost (Ghaffour et al., 2013)

However, due to the relatively high price of electricity in Northern Cyprus, various economic analyses showed a high specific price of desalinated water in Northern Cyprus, ranging between 2.2 $/m^3 and 2.1 $/m^3 (Abbasighadi, 2013; Oner, 2019).

There is a lack of detailed technical design of a water desalination plant for Northern Cyprus. In this study, a technical design of a high-efficiency energy-saving RO desalination plant for Northern Cyprus is provided as a sustainable and reliable water source.

CHAPTER 3

STUDY AREA AND DATA

In this study, rainfall patterns and the water balance components are analysed. Furthermore, seawater desalination as a sustainable and reliable source of potable water is investigated for Northern Cyprus. Cyprus island is located in the Mediterranean climate zone. The only conventional source of water on the island is rainfall. The study area contains 33 metrological stations, where daily rainfall data have been collected in 36 hydrological years between (1978-79 and 2014-15), by the Meteorological Authority of Northern Cyprus. The spatial distribution of rainfall stations spread across the study area covering all local hydro-climatologic patterns, as shown in Figure 3.1. Additionally, the figure illustrates the regions that are Karpass Peninsula, North Coast and Kyrenia Mountains, East Coast, and Mesaoria Plain (East, Central, and West), classified by Meteorological Authority with a total area of 3355 km^2. The quality and homogeneity of the rainfall data have been tested and missing data filled by (Zaifoğlu et al., 2017).

The Meteorological Authority of Northern Cyprus has also provided the temperature data. The data quality has been tested, and the missing data have been filled by (Cakal, 2016). The temperature data has been collected in 24 stations. However, the averaged temperature has been estimated for the remaining stations (Cakal, 2016). Hence, the same 33 stations, shown in Figure 3.1, have also monthly temperature data.

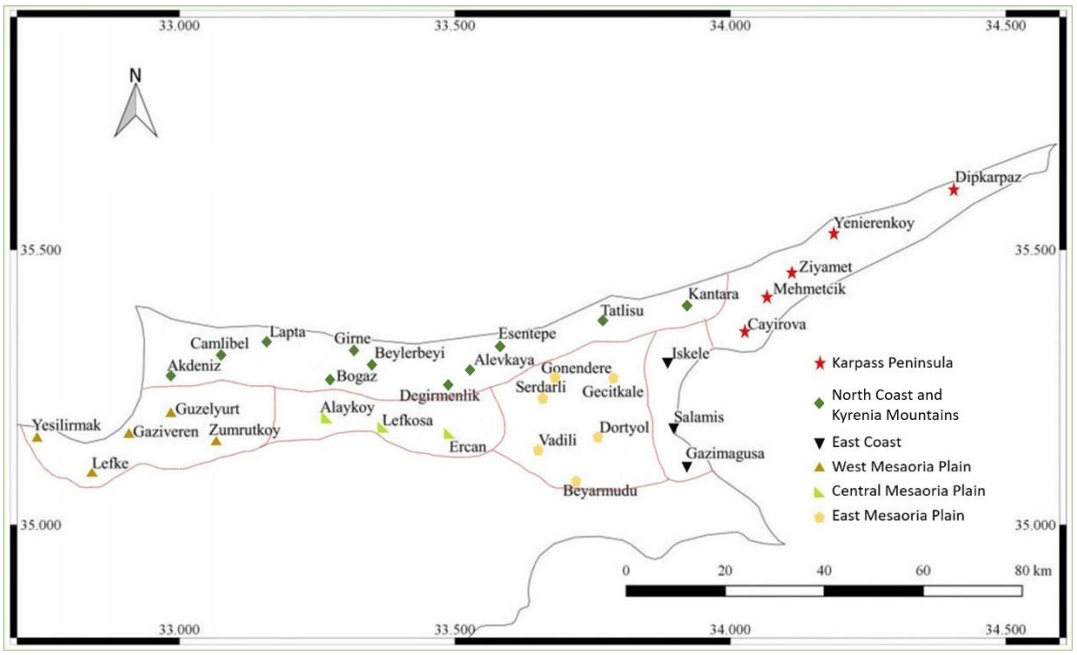

Figure 3.1. The spatial distribution of the metrological stations and the regions in the study area.

The location of each station in term of longitude, latitude, and region is listed in Table 3.1. Additionally, the average yearly total rainfall and the annual average temperature of each station are shown in Figure 3.1. It could be noted that the Karpass Peninsula and Kyrenia Mountains and North Cost receive relatively higher annual rainfall compared with East Coast, east, central and west Mesaoria Plain.

The maximum average annual rainfall in the study area is 558 mm, and it is observed in Kantara. In comparison, the minimum is 266 mm in Dortyol, as presented in Figure 3.2. On the other hand, the average annual temperature ranged from 16.3 to 20.4 across the study area, as shown in Figure 3.3.

Table 3.1. Region name, longitude, latitude, annual average precipitation ($\bar{P}$) and annual average tempreture ($\bar{T}$) of each station in the study area

Region	*Station Name*	*Latitude*	*longitude*	$\bar{P}$ *(mm)*	$\bar{T}$ *(°C)*
Karpass Peninsula	Cayirova	35.35	34.03	392	19.3
	Dipkarpaz	35.60	34.38	498	19.3
	Mehmetcik	35.42	34.08	414	20.1
	Yenierenkoy	35.54	34.19	454	19.6
	Ziyamet	35.45	34.12	431	19.6
Kyrenia Mountains and North Coast	Alevkaya	35.29	33.53	483	16.3
	Beylerbeyi	35.30	33.35	493	19.3
	Bogaz	35.29	33.28	400	18.9
	Degirmenlik	35.25	33.47	335	17.9
	Kantara	35.40	33.91	558	18.3
	Akdeniz	35.30	32.97	381	19.6
	Camlibel	35.32	33.07	453	18.2
	Esentepe	35.33	33.58	452	19.0
	Girne	35.34	33.33	470	20.3
	Lapta	35.34	33.16	544	19.9
	Tatlisu	35.36	33.75	479	19.7
East Coast	Iskele	35.29	33.88	339	19.0
	Gazimagusa	35.14	33.94	335	19.7
	Salamis	35.18	33.90	325	19.8
East Mesaoria Plain	Beyarmudu	35.05	33.70	339	19.4
	Dortyol	35.18	33.76	266	19.5
	Gecitkale	35.23	33.73	330	19.5
	Gonendere	35.25	33.66	325	18.1
	Serdarli	35.25	33.61	333	18.0
	Vadili	35.14	33.65	293	20.4
	Alaykoy	35.18	33.26	286	18.9

Central Mesaoria Plain	Ercan	35.16	33.50	314	19.3
	Lefkosa	35.20	33.35	305	19.2
West Mesaoria Plain	Gaziveren	35.17	32.92	273	18.2
	Guzelyurt	35.19	32.98	287	18.2
	Lefke	35.10	32.84	312	19.5
	Yesilirmak	35.15	32.73	363	20.0
	Zumrutkoy	35.17	33.05	285	18.2

The soil map of northern Cyprus has been developed by (Derici, Kapur, Kaya, Gök, & Ortas, 2000), and the soil types and classifications for the study area has been computed by (Cakal, 2016). The DEM was created for the island by (Paraskeva, 2016) with 25-meter resolution.

The average total rainfall across the study area is given in Figure 3.2. A noticeable variation of monthly rainfall across the study area is observed from the difference between the maximum, and the minimum values of the average total monthly precipitation noted from Figure 3.2.

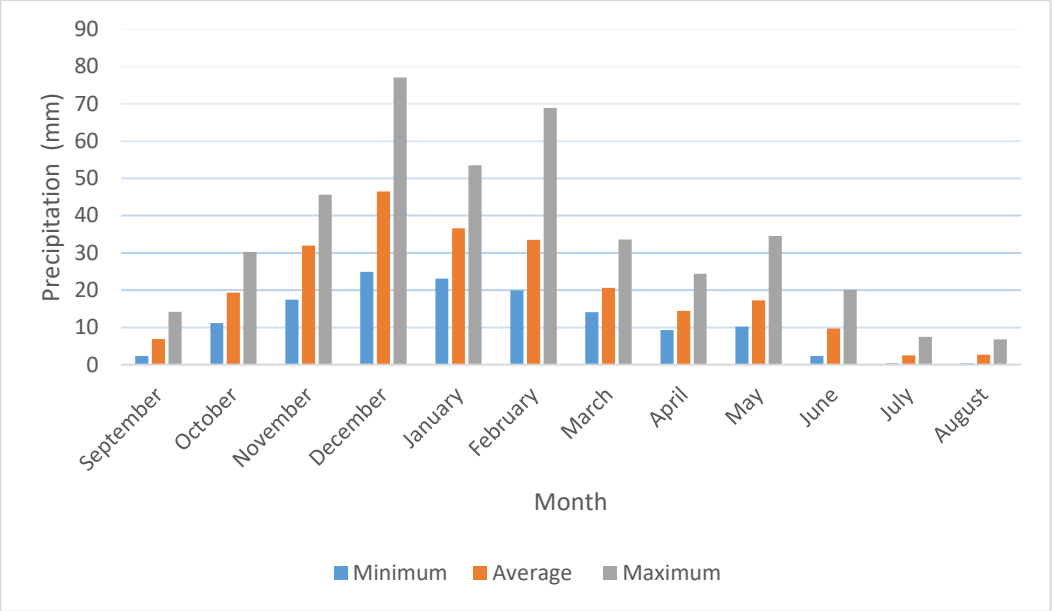

Figure 3.2. Average and the maximum and minimum average rainfall for each month across Northern Cyprus

The average temperature across Northern Cyprus is demonstrated in Figure 3.3. In the average monthly temperature, no significant variation is observed across the study area as the maximum, and the minimum average values are close to each other.

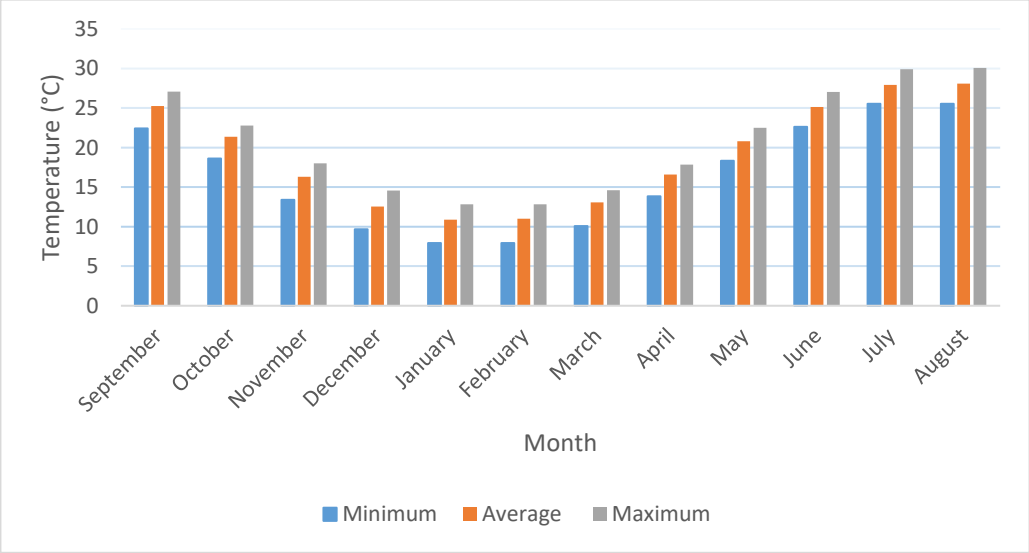

Figure 3.3. Average and the maximum and minimum average temperature for each month across Northern Cyprus

Additionally, the estimation of the needed drinking water capacity in this study is based on the amount of potable water could be imported from Turkey, with a capacity of 75 Mm^3/year (Oner, 2019).

On the other hand the quality of the Mediterranean seawater which is important in desalination processes is presented in Table 3.2.

Table 3.2. Mediterranean seawater quality (Gude, 2018b)

Water quality parameter	*Mediterranean seawater quality*
Temperature (°C)	16-28
pH	8.1
Ca^{2+} (mg/L)	480
Mg^{2+} (mg/L)	1558
Na^{+} (mg/L)	12200
K^{+} (mg/L)	480
CO_3^{2-} (mg/L)	5.6
HCO_3^{-} (mg/L)	160
SO_4^{2-} (mg/L)	3190
Cl^{-} (mg/L)	22340
F^{-} (mg/L)	1.4
Boron (mg/L)	5
TDS (mg/L)	40500

CHAPTER 4

METHODOLOGY

4.1 Rainfall Patterns Analysis

Both the precipitation quantity and its distribution have a substantial influence on the water balance components. Therefore, in this study, first of all various indices are used to study the spatial and temporal characteristic of daily, monthly, seasonal and yearly rainfall patterns. The results of each index are given in Chapter 5.

4.1.1 Daily, Monthly and Seasonal Rainfall Patterns Analysis

4.1.1.1 Concentration Index

CI, which is a statistical index, employed to compute the changing weight of daily rainfall values (Coscarelli & Caloiero, 2012; Martin-Vide, 2004; Zhang et al., 2009). It uses an exponential curve to relate the rainfall percentage to the percentage of the rainy days. The exponential curve, also known as the Lorenz curve, is shown in Figure 4.1.

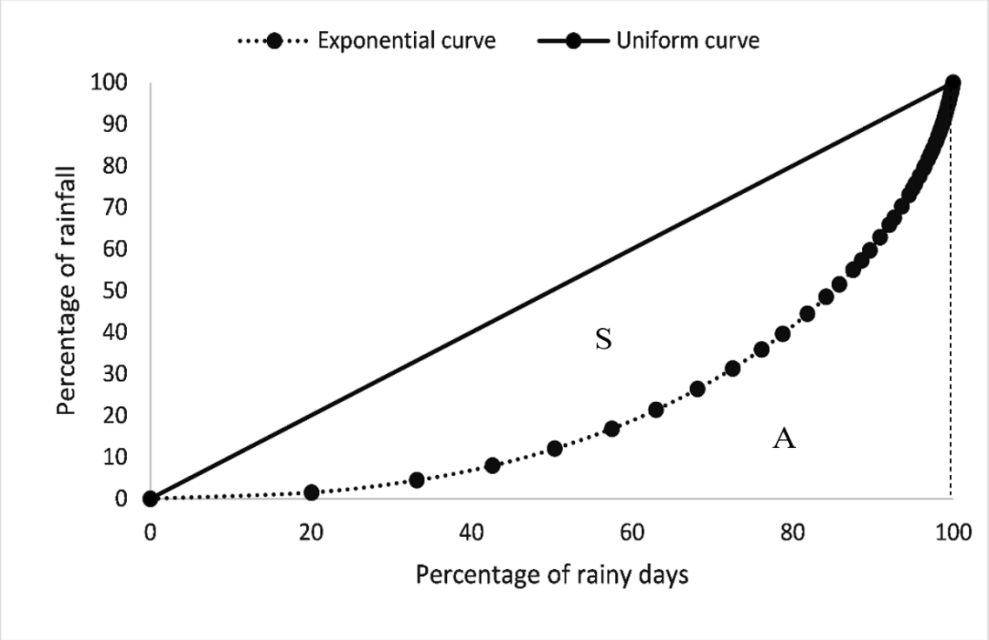

Figure 4.1. Lorenz curve showing the relation between the percentage of precipitation and the percentage of the rainy days

The curve is computed as:

$$Y = aX\,exp(bX) \tag{4.1}$$

$$\ln a = \frac{\sum X_i^2 \sum \ln Y_i + \sum X_i \sum X_i \ln X_i - \sum X_i^2 \sum \ln X_i - \sum X_i \sum X_i \ln Y_i}{N \sum X_i^2 - (\sum X_i)^2} \tag{4.2}$$

$$b = \frac{N \sum X_i \ln Y_i + \sum X_i \sum \ln X_i - N \sum X_i \ln X_i - \sum X_i \sum \ln Y_i}{N \sum X_i^2 - (\sum X_i)^2} \tag{4.3}$$

Where a and b are constants, Y is the precipitation percentage, X is the percentage of rainy days, and N is the total number of class limits excluding the days without rain.

CI is computed with a mathematical equation as:

$$CI = \frac{S}{5000} \tag{4.4}$$

$$S = 5000 - A \tag{4.5}$$

$$A = \left[\frac{a}{b}\, e^{bX} \left(x - \frac{1}{b}\right)\right]_0^{100} \tag{4.6}$$

which describes the ratio between S, the area between the uniform curve and the exponential curve (i.e. Lorenz curve), and *A*, which is the area under the Lorenz curve as shown in Figure 4.1. (Coscarelli & Caloiero, 2012). Uniform curve represents a dataset in which the same amount of rainfall is obtained in each day over a period of time. In contrast, the exponential curve is an example of a real dataset in which irregular rainfall is observed through the period of study.

CI ranges between zero and one. Zero value refers to completely uniform rainfall through the study period, whereas one means that all the rain comes in one day. In other words, high CI indicates that the majority of rainfall is obtained in fewer days. In contrast, low CI indicates homogeneity in rainfall distribution. Table 4.1 represents the ranges of CI values with the corresponding rainfall pattern.

Table 4.1. Precipitation patterns with corresponding CI values

CI	*Precipitation Pattern*
< 0.25	Uniform
0.25 – 0.50	Moderately concentrated
0.50 – 0.75	Concentrated
> 0.75	Extremely concentrated

4.1.1.2 Precipitation Concentration Index

PCI gives patterns of the relative distribution of rainfall throughout the year as:

$$PCI = \frac{100}{12} \times \left[1 + \left(\frac{CV}{100}\right)^2\right] \tag{4.7}$$

$$CV = 100 \times \frac{s}{\bar{P}} \tag{4.8}$$

where CV is the coefficient of variance, s represents the standard deviation, and $\bar{P}$ is the arithmetic mean of the monthly total rainfall data of the year. PCI is calculated for each year and then averaged over the whole set of years. PCI values range

between 8.33 and 100; the lower limit represents a uniform monthly rainfall pattern. Table 4.2 gives the ranges of PCI values relative to monthly rainfall pattern.

Table 4.2. Precipitation patterns with corresponding PCI values (Michiels et al., 1992)

PCI	*Precipitation Pattern*
< 10	Uniform
11 – 15	Moderate concentrated
16 – 20	Concentrated
> 20	Strong concentrated

4.1.1.3 Seasonality Index

SI is estimated to understand the seasonal variation in a region throughout a year using monthly total rainfall data (Kanellopoulou, 2002).

$$SI = \frac{1}{R_i}\sum_{j=1}^{12}\left|M_{ij} - \frac{R_i}{12}\right| \tag{4.9}$$

where R_i is the annual total rainfall of year i, and M_{ij} is the monthly total rainfall of month j in the year i.

SI is in the range of 0 and 1.83. Zero is obtained when each month of the year receives the same amount of total rainfall. SI value of 1.83 is obtained when all of the rain is received only in one month of the year. In other words, a low value of SI indicates uniformity, whereas a high value suggests a considerable degree of variability in monthly total precipitation throughout the year. The value of SI and the corresponding class of rainfall pattern are presented in Table 4.3.

Table 4.3. Precipitation patterns with corresponding SI values (Coscarelli & Caloiero, 2012)

SI	*Precipitation Pattern*
≤ 0.19	Very moderate
0.20 – 0.39	Moderate with a wet season
0.40 – 0.59	Rather seasonal with a short dry season
0.60 – 0.79	Seasonal
0.80 – 0.99	Significantly seasonal with a long dry season
1.00 – 1.19	Receiving most rain in 3 or fewer months
≥ 1.20	Extreme, receiving almost all rain in 1-2 months

4.1.2 Annual Rainfall Patterns Analysis

The annual rainfall patterns of the study area are analysed using Gamma Distribution as it is the most suitable statistical distribution for rainfall data. It is controlled by two parameters, namely, shape (α) and scale ($1/\beta$) paraments (Michaelides et al., 2009).

Probability density function (PDF) of incomplete gamma distribution calculated as:

$$f(x,\beta,\alpha) = \frac{\beta^{\alpha}}{\Gamma(\alpha)} \times x^{\alpha-1} \times e^{-\beta x} \tag{4.10}$$

$$\Gamma(\alpha) = \int_0^{\infty} e^{-t}\, t^{\alpha-1} dt \tag{4.11}$$

$$\alpha = \frac{1}{4A}\left(1 + \sqrt{1 + \frac{4A}{3}}\right) \tag{4.12}$$

$$A = \ln(\bar{x}) - \frac{\sum \ln(x)}{n} \tag{4.13}$$

$$\frac{1}{\beta} = \frac{\bar{x}}{\alpha} \tag{4.14}$$

where $\bar{x}$ and x refer to the arithmetic mean of annual rainfall over n years and annual rainfall, respectively. $1/\beta$ is the scale parameter, α is the shape parameter, A is the intermediate constant, while $\Gamma(\alpha)$ refers to complete gamma function. The whole study period is used to calculate both of the parameters for each station. Furthermore, the gamma distribution is used to interpret the thresholds of dry, normal and rainy years for each station for the whole study period. The thresholds of dry, normal and rainy annual precipitation values are estimated using Table 4.4.

Additionally, to evaluate the changes in annual precipitation patterns, the study period is divided into two sub-periods. The shape parameter and scale parameter of each station are calculated both for the sub-periods. Stations are classified depending on the change in their shape parameter values between the two sub-periods.

Table 4.4. Classification of rain season with corresponding threshold probabilities

Type of Travel	*Thresholds (probability)*
Dry	≤ 25%
Normal	25% - 75%
Rainy	≥75%

4.2 Water Balance Analysis

Using Thornthwaite and Mather (TM) models, the main components of the water balance are calculated. The inputs of the models are the monthly total precipitation (MP), the monthly average temperature (MT) and the soil moisture storage capacity (STC).

The study area his divided into 33 polygons, where each metrological station is used to represent one polygon. The polygons boundary and distribution is shown in Figure 4.2.

Figure 4.2. Boundaries of the 33 polygons in the study area (Cakal, 2016)

4.2.1 Soil Storage Capacity

STC value is determined for each polygon based on the soil type and land cover using Thornthwaite and Mather (1957) tables. The STC values with the corresponded land cover and soil type are given in Table 4.5.

Table 4.5. The soil storage capacity with the corresponding land cover and soil type (Jasrotia et al., 2009; Nugroho et al., 2019; USGS, 2007)

Land cover	*Soil type*	*STC (mm)*
Shallow-rooted crops (Spinach, Peas, Beans, Beets, Carrots, etc.)	Fine Sand	50
	Fine Sandy Loam	75
	Silt Loam	125
	Clay Loam	100
	Clay	75
Moderately Deep-Rooted Crops (Corn, Cotton, Tobacco, Cereal, Grains)	Fine Sand	75
	Fine Sandy Loam	150
	Silt Loam	200
	Clay Loam	200
	Clay	50
	Fine Sand	100

Deep Rooted Crops (Alfalfa, Pastures, Shrubs)	Fine Sandy Loam	150
	Silt Loam	250
	Clay Loam	250
	Clay	50
Orchards and Open Forest	Fine Sand	150
	Fine Sandy Loam	250
	Silt Loam	300
	Clay Loam	250
	Clay	200
Closed Mature Forest	Fine Sand	250
	Fine Sandy Loam	300
	Silt Loam	400
	Clay Loam	400
	Clay	350
Built-up area	Fine Sand	40
	Fine Sandy Loam	60
	Silt Loam	100
	Clay Loam	80
	Clay	240
High-density urban areas	Fine Sand	10
	Fine Sandy Loam	15
	Silt Loam	20
	Clay Loam	25
	Clay	35

A portion of the monthly total precipitation is converted to direct runoff while the rest of the precipitation (P_{eff}) is used to charge the soil until it reaches its maximum capacity, all of the excessive rainfall becomes available as water (Jasrotia et al., 2009; Mccabe & Markstrom, 2018). The flow diagram of the water balance analysis is presented in Figure 4.3, where the expected inputs and output are also indicated.

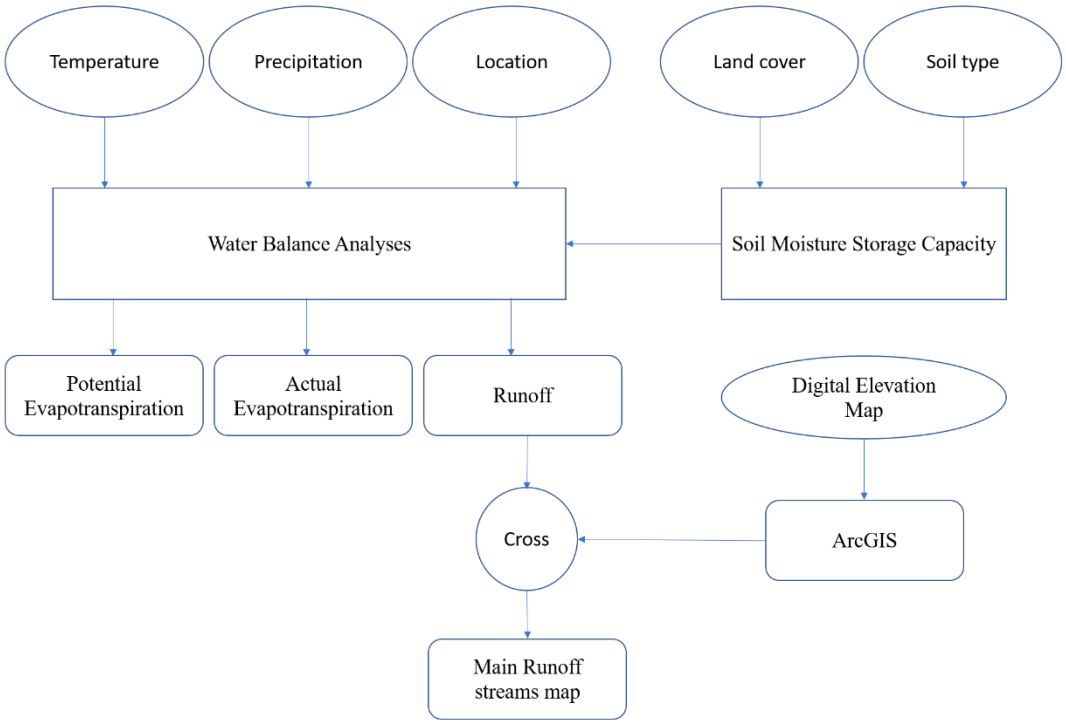

Figure 4.3. Flow diagram of the water balance analysis methodology

4.2.2 Monthly Potential Evapotranspiration

PET is calculated using Harmon's equation as follows:

$$PET = 13.97 \times d \times D^2 \times w \tag{4.15}$$

where d is the number of days in the month, D is the monthly daylight hours, and w represent the saturated water vapour density, calculated as:

$$w = \frac{4.95 \times e^{0.062 \times T}}{100} \tag{4.16}$$

where T is the mean monthly temperature in °C.

4.2.3 Monthly Actual Evapotranspiration

The monthly AET calculation method is dependant on the rainfall and PET of that month, as shown in Figure 4.4. When the monthly total rainfall is higher than the

monthly PET for the same month, the monthly AET is equal to the monthly PET. The extra precipitation is stored in the soil until it reaches its maximum soil moisture storage capacity (STC).

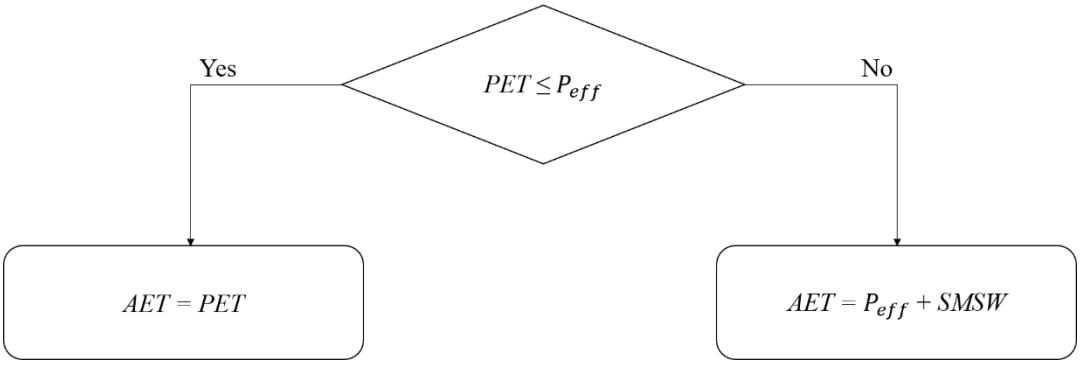

Figure 4.4. Flow diagram of the AET calculation methodology. Where P_{eff} is 95% of the total precipitation and *SMSW* is the soil moisture storage withdrawal rate

On the other hand, when the monthly PET is higher than the monthly total rainfall, the AET of the month is computed as:

$$AET = P_{eff} + SMSW \tag{4.17}$$

$$SMSW = \left|P_{eff} - PET\right| \times \frac{ST_{i-1}}{STC} \tag{4.18}$$

where P_{eff} is 95% of the total precipitation (P_{total}). $SMSW$ is soil moisture storage withdrawal, which represents a linear decrease in evapotranspiration from the soil as the water storage in the soil decreases. ST_{i-1} is the soil moisture storage of the previous month, and STC represents the soil moisture storage capacity and it is computed using Table 4.5. The soil moisture storage of a month ST_i is calculated as follows:

$$ST_i = ST_{i-1} - SMSW_i \tag{4.19}$$

The weighted average is used to calculate the STC value for each polygon based on the percentage of each soil type and the land cover in the area.

4.2.4 Monthly Water Surplus and Runoff

The surplus is generated after the soil moisture storage reaches its maximum capacity, and the P_{eff} is higher than the PET. In this case, all of the excessive rainfall is converted to surplus. While 5% of the P_{total} converts to direct runoff, 50% of the surplus is assumed to convert as runoff. At the same time, the rest is detained in small ponds, channels and subsoil of the study area, known as surface depression areas. Total of runoff (RO_{total}) is calculated as:

$$RO_{total} = 0.05 \times P_{total} + 0.5 \times S + RS \quad (4.20)$$

where P_{total} and S are the total precipitation and the surplus, respectively. RS is the remaining surplus of the previous months, and it is added to the runoff in the following months if the amount of rainfall is higher than PET.

Additionally, ArcGIS, DEM, and the TM analysis' results are used to determine the water flowing direction, junctions and water basins. Then, using the RO_{total} value of each station, the average annual discharge rate is calculated for the main water streams in the study area, as shown in Figure 4.5 where each polygon has a yearly RO_{total} value. This value is multiplied with the basin area under that polygon to determine the discharge rate of a specific part in the basin. In other words, the discharge rate value in the discharging point shown in Figure 4.5 is computed as:

$$DR = \sum_{i=1}^{n} (A_i \times TRO_i) \quad (4.21)$$

where DR is the discharge rate in the discharging point, TRO_i is the total depth of runoff for the i polygon, and A_i is the area of the basin under the i polygon and n is the number of basins.

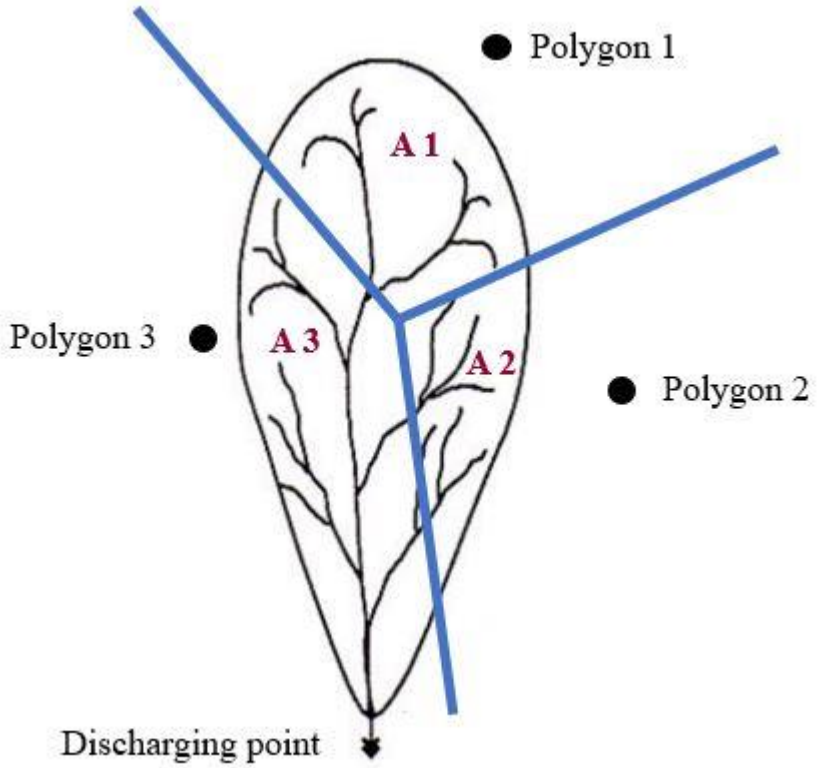

Figure 4.5. Demonstration of the discharge rate using basin boundary and rainfall station polygons

Furthermore, the available water for harvesting using a city drainage system or domestic water harvesting systems in the high-density residential area in the main cities is estimated using the average RO_{total}. The residential area's RO_{total} value is calculated separately using an average value of STC as 20 mm (see Table 4.5, High density urban areas), and the polygon monthly total rainfall and temperature for the whole study period.

4.3 Mann-Kendall Trend Test

MK is a non-parametric trend test commonly used to measure temporal changes in hydrological time series data.

MK trend test statistic *S* is calculated as:

$$S = \sum_{j=i+1}^{n} \sum_{j=i+1}^{n} \operatorname{sgn}(x_j - x_i) \tag{4.22}$$

where n is the sample size, and sgn $(x_j - x_i)$ is the mathematical function that extracts the sign of the time-series x given as:

$$\operatorname{sgn}(x_j - x_i) = \begin{cases} +1, & x_j > x_i \\ 0, & x_j = x_i \\ -1, & x_j < x_i \end{cases} \tag{4.23}$$

the variance Var(S) is computed as:

$$\operatorname{Var}(S) = \frac{n(n-1)(2n+5) - \sum_{i=1}^{n} t_i i(i-1)(2i+5)}{18} \tag{4.24}$$

where t_i is the number of ties of extent i. The standardised statistics Z for the one-tailed test is formulated as:

$$Z = \begin{cases} \dfrac{S-1}{\sqrt{\operatorname{Var}(s)}}, & S > 0 \\ 0, & S = 0 \\ \dfrac{S+1}{\sqrt{\operatorname{Var}(s)}}, & S < 0 \end{cases} \tag{4.25}$$

Table 4.6 shows the trend type and class with the corresponding significance level and Z value, which are considered in this study to classify the temporal trends in rainfall patterns. R-package prepared by (Kendall, 2015) has been employed in this study to determine MK values on the time-series data.

Table 4.6. Classification of trend types in terms of significance level and standardised statistics (Z) computed by the Mann-Kendall (MK) trend test (Tao et al., 2018)

Z	*Significance level (α)*	*Class*	*Trend type*
	$\alpha < 0.01$	3	Very significant increase
$Z > 0$	$0.01 \leq \alpha < 0.05$	2	Significant increase
	$0.05 \leq \alpha \leq 0.1$	1	Slight increase
$Z = 0$	$0.1 < \alpha$	0	No trend
	$0.05 \leq \alpha \leq 0.1$	-1	Slight decrease
$Z < 0$	$0.01 \leq \alpha < 0.05$	-2	Significant decrease
	$\alpha < 0.01$	-3	Very significant decrease

4.4 Seawater Desalination

A water desalination system's performance is a function of both the water source quality and the produced water quality. The quality of the Mediterranean Sea is shown in Table 3.2. Both of the mentioned factors and the required amount of treated water are crucial in the RO design (Gude, 2018a).

Additionally, the World Health Organization guidelines for drinking water are presented in Table 4.7 and were taken as reference. In that respect, the 75 million m^3/year of drinking water capacity was targeted in the plant design, which is the capacity of water that could be imported from Turkey.

Table 4.7. Water intended for drinking quality standards (IUCN, UNEP, 2000; WHO, 2006)

Water quality parameter	*Drinking water quality guidelines*
pH	6.5 – 8
Ca^{2+} (mg/L)	60 – 180
Mg^{2+} (mg/L)	2.3 – 52.1
Na^{+} (mg/L)	< 200
K^{+} (mg/L)	200 – 300
CO_3^{2-} (mg/L)	< 5.6
HCO_3^{-} (mg/L)	< 160
SO_4^{2-} (mg/L)	< 500
Cl^{-} (mg/L)	200 – 300
F^{-} (mg/L)	< 0.2
Boron (mg/L)	< 1
TDS (mg/L)	600 – 1000

4.4.1 Theory

Estimating the water desalination plant size, product quality, energy consumed per unit of the product, i.e. specific energy consumption (SEC), and the system recovery for the whole design and in each stage and pass, using real data is possible using WAVE. WAVE is a water treatment design software that has been introduced by DUPONT. Pictures of the software interface are given in appendix D.

The required amount of pressure to stop the osmotic phenomena is called the osmotic pressure (Π). It is a function of the solution concentration and its temperature. The mathematical formula to determine the Π in Pa is:

$$\Pi = C\ R\ T \tag{4.26}$$

where the temperature in Kelvin is donated as T, C is the ion concentration in mol/m^3, and R is the perfect gas constant, and its value is 8.341 J/mol/K. The osmotic pressure of the feedwater is calculated using this equation.

Transmembrane pressure (TMP) is equal to the pressure difference between the feed and the permeate pressure across the membrane, as shown in (4.27).

$$TMP = \frac{P_f + P_c}{2} - P_p \tag{4.27}$$

where P_f and P_c are the feed and the concentrate pressure, respectively, while P_p refers to the permeate pressure all in bar.

However, the transmembrane osmotic pressure is the difference between the feed and the permeate osmotic pressure, and it is calculated as:

$$\Pi_{TMP} = \frac{\Pi_f + \Pi_c}{2} - \Pi_p \tag{4.28}$$

where Π_f and Π_c are the feed and the concentrate osmotic pressure, respectively. Π_p if the permeate osmotic pressure whereas Π_{TMP} is transmembrane osmotic pressure all in bar.

The net driving pressure measures the difference between the TMP and transmembrane osmotic pressure, and it is calculated as:

$$NDP = TMP - \Pi_{TMP} \tag{4.29}$$

where NDP refers to the net driving pressure in bar.

RO modules flux in m^3/h/m^2 which represents the permeate flow rate per unit area is calculated as:

$$Flux = \frac{Q_p}{S} \tag{4.30}$$

where S is the membrane surface area in m^2, and it is provided by the manufacturer.

The module permeability is the ratio between the change in flux and the net driving pressure change. The permeability is calculated as:

$$L_p = \frac{Flux}{NDP} \tag{4.31}$$

where L_p refers to the permeability in $m^3/h\ /m^2/bar$.

Additionally, the percentage of rejected solute by the membrane is determined as:

$$R = \left(1 - \frac{C_p}{C_f}\right) \times 100 \tag{4.32}$$

where R is the salt rejection percentage, C_p and C_f stands for the salt concentration in the permeate and the feedwater in mg/L, respectively.

The difference between the feed pressure and the concentrate pressure across modules is commonly referred to as the pressure drop, and it is found as:

$$dp = P_f - P_c \tag{4.33}$$

where pressure drop is noted as dp in bar.

The system recovery (SR) is the ratio between the permeate water and the feedwater, which is calculated as:

$$SR = \frac{Q_p}{Q_f} \tag{4.34}$$

where Q_p and Q_f are the flow rate of the permeate and the feedwater in m^3/h, respectively. The system pressure and the membrane characteristics influence the system recovery.

WAVE software is used to design the RO system using the previous equations and module's datasheets, shown in Appendix D.

Based on the flow rate and the pressure in the concentrate, the optimum ERD is introduced to the system. The energy saved by the ERD is calculated as:

$$Es = (Q_c \times P_c) \times \eta \tag{4.35}$$

where Es is the energy saved by ERD in W, Q_c and P_c are the flow rate of the concentrate in m^3/s and its pressure in Pa, and η is the efficiency of the used ERD device (Huang et al., 2020).

However, the energy consumed by the pumps could be calculated as:

$$E_c = \frac{Q_f \times P_f}{\eta} \tag{4.36}$$

where Ec is the energy consumed by the pump. The actual efficiency of high-pressure pumps is used in the calculations, which is 79% as provided by the software. For determining the concentration of TDS or a specific ion, the mass balance equation is used.

The system operation conditions have a direct influence on the RO system flux and salt rejection. The summary of the effects of the change in various operation conditions is presented in Table 4.8. The impact of these changes on the system performance causes the uniqueness of each design.

Table 4.8. The effects of changing in operation conditions on the RO system (Gude, 2018b).

Change in operating condition	*System flux*	*Salt rejection*
Increase of the feedwater pressure	Increase	Increase
Increase of the feedwater TDS concentration	Decrease	Increase
Increase of feedwater temperature	Increase	Decrease

The change of the system flux has a direct relation with the feedwater temperature, and it depends on the materials used in the RO modules. Additionally, assuming a 3% increase in permeate flux per each degree Celsius is used in the literature (Al-Mutaz & Al-Ghunaimi, 2001).

4.4.2 System Configurations

The system starts with an open seawater intake coupled with mechanical screening to avoid large size particles. The feedwater is subjected to disinfectant injection,

commonly chlorine, to prevent the build-up of biological growth in the pipeline system. Then the feedwater is pretreated before it is desalinated. The final step before the distribution of water to the users is posttreatment, as shown in Figure 4.6. Moreover, the concentrate produced during the process is treated separately.

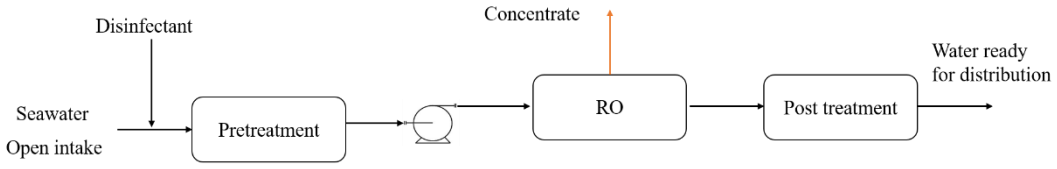

Figure 4.6. Water desalination flow diagram

4.4.2.1 Pretreatment

The pretreatment step consists of coagulation, flocculation, DAF, and UF to provide the RO system with steady high-quality feedwater. The flow diagram of raw water pretreatment is demonstrated in Figure 4.7. The usage of combined conventional systems and membrane technology aims to ensure high-quality feedwater to the RO system to reduce the required maintenance.

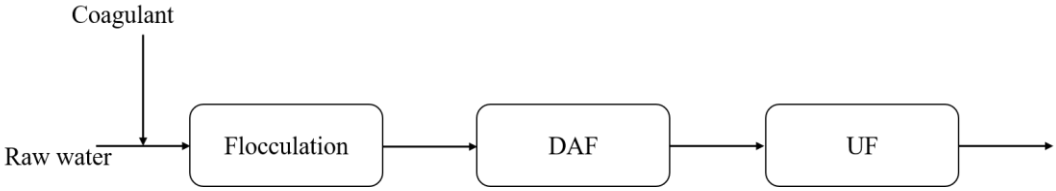

Figure 4.7. Flow diagram of Seawater pretreatment for RO water desalination system

4.4.2.2 Reverse Osmosis System

Feedwater is injected with antiscalant ($Na_6P_6O_{18}$) and acid (HCl) to prevent scaling on the membranes since feedwater with high pH would cause scaling and damage the RO membranes modules. Therefore, four mg/L of ($Na_6P_6O_{18}$) are added to the feedwater, and its pH is decreased to 6.5 using (HCl). Various system configurations

are studied and optimised, and the results are analysed before finding the final optimal system, starting with a one-pass RO system with three stages. Sodium hydroxide is added to the feed of the second pass to increase its pH up to 10 and improve the boron rejection. Two types of modules are used in the design, which are SEAMAXX-440™ for the first pass and BW30HRLE-440™ for the second pass. Both modules are produced by DUPONT; more information on the modules is available in Appendix D.

4.4.2.3 Posttreatment

The permeate could be neutralised by adding carbon dioxide and hydrated lime to the desalinated water to ensure its stability while being distributed without harming the water distribution system, as shown in Figure 4.8. Langelier Saturation Index (LSI) is commonly used to measure the water aggressiveness. LSI's negative values indicate aggressive water, while positive values indicate the possibility of scale formation in the pipelines (Anwar, Sembiring, & Irawan, 2020). LSI could be calculated as:

$$LSI = pH - pHs \tag{4.37}$$

where pH is the measured pH value of the water sample, and pHs is saturated water pH. LSI value is dependent on the water pH, TDS concentration, temperature, calcium hardness and alkalinity. WAVE software results include LSI value of the produced water.

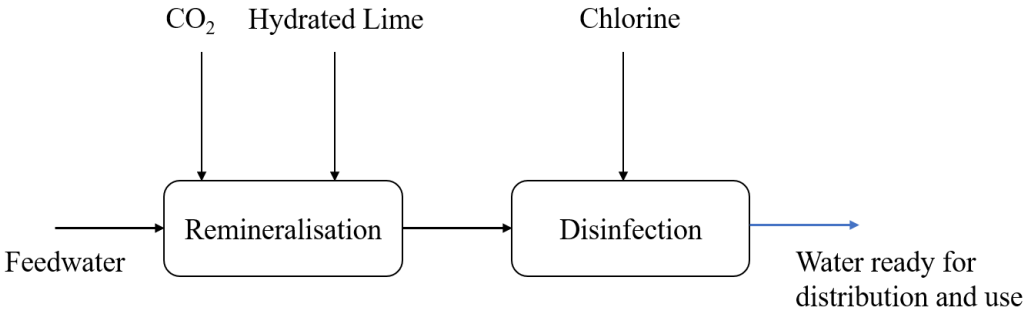

Figure 4.8. Posttreatment schematic diagram

Furthermore, the water must be disinfected, and disinfectant residues must be present in the water before distribution to avoid contamination during the process. Therefore, chlorine would be the most suitable alternative for disinfection. The chlorine concentration should not exceed five mg/L for the water intended drinking (WHO, 2004).

4.4.2.4 Concentrate Treatment

The concentrate could be discharged to the sea. However, mixing the treated used water with the concentrate before discharging it to the sea is a possible choice. The aim of the mixing is to minimise the environmental effect around the discharging point. Additionally, combining the water desalination with a salt extraction industry could decrease the concentrate significantly and would save energy in the salt extraction. Therefore, it could be the most sustainable solution, if available.

CHAPTER 5

RESULTS AND DISCUSSION

5.1 Spatial and Temporal Analysis of Rainfall Patterns

The spatial and temporal rainfall patterns are investigated in this study. The results of the CI, PCI and SI as well as gamma distribution analysis are given in the following subsections.

5.1.1 Daily Rainfall Patterns

CI is applied to evaluate the daily precipitation pattern over the whole study area. The analysis results show that CI is in the range of 0.52 to 0.63, as given in Table 5.1. It is found that most rainfall is received for higher CI values in fewer days, as given in Table 5.1 where average annual rainfall and precipitation percentage of 25% of high-intensity rain days are also presented.

Table 5.1. Average annual rainfall ($\overline{P}$), precipitation percentage of 25% of rainiest days (P_{25}), CI of the corresponding station

Region	*Station Name*	$\bar{P}$ *(mm)*	P_{25} *(%)*	*CI*
Karpass Peninsula	Cayirova	392	70.35	0.60
	Dipkarpaz	498	67.90	0.59
	Mehmetcik	414	66.05	0.58
	Yenierenkoy	454	67.56	0.58
	Ziyamet	431	67.54	0.59

Kyrenia Mountains and North Coast	Alevkaya	483	68.67	0.59
	Beylerbeyi	493	69.61	0.60
	Bogaz	400	69.10	0.60
	Degirmenlik	335	66.90	0.56
	Kantara	558	68.54	0.58
	Akdeniz	381	65.50	0.57
	Camlibel	453	65.20	0.55
	Esentepe	452	68.02	0.58
	Girne	470	73.50	0.61
	Lapta	544	69.10	0.59
	Tatlisu	479	71.32	0.62
East Coast	Iskele	339	68.41	0.58
	Gazimagusa	335	73.56	0.63
	Salamis	325	69.75	0.59
East Mesaoria Plain	Beyarmudu	339	71.03	0.62
	Dortyol	266	64.06	0.54
	Gecitkale	330	71.20	0.60
	Gonendere	325	61.54	0.52
	Serdarli	333	66.46	0.58
	Vadili	293	68.37	0.59
Central Mesaoria Plain	Alaykoy	286	66.40	0.56
	Ercan	314	74.32	0.63
	Lefkosa	305	72.84	0.63
West Mesaoria Plain	Gaziveren	273	62.60	0.54
	Guzelyurt	286	60.65	0.59
	Lefke	312	64.14	0.56
	Yesilirmak	363	64.08	0.55
	Zumrutkoy	285	64.23	0.55

It is found that Central Mesaoria Plain, East Coast, and Karpass Peninsula regions have relatively high CI values. In contrast, West and East Mesaoria Plain and North Coast and Kyrenia Mountains regions show relatively low CI values as illustrated in Figure 5.1. The CI values across the study area represent a concentrated daily rainfall pattern.

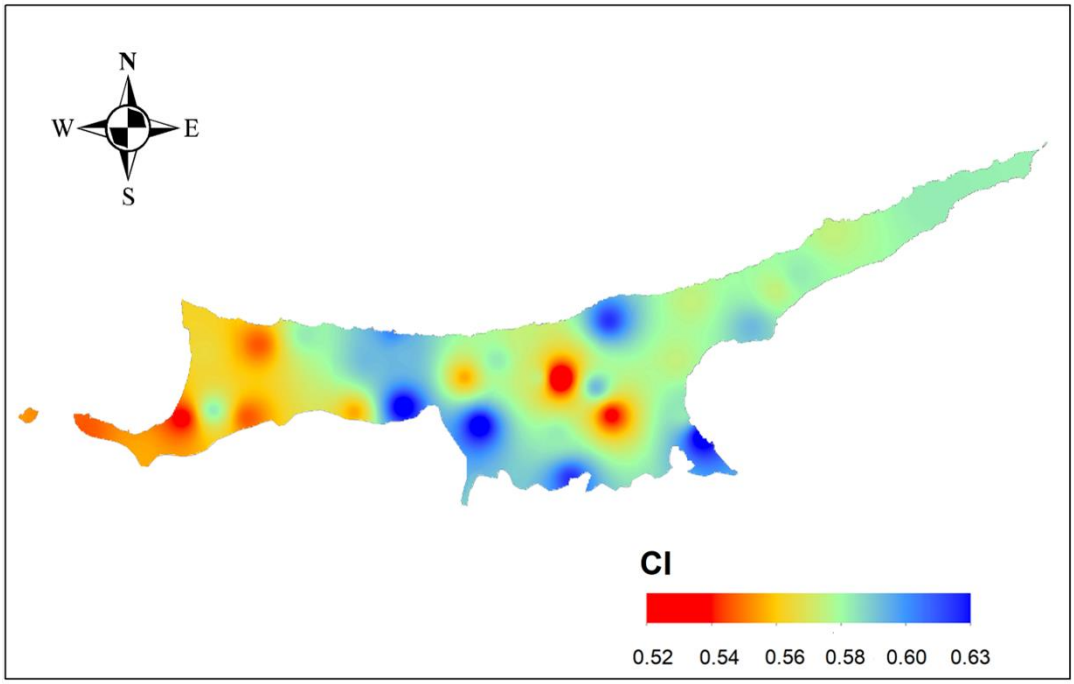

Figure 5.1. Spatial distribution of the average CI values in Northern Cyprus for a period of 1978 – 2014

The yearly CI of each station is calculated by using MK trend test. The trend of the annual CI value is determined as illustrated in Figure 5.2.

Figure 5.2. Spatial distribution temporal trends of CI values for a period of 1978 – 2014

Results of the trend test are analysed according to Table 4.6. The spatial distribution of MK trend test applied to CI is given in Figure 5.2, which presents that the majority of the stations show an upward trend where ten stations are categorised as a significant increase. Furthermore, none of the stations show a negative trend. The CI trend results indicate that the concentration of rainfall increases in Northern Cyprus, which would influence the frequency of extreme rainfall events and consequently flash floods and even drought events.

5.1.2 Monthly and Seasonal Rainfall Patterns

Each year's monthly total rainfall data over the whole study period are used and averaged to estimate PCI at each station. Results of the averaged PCI for each station are given in Table 5.2. PCI values range between 19.55 and 23.74 whose spatial distribution is illustrated in Figure 5.3. The majority of the stations fall under the strongly concentrated rainfall class. The eastern part of the study area that includes

Karpass Peninsula and East Coast regions show the most concentrated monthly rainfall patterns. In contrast, the relatively lowest values dominate the south-western part of the study area, which are Central and West Mesaoria Plain regions, as shown in Figure 5.3.

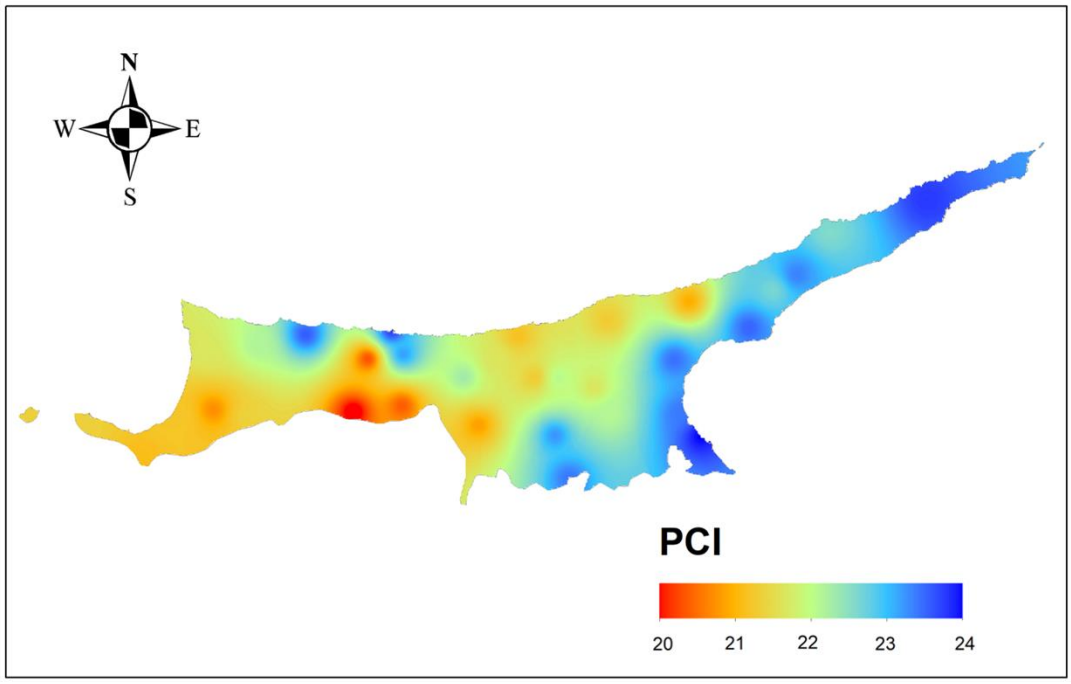

Figure 5.3. Spatial distribution of the average PCI values in Northern Cyprus for a period of 1978 – 2014

Additionally, SI is calculated for each year using the monthly data and averaged over the study period for each station. The spatial distribution of SI is presented in Figure 5.4.

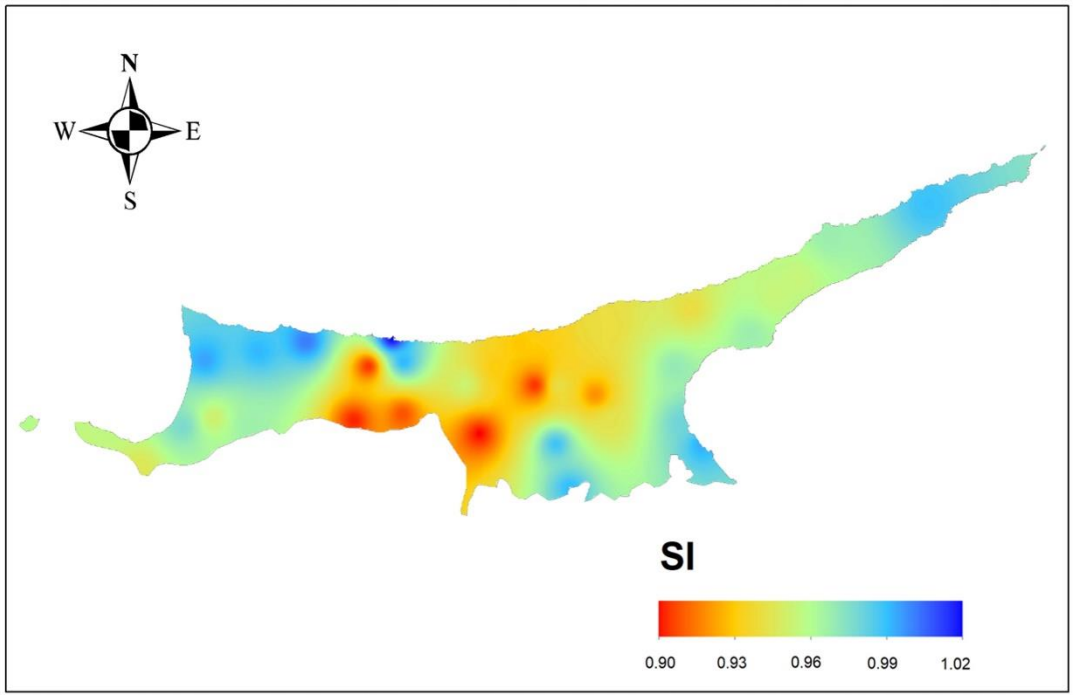

Figure 5.4. Spatial distribution of the average SI values in Northern Cyprus for a period of 1978 – 2014

SI values range between 0.90 and 1.01, which show that the seasonality is spatially homogeneous across the study area. All the stations except Girne station are in the range that concludes significantly seasonal with a long dry season, and the lowest values for SI are located in the centre of the study area. The numerical values of SI are presented in Table 5.2.

Annual PCI and SI values calculated for the 33 stations are tested for possible temporal trends over the study period using the MK trend test. The results suggest that there is no statistically significant upward or downward trend across the study area.

Table 5.2. PCI and SI values with the corresponding station and region

Region	*Station Name*	*PCI*	*SI*
Karpass Peninsula	Cayirova	23.25	0.97
	Dipkarpaz	23.51	0.99
	Mehmetcik	22.35	0.95
	Yenierenkoy	22.28	0.97
	Ziyamet	23.07	0.95
Kyrenia Mountains and North Coast	Alevkaya	21.33	0.93
	Beylerbeyi	22.90	0.99
	Bogaz	20.10	0.91
	Degirmenlik	22.00	0.95
	Kantara	20.62	0.94
	Akdeniz	21.36	0.99
	Camlibel	21.87	0.99
	Esentepe	20.83	0.93
	Girne	23.45	1.02
	Lapta	23.30	1.00
	Tatlisu	20.97	0.94
East Coast	Iskele	23.18	0.97
	Gazimagusa	23.74	0.99
	Salamis	23.14	0.98
East Mesaoria Plain	Beyarmudu	23.14	0.99
	Dortyol	21.81	0.94
	Gecitkale	21.34	0.92
	Gonendere	21.76	0.94
	Serdarli	20.97	0.91
	Vadili	22.96	0.99
Central Mesaoria Plain	Alaykoy	19.66	0.90
	Ercan	20.54	0.90

	Lefkosa	20.15	0.91
West Mesaoria Plain	Gaziveren	20.90	0.97
	Guzelyurt	20.43	0.95
	Lefke	20.77	0.95
	Yesilirmak	21.04	0.95
	Zumrutkoy	21.05	0.97

5.1.3 Annual Rainfall Patterns

Both the shape and scale parameters are calculated for each station using the annual rainfall data, as presented in Table 5.3. Additionally, to illustrate the temporal change in the annual rainfall patterns over the study period, the parameters' values of each station for the subperiods are calculated and tabulated in Table 5.3.

Table 5.3. Values of α and 1/β for each station during different periods

	Over 37 years		*Subperiod 1*		*Subperiod 2*		*Changing of shape parameter α between the two periods*
	1978-2014		*1978-1996*		*1997-2014*		
Station	*α*	*1/β*	*α1*	*1/β1*	*α2*	*1/β2*	
Akdeniz	10.72	35.54	12.39	35.54	9.660	41.02	α1 > α2
Alaykoy	10.76	26.59	15.76	26.59	8.090	35.65	α1 > α2
Alevkaya	13.07	36.57	17.70	36.57	10.80	46.51	α1 > α2
Beyarmudu	8.990	38.01	13.14	38.01	7.690	48.80	α1 > α2
Beylerbeyi	11.54	42.78	15.88	42.78	9.120	55.81	α1 > α2
Bogaz	12.02	33.66	17.24	33.66	9.950	43.50	α1 > α2
Camlibel	10.10	44.91	17.06	44.91	9.570	54.01	α1 > α2
Cayirova	12.47	31.48	15.86	23.18	11.12	37.63	α1 > α2

Degirmenlik	8.580	38.82	10.51	38.82	7.980	45.30	$\alpha1 > \alpha2$
Dipkarpaz	11.22	44.39	11.91	44.39	10.69	47.70	$\alpha1 > \alpha2$
Dortyol	9.361	29.17	11.63	23.62	7.710	35.22	$\alpha1 > \alpha2$
Ercan	11.01	28.49	15.33	28.49	8.990	36.94	$\alpha1 > \alpha2$
Esentepe	8.760	50.56	12.67	50.56	7.270	66.11	$\alpha1 > \alpha2$
Gaziveren	13.99	19.49	17.47	19.49	12.00	23.64	$\alpha1 > \alpha2$
Gecitkale	8.970	36.76	8.970	36.76	9.450	36.81	$\alpha1 < \alpha2$
Girne	10.03	46.87	10.26	46.87	9.810	48.33	$\alpha1 > \alpha2$
Gonendere	10.65	30.43	12.83	30.43	9.510	35.92	$\alpha1 > \alpha2$
Guzelyurt	12.76	22.47	17.40	22.47	10.48	28.74	$\alpha1 > \alpha2$
İskele	10.83	31.38	12.72	31.38	9.470	36.79	$\alpha1 > \alpha2$
Kantara	14.97	37.31	20.54	37.31	11.96	48.29	$\alpha1 > \alpha2$
Lapta	7.640	71.24	8.830	71.24	7.100	81.87	$\alpha1 > \alpha2$
Lefke	12.73	24.56	18.21	24.56	11.03	30.65	$\alpha1 > \alpha2$
Lefkosa	11.25	27.29	19.96	27.29	8.410	39.24	$\alpha1 > \alpha2$
Magusa	12.12	27.64	11.79	27.64	12.68	27.10	$\alpha1 < \alpha2$
Mehmetcik	10.80	38.39	14.33	38.39	9.620	46.60	$\alpha1 > \alpha2$
Salamis	10.18	31.63	10.82	31.63	9.940	30.95	$\alpha1 > \alpha2$
Serdarli	9.790	33.53	13.97	33.53	7.850	44.32	$\alpha1 > \alpha2$
Tatlisu	7.140	66.89	7.550	66.89	8.140	65.49	$\alpha1 < \alpha2$
Vadili	10.08	29.04	9.990	29.04	10.40	29.09	$\alpha1 < \alpha2$
Yeni Erenkoy	12.46	36.42	15.03	36.42	10.65	41.72	$\alpha1 > \alpha2$
Yesilirmak	6.530	55.60	11.69	55.60	4.960	81.15	$\alpha1 > \alpha2$
Ziyamet	12.87	33.48	11.40	33.48	14.93	28.69	$\alpha1 < \alpha2$
Zumrutkoy	12.39	22.99	19.05	22.99	10.97	28.58	$\alpha1 > \alpha2$

Also, the thresholds of dry, normal and rainy day for each station are given in Table 5.4. East, Central and West Mesaoria Plain showed relatively low annual rainfall values under the normal year threshold. In contrast, higher annual rainfall values

categorised as normal year are observed in Karpass Peninsula region. This difference between the two regions is due to the significant variation of rainfall patterns in the study area.

Table 5.4. Annual rainfall thresholds of rainy, normal, and dry year with corresponding station and region

Region	*Station Name*	*Dry year (mm)*	*Normal year (mm)*	*Rainy year (mm)*
Karpass Peninsula	Cayirova	≤310	310-450	≥450
	Dipkarpaz	≤390	390-580	≥580
	Mehmetcik	≤320	320-490	≥490
	Yenierenkoy	≤360	360-530	≥530
	Ziyamet	≤340	340-500	≥500
Kyrenia Mountains and North Coast	Alevkaya	≤220	220- 330	≥330
	Beylerbeyi	≤380	380-580	≥580
	Bogaz	≤320	320-470	≥470
	Degirmenlik	≤250	250-400	≥400
	Kantara	≤450	450-640	≥640
	Akdeniz	≤290	290-450	≥450
	Camlibel	≤340	340-530	≥530
	Esentepe	≤330	330-520	≥520
	Girne	≤360	360-550	≥550
	Lapta	≤400	400-660	≥660
	Tatlisu	≤340	340-580	≥580
East Coast	Iskele	≤260	260-400	≥400
	Gazimagusa	≤260	260-390	≥390
	Salamis	≤240	240-380	≥380
East Mesaoria Plain	Beyarmudu	≤240	240-350	≥350
	Dortyol	210	210-320	320
	Gecitkale	≤240	240-390	≥390

	Gonendere	≤240	240-380	≥380
	Serdarli	≤250	250-380	≥380
	Vadili	≤220	220-340	≥340
Central Mesaoria Plain	Alaykoy	≤220	220- 330	≥330
	Ercan	≤240	240-370	≥370
	Lefkosa	≤240	240-360	≥360
West Mesaoria Plain	Gaziveren	≤210	210-310	≥310
	Guzelyurt	≤230	230-330	≥330
	Lefke	≤250	250-360	≥360
	Yesilirmak	≤250	250-440	≥440
	Zumrutkoy	≤220	220-330	≥330

Additionally, to illustrate the temporal change in the annual rainfall patterns over the study period, the values of shape and scale parameters of each station for the subperiods are calculated and tabulated in Table 5.3. Based on the percentage change of the shape parameter, the stations are classified under three categories, as presented in Table 5.5. Group A includes stations with an increase in α between the first and the second period, group B for the station with an insignificant decrease of α value (less than 30%), and group C representing the stations with a significant decline in α, (higher than 30%). The majority of the stations are categorized under Group C, as shown in Table 5.5.

Table 5.5. Classification of the stations based on the change in the scale parameter

Group A – increase in α		Group B – less than 30% decrease in α		Group C – more than 30% decrease in α	
Station	% change in α	*Station*	% change in α	*Station*	% change in α
Ziyamet	30.9	Girne	-4.42	Gaziveren	-31.2
Tatlisu	7.83	Salamis	-8.11	Mehmetcik	-32.8
Gazimagusa	7.55	Dipkarpaz	-10.2	Dortyol	-33.7
Gecitkale	5.32	Lapta	-19.5	Alevkaya	-39.0
Vadili	4.14	Akdeniz	-22	Lefke	-39.4
		Degirmenlik	-24	Guzelyurt	-39.7
		Iskele	-25.5	Ercan	-41.3
		Gonendere	-25.8	Beyarmudu	-41.5
		Yenierenkoy	-29.1	Kantara	-41.7
				Bogaz	-42.3
				Cayirova	-42.6
				Zumrutkoy	-42.4
				Beylerbeyi	-42.5
				Esentepe	-42.6
				Serdarli	-43.7
				Camlibel	-43.8
				Alaykoy	-48.6
				Yesilirmak	-57.6
				Lefkosa	-57.8

The spatial distribution of the three categories is presented in Figure 5.5, where it is observed that Group C dominates West and Central Mesaoria Plain, most of North Coast and Kyrenia Mountains.

Figure 5.5. Spatial distribution of the stations based on the categories

To demonstrate the difference in temporal change between the three categories, a sample station from each type is shown in Figure 5.6. Gazimagusa station is selected to represent group A with a slight increase in α. It could be observed that there is no noticeable change in the rainfall distribution between the first and the second subperiods, as shown in Figure 5.6-a. Additionally, Akdeniz station is chosen to represent group B. It could be noticed from Figure 5.6-b that the probability of extreme annual events increases in the second subperiod. Finally, Lefkosa station represents group C, as shown in Figure 5.6-c. The increase in the probability of extreme annual rainfall values in the second subperiod in most of the station is linked to the increase in the extreme daily precipitation events due to the upward trends in CI. The majority of the stations having an upward trend in the intensity of daily rainfall events could increase the risk of flash floods in various areas across Northern Cyprus.

The results of gamma analysis are aligned with the results of another study conducted in Southern Cyprus. The study used the same methodology to study the temporal changes in rainfall patterns. The results suggested an increase in the probability of extreme annual rainfall values in the study area (Michaelides et al., 2009).

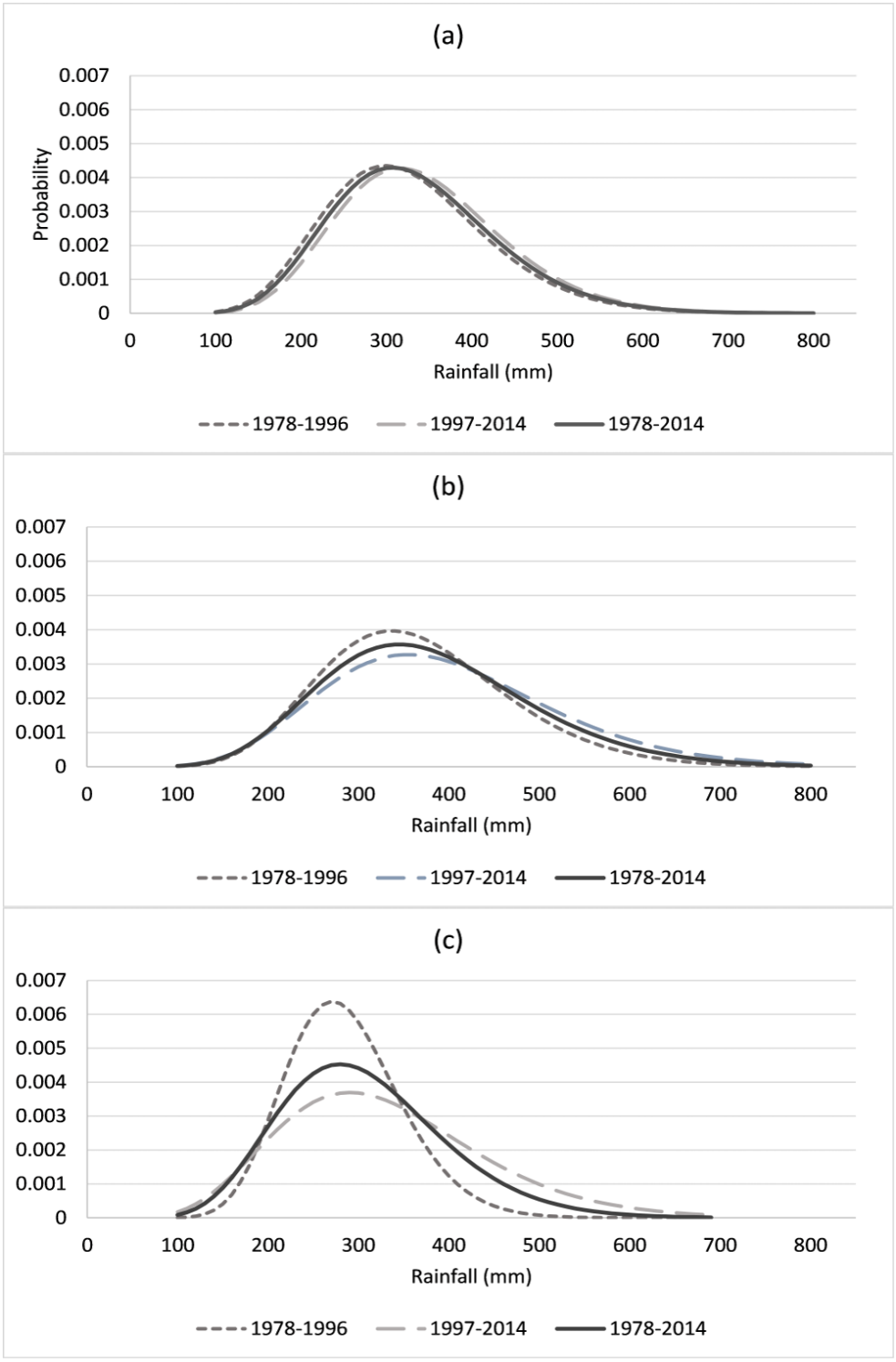

Figure 5.6. Gamma probability density curves for three stations from the three categories; (a) Group A - Gazimagusa, (b) Group B - Akdeniz, (c) Group C - Lefkosa

5.2 Water Balance Analysis

The results of the monthly TM water balance analysis are given in this section. The STC, PET, AET, and water surplus and runoff results for each polygon are given in the following subsections. The 36 years of data is used to obtain the average results.

5.2.1 Soil Moisture Storage Capacity

Using the arithmetic mean of the soil type and the land cover of each station listed in Table 5.6, an STC value of each polygon was determined, as shown in Table 5.7.

Table 5.6. The percentage of each type of land cover for each polygon in the study area

Station	*Land Cover*				
	Open Forest	*Built-up Area*	*High-density Urban areas*	*Moderately Deep-Rooted Crops*	*Empty Sand*
Akdeniz	5.9	0.8	0.1	83.9	9.3
Alaykoy	0.0	1.3	3.7	95.0	0.0
Alevkaya	52.7	0.9	0.0	46.4	0.0
Beyarmudu	0.0	1.9	0.0	98.1	0.0
Beylerbeyi	25.6	21.0	0.0	53.4	0.0
Bogaz	15.1	8.7	0.0	76.2	0.0
Camlibel	23.3	4.7	0.0	72.1	0.0
Cayirova	8.8	2.9	0.0	88.3	0.0
Degirmenlik	8.3	9.1	0.2	82.4	0.0
Dipkarpaz	34.1	2.6	0.0	47.5	15.7
Dortyol	0.0	4.0	0.0	96.0	0.0
Ercan	0.0	3.9	0.0	96.1	0.0
Esentepe	46.0	3.7	0.0	50.3	0.0
Gazimagusa	0.0	0.0	27.2	71.7	1.1

Gaziveren	11.0	4.4	1.0	68.4	15.3
Gecitkale	0.0	4.5	0.9	94.6	0.0
Girne	19.6	11.0	50.2	15.3	3.9
Gonendere	22.1	2.5	0.0	75.4	0.0
Guzelyurt	24.7	2.1	2.4	70.8	0.0
Iskele	0.0	6.8	0.8	92.5	0.0
Kantara	39.7	20.5	0.0	39.9	0.0
Lapta	29.3	23.2	5.5	42.0	0.0
Lefke	6.3	7.0	0.5	86.2	0.0
Lefkosa	0.0	3.0	27.0	70.0	0.0
Mehmetcik	16.5	2.2	0.0	81.3	0.0
Salamis	0.0	17.5	0.6	81.9	0.0
Serdarli	0.0	5.1	0.6	94.3	0.0
Tatlisu	41.6	1.0	0.0	57.4	0.0
Vadili	0.0	3.2	2.0	94.8	0.0
Yenierenkoy	29.2	4.8	0.0	66.0	0.0
Yesilirmak	14.3	0.4	0.0	85.3	0.0
Ziyamet	27.6	5.1	0.0	67.4	0.0
Zumrutkoy	5.8	2.3	0.6	91.3	0.0

As noted in Table 5.7, stations with high-density urban areas like cities have the lowest STC value, Girne station is a case in point. These low values reflect the significance of land cover on the ability of soil to hold water.

Table 5.7. STC values of the polygons with the corresponding station name and polygon area

Station	*STC (mm)*	*Area (km^2)*
Akdeniz	150	119
Alaykoy	158	115
Alevkaya	244	74

Beyarmudu	206	102
Beylerbeyi	180	90
Bogaz	190	86
Camlibel	211	143
Cayirova	199	92
Degirmenlik	218	105
Dipkarpaz	178	168
Dortyol	210	152
Ercan	168	202
Esentepe	257	63
Gazimagusa	172	91
Gaziveren	168	75
Gecitkale	160	115
Girne	114	26
Gonendere	247	68
Guzelyurt	222	86
Iskele	196	117
Kantara	199	126
Lapta	203	75
Lefke	178	64
Lefkosa	136	102
Mehmetcik	210	98
Salamis	160	83
Serdarli	179	83
Tatlisu	237	125
Vadili	152	164
Yenierenkoy	220	120
Yesilirmak	181	36
Ziyamet	202	88
Zumrutkoy	158	96

Northern Cyprus	190	3350

5.2.2 Potential and Actual Evapotranspiration

The annual average PET and the yearly average percentage AET of the precipitation are determined for each polygon using TM over the study period as presented in Table 5.8. Girne area has the lowest percentage of rainfall converted to AET around 76%, and Gonendere polygon has the highest percentage, almost 95%. The average rate of precipitation converted to AET across the study area is 90%.

Table 5.8. PET and AET values of the polygons with the corresponding station name and polygon area

Station	*PET (mm)*	*AET(mm)*	*%AET*
Akdeniz	84.6	322	86.6
Alaykoy	81.6	266	93.7
Alevkaya	84.6	445	91.9
Beyarmudu	82.9	313	92.4
Beylerbeyi	82.3	388	82.7
Bogaz	81.0	341	87.3
Camlibel	76.0	375	86.4
Cayirova	81.6	349	90.7
Degirmenlik	77.0	311	94.6
Dipkarpaz	81.4	387	81.4
Dortyol	83.5	261	92.4
Ercan	84.9	290	93.8
Esentepe	80.4	399	91.6
Gazimagusa	83.5	303	91.8
Gaziveren	76.7	259	94.7
Gecitkale	85.0	303	92.9
Girne	86.0	331	75.8
Gonendere	77.0	306	95.0

Guzelyurt	76.8	272	94.8
Iskele	80.2	313	93.0
Kantara	77.3	438	81.1
Lapta	84.0	408	81.1
Lefke	84.0	293	93.8
Lefkosa	84.1	282	93.3
Mehmetcik	86.5	368	90.8
Salamis	84.8	289	91.6
Serdarli	77.0	307	94.3
Tatlisu	86.7	413	88.3
Vadili	90.1	274	93.7
Yenierenkoy	83.0	392	89.0
Yesilirmak	86.9	316	89.8
Ziyamet	83.0	378	89.8
Zumrutkoy	76.7	266	93.7

The study area receives an average of 1.2 billion m^3 annually, calculated from the average annual rainfall. Around 1 billion of it is lost as annual AET. On average 84% of the yearly precipitation on Cyprus is evaporating as AET.

The spatial distribution of AET percentage is illustrated in Figure 5.7. Where Karpass Peninsula, the North Coast and Kyrenia Mountains shows the lowest percentage of AET. In contrast, the West and Central Mesaoria Plain are dominated by the highest AET percentage. The temporal change of the AET is estimated using MK test. However, no significant trend is found in any of the stations.

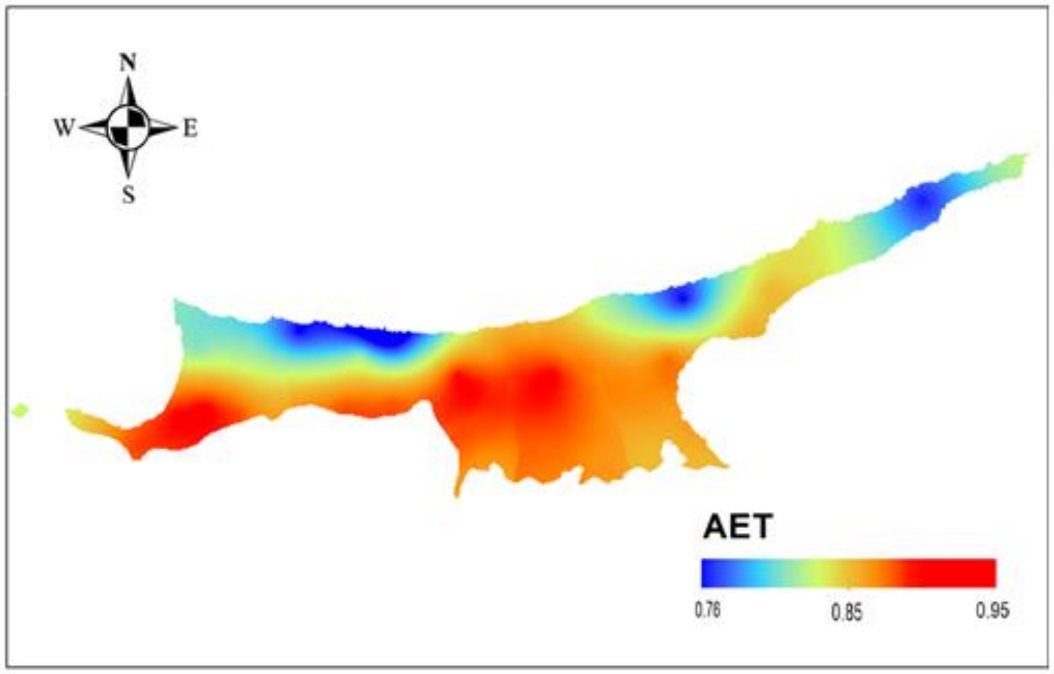

Figure 5.7. Spatial distribution of AET

5.2.3 Water Surplus and Runoff

The average annual RO_{total} depth in mm and the average yearly volume of RO_{total} in m^3 for each station are presented in Table 5.9. Dortyol has the lowest yearly $RO_{total,}$ while Girne has the highest values. Additionally, the maximum and minimum annual RO_{total} evaluated during the study period for each station are given in Table 5.9, which demonstrates the significant variation in RO_{total} from rainfall season to another. Also, the average yearly volume of RO_{total} for each station is calculated using each polygon area and its average RO_{total} value and given in Table 5.9. The average annual RO_{total} volume over the whole study area is estimated as 159.1 million m^3, which stands as 13% of the total rainfall on the study area.

Table 5.9. PET and AET values of the polygons with the corresponding station name and polygon area

Station	*Average* RO_{total} *(mm)*	*Maximum* RO_{total} *(mm)*	*Minimum* RO_{total} *(mm)*	*Average* RO_{total} $(m^3) *10^6$
Akdeniz	60.6	233.2	8.3	7.2
Alaykoy	20.2	128.9	5.5	2.3
Alevkaya	30.6	141.7	8.2	2.3
Beyarmudu	30.4	167.1	8.1	3.1
Beylerbeyi	105.7	371.7	8.5	9.5
Bogaz	60.8	367.3	10.1	5.2
Camlibel	78.2	376.8	9.6	11.2
Cayirova	44.5	234.4	10.1	4.1
Degirmenlik	20.0	81.8	4.1	2.1
Dipkarpaz	112.7	449.8	9.3	18.9
Dortyol	14.5	35.8	5.7	2.2
Ercan	21.6	114.7	4.4	4.4
Esentepe	46.0	215.2	6.8	2.9
Gazimagusa	33.6	220.6	8.3	3.1
Gaziveren	15.8	61.1	6.9	1.2
Gecitkale	26.4	107.4	5.6	3.0
Girne	139.2	477.9	11	3.6
Gonendere	18.2	74.9	5.6	1.2
Guzelyurt	17.2	68.8	6.8	1.5
Iskele	27.6	146.9	7.5	3.2
Kantara	121.8	377.3	14.4	15.4
Lapta	138.2	562.3	11.2	10.4
Lefke	21.5	83.7	8.7	1.4
Lefkosa	23.5	130.4	5.0	2.4
Mehmetcik	47.3	338.3	10.2	4.6
Salamis	33.0	177.9	7.5	2.7

Serdarli	20.4	82.3	4.1	1.7
Tatlisu	69.8	294	9.2	8.7
Vadili	20.4	87.6	6.0	3.3
Yenierenkoy	62.9	333.9	8.4	7.5
Yesilirmak	49.3	203.4	8.5	1.8
Ziyamet	55.1	379.1	10.4	4.8
Zumrutkoy	21.2	148.5	6.7	2.0

Using ArcGIS and the DEM, it was estimated that on average, around 137 million m^3 (85% of the available RO_{total}) water flows towards the sea by 25 main streams annually. The main RO_{total} streams across the study area are shown in Figure 5.8. The main streams are categorised into three classes based on the average annual RO_{total} carried by the stream. The first category includes three streams, each carries an average RO_{total} between 10 to 55 million m^3 presented in blue in Figure 5.8. The second class is the RO_{total} streams with annual average values ranging between 1.5 to 10 million m^3, indicated with the black colour in Figure 5.8. The last group which presented in grey colour in Figure 5.8, includes the streams with average RO_{total} lesser than 1.5 million m^3/year. This classification could be useful for water resources management by the authorities as it could be used in sizing water-holding structures as well as for flash flood mitigation strategies. However, in this study, it has been assumed that no water comes from the southern part of the island, as there are many dams which keep most of the runoff on that side.

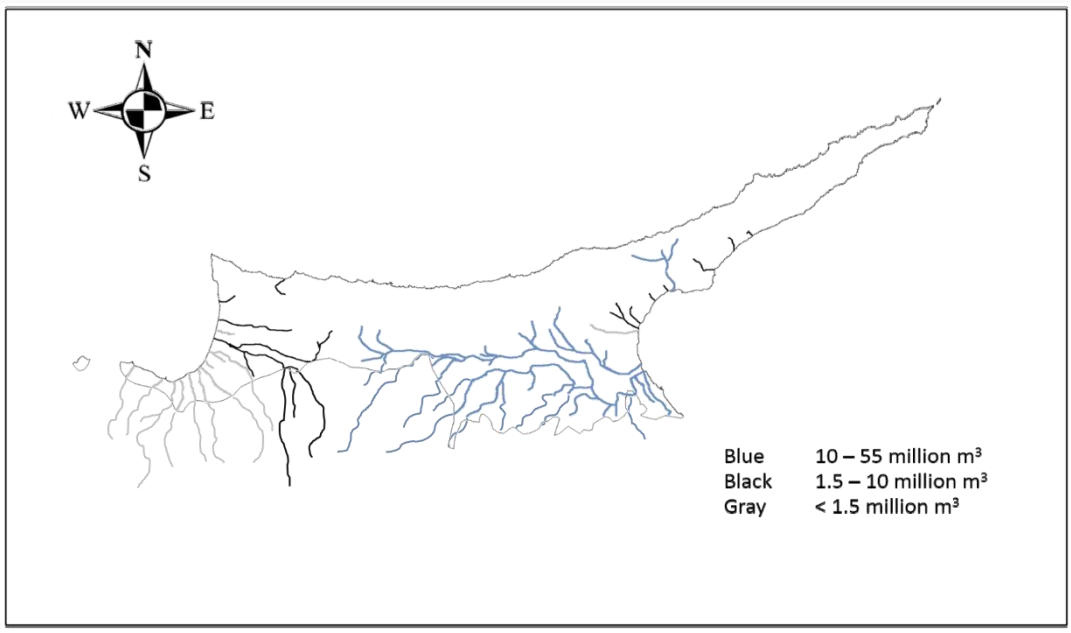

Figure 5.8. Spatial distribution of RO_{total} streams classes based on the discharge volume

MK trend test is applied to the annual RO_{total} values to evaluate the temporal change in its values. However, no significant trend is detected in any of the stations.

The spatial distribution of RO_{total} is presented in Figure 5.9, where the East, Central and West Mesoaria Plain and the East Coast have the lowest values of RO_{total}. On the other hand, The Karpass Peninsula and North Coast and Kyrenia Mountains show significantly higher RO_{total} values.

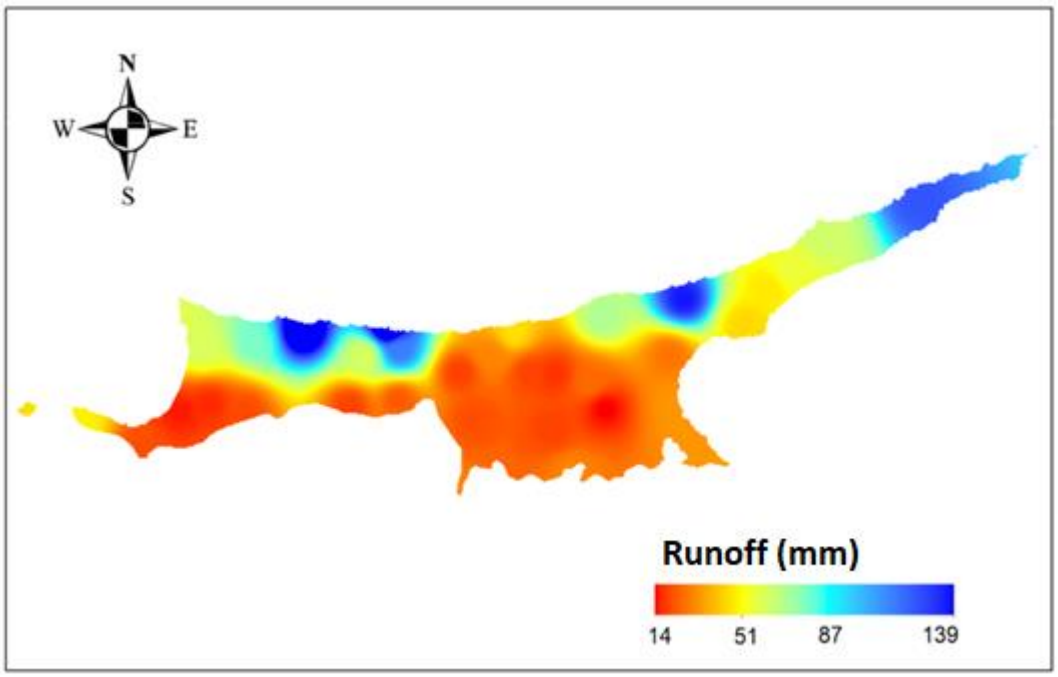

Figure 5.9. Spatial distribution of RO_{total}

The results of the water analysis suggest that more than 137 million m^3 rainfall could be harvested only from the 25 main water streams whose pourpoints are the sea. Additionally, in areas with a significant percentage of a high-density urban area, including the North Coast and Kyrenia region, a small scale domestic rainfall harvesting system or city drainage water collection system would provide a significant amount of water collection. This two option could also play an essential role in mitigating the frequent flash floods in these areas. The average amount of available water for domestic harvesting in the dense urban areas, which stands for more than 20% of the polygon's area, is presented in Table 5.10.

Table 5.10. Average, maximum and minimum annual runoff and available water volume for domestic harvesting in the main cites of Northern Cyprus

Polygon name	*Average annual RO_{total} (mm)*	*Maximum annual RO_{total} (mm)*	*Minimum annual RO_{total} (mm)*	*Dense urban area (km^2)*	*Average annual available water for harvesting (m^3)*
Lefkosa	78.7	247.3	5.2	27.5	2164250
Gazimagusa	120.7	373.7	9.2	25	3017500
Girne	222.4	573.2	28.5	13.1	2913440

It should be noted that in areas with higher average runoff depth like Girne, domestic water harvesting would be more effective. The total annual volume of runoff available for collecting in all of the high-density urban areas is around 8.1 million m^3 on average.

Additionally, the three cities showing an upward trend in CI indicates a possible increase in the runoff amount. Furthermore, Lefkosa and Girne stations exhibit an increase in extreme annual rainfall patterns, emphasising the need for water harvesting systems.

Over the study area, it is evident that the frequency of rainfall extreme events are increasing. This increase would directly impact water resources and consumption and could result in frequent flash floods. However, these effects could be mitigated by collecting the runoff resulting from the extreme events from the main streams as well as in the main cities.

A summary of the water balance is given in Figure 5.10, where 84% of the rainfall is lost as AET each year on average. The remaining 16% is divided into 3%, which stays on the surface depression, and 13%, which is available as runoff. 84.6% of runoff is discharged by the main 25 streams shown in Figure 5.8. On the other hand,

7.6% of runoff is available in the main three cities, while the remaining runoff is available in the rest of the study area.

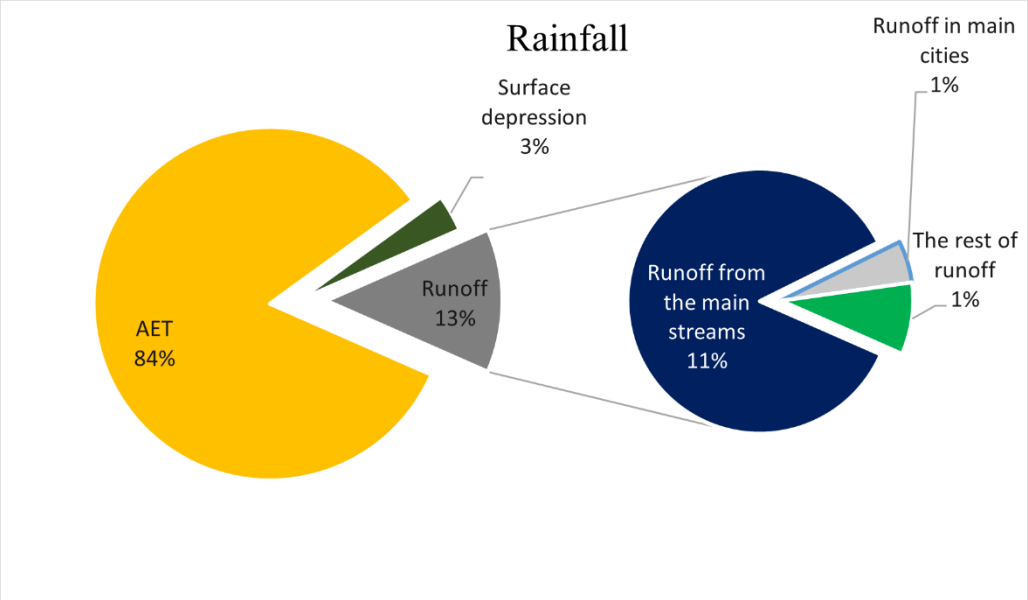

Figure 5.10. Pie chart of the water balance results in the study area

Due to the lack of real data, the TM model could not be compared with measured runoff and calibrated. However, it should be noted that this model has been used in various countries and climates and showed acceptable accuracy when compared with measured data.

From Table 5.9 and Table 5.10, a significant variation in the annual runoff values could be observed. Hence, there is a need for a climate independent source of potable water. In the following section, the technical aspect of RO seawater desalination plant as an alternative and reliable source of drinking water is investigated.

5.3 Seawater Desalination

The first step in the seawater desalination is the pretreatment, where a combination of conventional pretreatment UF systems is used. In the UF system, the number of the train is 40. Train refers to the structure that contains a specific number of pressure vessels (PV) combined with a pump. Each train has 200 modules. The total number

of modules is 8000. The system flux is 97 $m^3/m^2/day$. The UF system recovery is 92.2%.

Various RO system configurations are analysed to find the optimum design, starting with a one-pass and three stages RO system. This RO system could not effectively produce a permeate with accepted boron concentration. The schematic diagram of the suggested design is demonstrated in Figure 5.11.

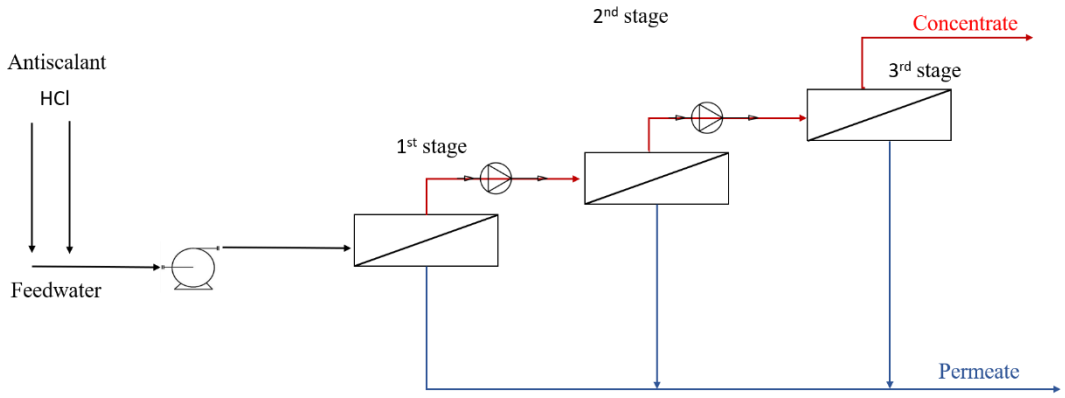

Figure 5.11. One pass three stages RO schematic diagram

The system shown in Figure 5.11 achieves 49% recovery. However, the boron concentration stays higher than 1.5 mg/L in the permeate. Also, TDS concentration in the produced water is higher than 700 mg/L. This system consumes a specific energy of 3.92 kW/m^3.

Adding a partial second pass to the system, as shown in Figure 5.11, was investigated to control both the TDS and boron concentration. In this design, 40% of the permeate from the first pass is further desalinated using the second pass. The second pass' feedwater pH is increased to enhance boron removal, as shown in Figure 5.12.

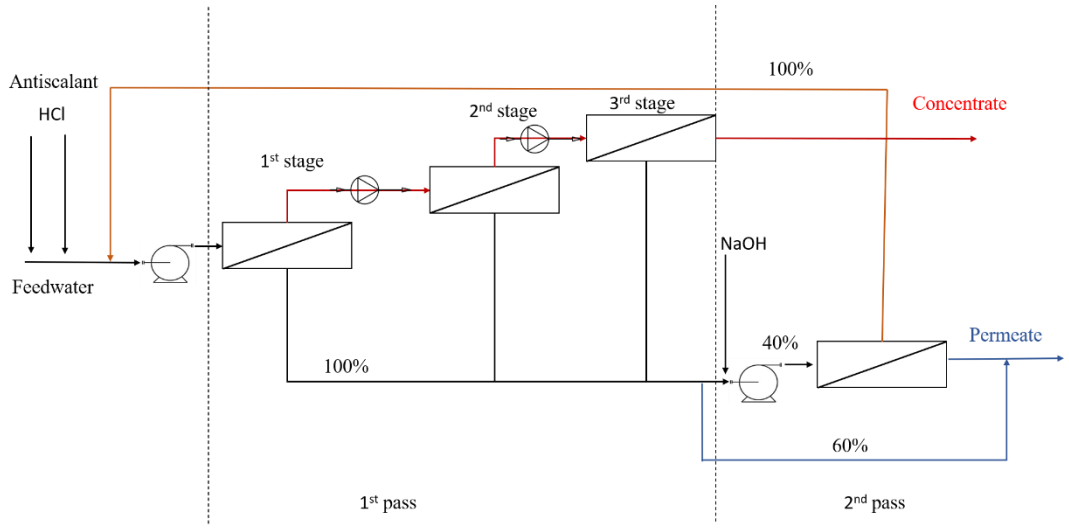

Figure 5.12. Two passes three stages RO schematic diagram

In this case, the system recovery decreased to 47.1%. The TDS concentration in the permeate of this system is around 450 mg/L, and the boron concentration remains less than 1 mg/L. On the other hand, specific energy consumption increases to 4.36 kW/m in this system.

The third stage is removed to decrease energy consumption, as shown in Figure 5.13. In this system, the first-pass has two stages that aim to increase the system's recovery. The first pass contains ten trains. Each train consists of 220 PV as the first stage and 110 PV as the second stage, in which each PV has 7 RO modules. The used RO module is SEAMAXX-440™.

A booster pump is introduced between the two stages to increase the permeate production from the second stage. The pressure of the feedwater in between first and second stages is increased by 14 bar. In this design, an extra train is available. This additional train will sustain the plant production in case of any emergency or during the maintenance.

25% of the permeate of the first pass is desalinated further in the second pass, where 75% of the first pass's permeate is bypassed to the final product directly. The configuration is used to ensure producing the required water quality with a minimum amount of energy. The concentrate of the second pass has TDS value lower than the

seawater. Therefore, it is blended with the feedwater, as shown in Figure 5.13. Additionally, sodium hydroxide is added to the feed of the second pass to increase its pH and improve the boron rejection, as illustrated in Figure 5.13.

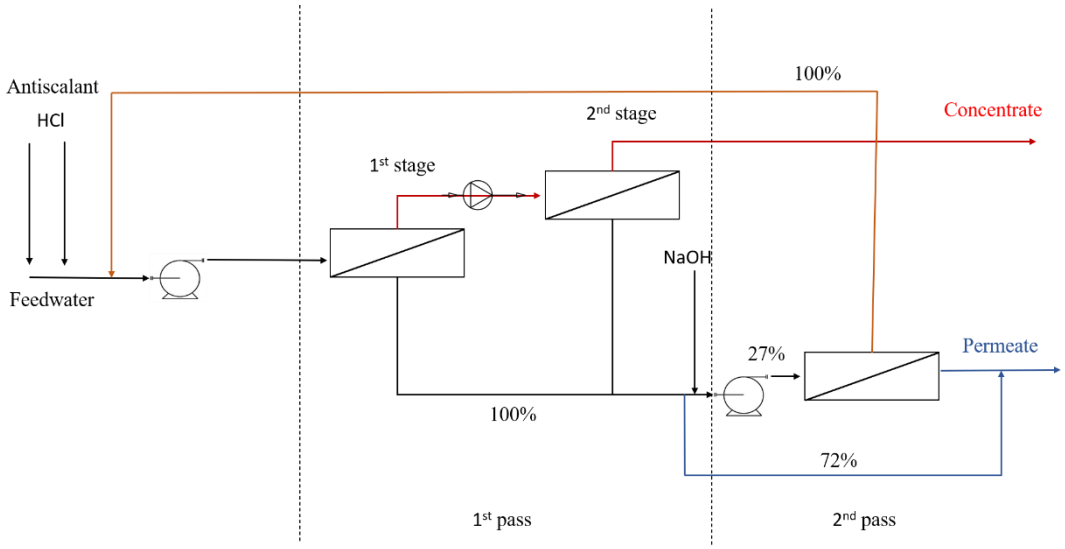

Figure 5.13. Two-pass two stages RO schematic diagram

The second pass is consist of two trains, containing 110 PV. Each PV contains 7 modules. The feedwater of the second pass includes a low concentration of TDS. Therefore, brackish water RO modules are used in this pass whose name is BW30HRLE-440™. The details of the system design and configuration are given in Table 5.11.

Table 5.11. System configurations details

Configuration	*1st pass*		*2nd Pass*
	1st stage	*2nd stage*	
Number of trains	10		2
Number of PV per train	220	110	110
Number of modules per PV	7	7	7
Feed flow rate per train (m^3/h)	2100	2790	2464
Working pressure (bar)	43.5	56	9.8
Recovery	47.0%		82.0%
Specific energy consumption (kwh/m^3)	3.91		0.42
Recycling from the concentrate to the feed	0.0		100%
From the pass permeate directly to the final product	72%		100%

The system flow diagram is demonstrated in Figure 5.14, where nine data points on the streamlines are shown in the diagram.

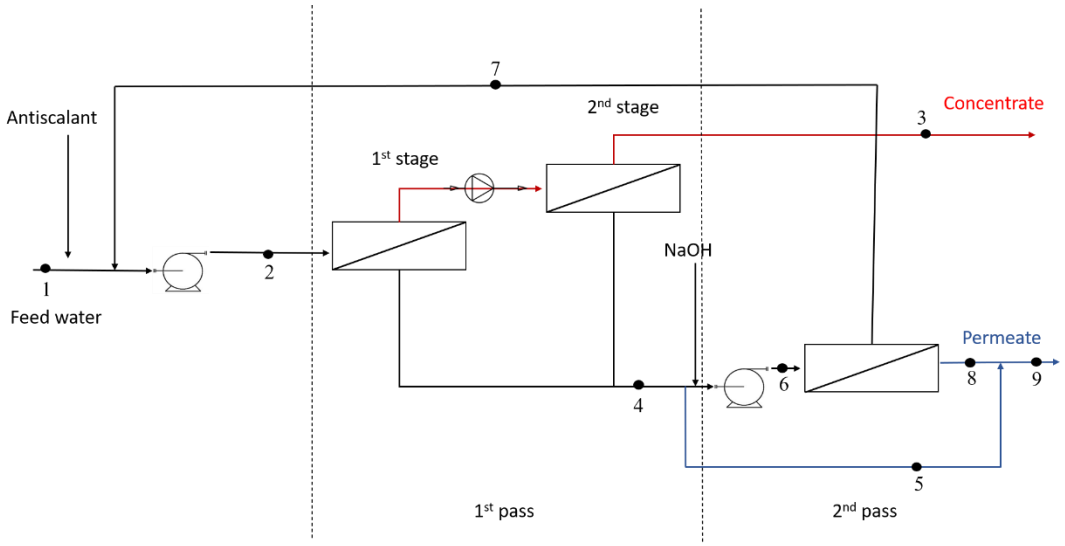

Figure 5.14. The RO system flow diagram

The flowrate, TDS concentration and working pressure for each one of the nine points is given in Table 5.12. The overall recovery of the system is 45.6%.

Table 5.12. Flow rate, TDS and pressure for the nine points in the RO system

Point number	*Flow rate (m^3/h)*	*TDS (mg/L)*	*Pressure (bar)*
1	20653	39626	1
2	20989	38907	43.8
3	11204	72758	53.2
4	9922	626	1
5	7144	626	1
6	2776	1167	9.8
7	500	6376	8.1
8	2277	22.97	1
9	9421	480.2	1

The RO system's overall specific energy is 4.21 kW/m^3. However, the system produces the maximum concentrate of 11204 m^3/h at 53.2 bar; the concentrate holds 107.5 MW which is a considerable amount of energy. The concentration carries 0.41% of the energy consumed by the RO system. However, this is the theoretical content of energy. The actual recovered energy would be lesser due to the used ERD efficiency.

Furthermore, the concentrate needs to preserve energy for the discharging process. By using Equation (4.36), the consumed energy is determined. Moreover, the energy recovery percentage could be estimated using Equation (4.35) in which the concentrate pressure and flow rate are read from Table 5.12, and the ERD efficiency is assumed to be 90%. The concentrate is discharged with two bar pressure to ensure enough pressure to transfer the concentrate without an additional pump after energy recovery.

The recovered energy using ERD from the concentrate stands for 0.37% of the consumed energy by the RO system. Therefore, the specific energy consumed by the RO system after utilising the ERD system is 2.65 kW/m^3.

Boron concentration in the permeate of the first pass is 1.39 mg/L. On the other hand, the second pass produces a very low boron concentration which is 0.11 mg/L. Therefore, the final product contains 0.97 mg/L of boron.

As presented in Table 5.12, the final product TDS concentration is 480 mg/L which is the blended permeate of the second pass with 23 mg/L TDS, and 72% of the first pass permeate with 861 mg/L TDS.

Table 5.13 shows the first pass's permeate quality, including both stages, second pass, and the final permeate. By comparing Table 5.13 with Table 4.7, the produced water from the first pass has a higher concentration than the accepted quality guidelines. However, the final permeate after mixing the first and the second-passes' permeate complies with the guidelines. The pH of the final permeate is higher than the guidelines. However, during the post-treatment and the injection of carbon dioxide, the pH value will be adjusted for human use. LSI value of the final permeate is equal to -3.0. The negative value of the permeate indicates significant corrosive water that could cause substantial damage in the pipelines network. However, by adding 49 mg of hydrated lime per each litre of permeate water and dissolving 120 mg of carbon dioxide per litre of water, LSI value of 0.18 could be achieved. This will ensure safe water distribution and use.

Finally, chlorine could be used as water disinfectant before the distribution. The suggested concentration of chlorine by the WHO for water intended for drinking is between 2 and 3 mg/L. Chlorine and water contact time must be more than 30 minutes (WHO, 2004).

Table 5.13. Quality of the produced water

Water quality parameter	*Permeate from the 1st Pass*		*Permeate from the 2nd pass*	*Final permeate*
	1st stage	*2nd stage*		
pH	8.1	8.2	9	8.2
Ca^{2+} (mg/L)	1.56	2.67	0.02	1.48
Mg^{2+} (mg/L)	5.42	8.74	0.05	4.85
Na^{+} (mg/L)	189.1	306.5	8.55	171
K^{+} (mg/L)	8.66	14.1	0.3	7.82
CO_3^{2-} (mg/L)	0.03	0.05	0.01	0.03
HCO_3^{-} (mg/L)	2.22	3.53	0.01	0.03
SO_4^{2-} (mg/L)	4.63	7.43	0.07	4.13
Cl^{-} (mg/L)	313	507.4	12.99	282.7
F^{-} (mg/L)	0.03	0.06	0.00	0.03
Boron (mg/L)	1.24	1.79	0.11	0.97
TDS (mg/L)	531.9	860.7	22.97	480

The economic analysis for the RO water desalination in Northern Cyprus has been conducted in various studies. The cost of water production depends on energy prices. In all of the analysis, it is found that government subsidies are needed for a competitive price. In literature, the cost of water desalination ranged between 2.2 $/m^3 and 2.1 $/m^3 (Abbasighadi, 2013). This is significantly higher than the cost of water coming from Turkey at 0.9 $/m^3 (Oner, 2019). Nevertheless, it would be a sustainable and more reliable solution for long term water resources management. Moreover, it could be a backup solution in case of extreme drought or main failure in the pipeline system coming from Turkey. Furthermore, as could be noted from the previous section, relying only on rainfall is not possible for Northern Cyprus due to the significant variation of annual rainfall.

The detailed quality of the concentrate produced from each stage and pass is listed in Table 5.14. This data would help the authorities on deciding the best concentrate treatment choice.

Table 5.14. Quality of the concentrate from each stage and pass

Water quality parameter	*1st pass*		*Concentrate from the 2nd pass*
	Concentrate from the 1st stage	*Concentrate from the 2nd stage*	
pH	8.8	8.8	12.7
Ca^{2+} (mg/L)	693.3	868.4	10.74
Mg^{2+} (mg/L)	2250	2819	35.16
Na^{+} (mg/L)	17643	22038	2934
K^{+} (mg/L)	691.4	863.1	55.42
CO_3^{2-} (mg/L)	122.5	153.5	0
HCO_3^{-} (mg/L)	138.5	172.7	0.01
SO_4^{2-} (mg/L)	4770	5978	29.86
Cl^{-} (mg/L)	31865	39815	1989
F^{-} (mg/L)	2.51	3.13	0.22
Boron (mg/L)	6.97	8.29	7.25
TDS (mg/L)	58215	72758	6376

To achieve 45000 mg/L TDS concentration in the concentrate before discharging it to the sea, a significant amount of treated used water, around 7000 m^3/h is required. Therefore, the authorities might consider salt extraction as a more sustainable solution.

Cyprus is an island; therefore, there are various choices for water desalination plant location. However, a ready infrastructure including water treatment plant, storage area and pumping station is available as a part of the water pipeline project in

Gecitkoy. Hence, the area of Gecitkoy shown in Figure 5.15 could be the optimum option for the seawater desalination plant.

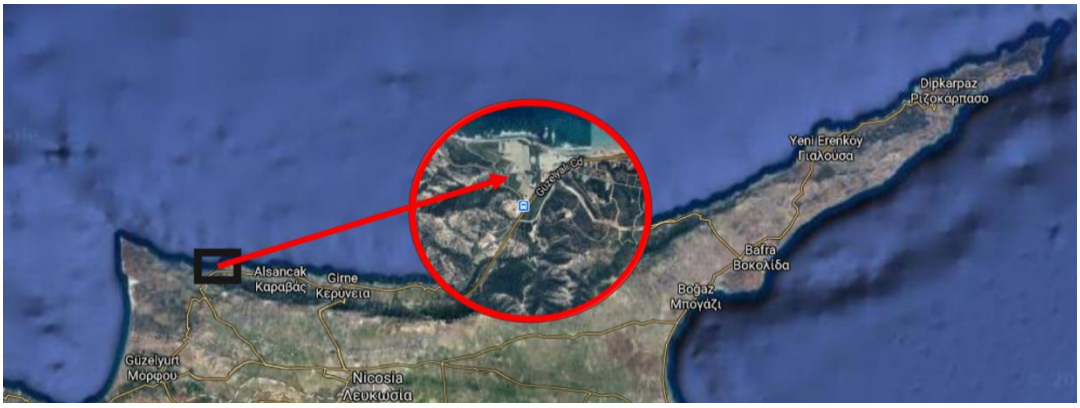

Figure 5.15. Suggested location for the seawater desalination plants in Northern Cyprus

CHAPTER 6

CONCLUSION

This study aims to provide the authorities with significant data for sustainable water resources management to sustain the remaining water reservoirs from seawater intrusion, by analysing various water balance components. Moreover, a design of Reverse Osmosis seawater desalination system is provided as an alternative reliable and sustainable choice for potable water production in Northern Cyprus, as the current water budget could collapse in the case of long term drought in the region or a significant failure in the pipeline system from Turkey. Thirty-six hydrological years of rainfall and temperature data between 1978 and 2015 collected in 33 meteorological stations distributed across Northern Cyprus is used in this study.

The spatial distribution of Northern Cyprus daily, monthly, seasonal, and yearly rainfall patterns are analysed using Concentration Index, Precipitation Concentration Index, Seasonality Index, and Gamma distribution. West and East Mesaoria Plane and the North Coast were found to have a relatively more spread distribution of daily rainfall than the rest of the study area. However, regarding the seasonal and monthly rainfall characteristics, the whole study area shows significant seasonal patterns where most of the precipitation occurs in a limited number of months. This pattern is observed relatively more substantial in the East Coast, Karpass Peninsula and parts of the North Coast. Additionally, the probability density function is calculated for each station using Gamma distribution. The results are used to study the annual rainfall patterns in the study area and to identify the thresholds for a dry, normal and rainy year for each station.

Furthermore, temporal changes in rainfall patterns across the study area are studied. The seasonal rainfall patterns do not show any significant trend during the study

period between 1978 and 2015. However, the annual rainfall patterns indicate an increase of the probability of extreme yearly precipitation across Northern Cyprus. This increase is explained by the rise in the daily rainfall concentration observed in the majority of the stations, where most of the annual rainfall is observed in a limited number of days.

Moreover, the rainfall and the temperature data are used to estimate the water balance components, including Potential Evapotranspiration, Actual Evapotranspiration, Surplus and runoff using Thornthwaite and Mather monthly water balance analysis. The spatial distribution of each element is evaluated and given in this study. The results showed that West, East and Central Mesaoria Plain and East Coast observed the highest Actual Evapotranspiration percentage. Also, it is found that the majority of the precipitation over the study area is lost due to Actual Evapotranspiration, as it stands for 84% of the total received rainfall on average. The remaining is the Surplus, where the significant amount of it becomes runoff. Around 85% of the runoff is concentrated in 25 main water streams. Moreover, the possibility of rainwater harvesting is estimated in dense urban areas. The results showed that 7.6% of the runoff could be harvested in the three main cities.

On the other hand, the result showed a considerable variation in precipitation, hence the available runoff for collecting. Therefore, a design of Reverse Osmosis seawater desalination is given as a sustainable, climate-independent and reliable source of potable water. The energy consumption and the permeate water quality are the primary consideration in the design. Using Energy Recovery Devices, specific energy consumption is reduced. WHO drinking water guidelines are followed. Additionally, solutions for the produced concentrate are suggested.

The optimum Reverse Osmosis system configuration is found to be a partial two-pass system, where the first pass consists of two stages. 28% of the first pass permeate is desalinated further to ensure meeting the drinking water guidelines. Total of twelve trains are used in the design, ten of which are used for the first-pass and two for the second pass. Moreover, an optimum location for the water desalination

plant is suggested. Also, a suitable pretreatment and posttreatment are suggested to ensure a steady operation and high-quality production.

Detailed studies for each district in Northern Cyprus could offer more information that could help the water resources authorities. A weekly or daily water balance analysis could also provide more insight into the effect of the temporal changes on the daily rainfall patterns in Northern Cyprus. Furthermore, there is a lack of work on water harvesting capacity optimisation for the study area and similar water-scarce Mediterranean regions. Finally, more data should be collected in the various possible seawater intake locations for the Reverse Osmosis desalination for a long period to specify the optimum location.

REFERENCES

Abbasighadi, A. (2013). *A Cost-Benefit Analysis of a Reverse Osmosis Desalination Plant with and without Advanced Energy Recovery Devices*. Retrieved from http://i-rep.emu.edu.tr:8080/xmlui/handle/11129/3279

Al-Karaghouli, A., & Kazmerski, L. L. (2013, August 1). Energy consumption and water production cost of conventional and renewable-energy-powered desalination processes. *Renewable and Sustainable Energy Reviews*. Elsevier Ltd. https://doi.org/10.1016/j.rser.2012.12.064

Al-Mutaz, I. S., & Al-Ghunaimi, M. A. (2001). *Performance of Reverse Osmosis Units at High Temperatures*.

Anwar, Sembiring, A., & Irawan, A. P. (2020). Analysis of the potential of crust formation and corrosiveness in the Way Rilau PDAM lampung distribution network using the langelier saturation index method. In *IOP Conference Series: Materials Science and Engineering* (Vol. 852, p. 012040). Institute of Physics Publishing. https://doi.org/10.1088/1757-899X/852/1/012040

Arslan, B., & Akün, E. (2019). Management, contamination and quality evaluation of groundwater in North Cyprus. *Agricultural Water Management*, *222*, 1–11. https://doi.org/10.1016/j.agwat.2019.05.023

Axelsson, G., & Stefánsson, V. (2003). *Sustainable management of geothermal resources*. *International Geothermal Conference*. Retrieved from http://www.jardhitafelag.is/media/pdf/s12paper075.pdf

Berezovskaya, S., Yang, D., & Hinzman, L. (2005). Long-term annual water balance analysis of the Lena River. *Global and Planetary Change*, *48*(1-3 SPEC. ISS.), 84–95. https://doi.org/10.1016/j.gloplacha.2004.12.006

Bhattarai, N., Dougherty, M., Marzen, L. J., & Kalin, L. (2012). Validation of evaporation estimates from a modified surface energy balance algorithm for land (SEBAL) model in the south-eastern United States. *Remote Sensing Letters*, *3*(6), 511–519. https://doi.org/10.1080/01431161.2011.632655

Boulet, G., Chehbouni, A., Braud, I., Vauclin, M., Haverkamp, R., & Zammit, C. (2000). A simple water and energy balance model designed for regionalization and remote sensing data utilization. In *Agricultural and Forest Meteorology* (Vol. 105, pp. 117–132). Elsevier. https://doi.org/10.1016/S0168-1923(00)00184-2

Cakal, S. (2016). *Palmer Drought Analysis of North Cyprus*. Middle East Technical University, Northern Cyprus Campus. Retrieved from http://etd.lib.metu.edu.tr

Chowdhury, R. K., & Beecham, S. (2009). Australian rainfall trends and their

relation to the southern oscillation index. *Hydrological Processes*, *24*(4), n/a-n/a. https://doi.org/10.1002/hyp.7504

Coscarelli, R., & Caloiero, T. (2012). Analysis of daily and monthly rainfall concentration in Southern Italy (Calabria region). *Journal of Hydrology*, *416–417*, 145–156. https://doi.org/10.1016/J.JHYDROL.2011.11.047

Darre, N. C., & Toor, G. S. (2018, June 1). Desalination of Water: a Review. *Current Pollution Reports*. Springer. https://doi.org/10.1007/s40726-018-0085-9

Davis, T. A. (2006). Production of purified water and high value chemicals from salt water. *US Patent*.

De Luís, M., Raventós, J., González-Hidalgo, J. C., Sánchez, J. R., & Cortina, J. (2000). Spatial analysis of rainfall trends in the region of valencia (East Spain). *International Journal of Climatology*, *20*(12), 1451–1469. https://doi.org/10.1002/1097-0088(200010)20:12<1451::AID-JOC547>3.0.CO;2-0

Deng, S., Chen, T., Yang, N., Qu, L., Li, M., & Chen, D. (2018). Spatial and temporal distribution of rainfall and drought characteristics across the Pearl River basin. *Science of The Total Environment*, *619–620*, 28–41. https://doi.org/10.1016/J.SCITOTENV.2017.10.339

Derici, M., Kapur, S., Kaya, Z., Gök, M., & Ortas, İ. (2000). Kuzey Kıbrıs Türk Cumhuriyeti detaylı toprak etüd ve haritalama projesi.

Easterling, D. R., Evans, J. L., Groisman, P. Y., Karl, T. R., Kunkel, K. E., & Ambenje, P. (2000). Observed Variability and Trends in Extreme Climate Events: A Brief Review *. *Bulletin of the American Meteorological Society*, *81*(3), 417–425. https://doi.org/10.1175/1520-0477(2000)081<0417:OVATIE>2.3.CO;2

Edzwald, J. K. (2010, April 1). Dissolved air flotation and me. *Water Research*. Elsevier Ltd. https://doi.org/10.1016/j.watres.2009.12.040

Ekin, M. (2016). *Experimental Investigation of an Inclined Combined Solar Hot Water and Desalination System*. Eastern Mediterranean University (EMU) - Doğu Akdeniz Üniversitesi (DAÜ). Retrieved from http://i-rep.emu.edu.tr:8080/xmlui/handle/11129/2843

Elkiran, G., Aslanova, F., & Hiziroglu, S. (2019). Effluent Water Reuse Possibilities in Northern Cyprus. *Water*, *11*(2), 191. https://doi.org/10.3390/w11020191

Ergil, M. E. (2000). The salination problem of the Guzelyurt aquifer, Cyprus. *Water Research*, *34*(4), 1201–1214. https://doi.org/10.1016/S0043-1354(99)00253-5

Ettouney, H., & Wilf, M. (2009). Conventional Thermal Process. In A. Cipollina, G. Micale, & L. Rizzuti (Eds.), *Seawater Desalination: Conventional and Renewable Energy Processes* (p. 306). Springer Science & Business Media.

https://doi.org/10.1007/978-3-642-01150-4

Fustos, I., Abarca-Del-Rio, · R, Moreno-Yaeger, · P, & Somos-Valenzuela, · M. (2020). Rainfall-Induced Landslides forecast using local precipitation and global climate indexes. *Natural Hazards*, *102*, 115–131. https://doi.org/10.1007/s11069-020-03913-0

Fylaktos, N., Mitra, I., Tzamtzis, G., & Papanicolas, C. N. (2015). Economic analysis of an electricity and desalinated water cogeneration plant in Cyprus. *Desalination and Water Treatment*, *55*(9), 2453–2470. https://doi.org/10.1080/19443994.2014.940219

Gasia-Bruch, E., Sehn, P., García-Molina, V., Busch, M., Raize, O., & Negrin, M. (2011). Field experience with a 20,000 m3/d integrated membrane seawater desalination plant in cyprus. *Desalination and Water Treatment*, *31*(1–3), 178–189. https://doi.org/10.5004/dwt.2011.2381

Ghaffour, N., Missimer, T. M., & Amy, G. L. (2013). Technical review and evaluation of the economics of water desalination: Current and future challenges for better water supply sustainability. *Desalination*, *309*, 197–207. https://doi.org/10.1016/j.desal.2012.10.015

Ghandhari, A., & Alavi Moghaddam, S. M. R. (2011). Water balance principles: A review of studies on five watersheds in Iran. *Journal of Environmental Science and Technology*, *4*(5), 465–479. https://doi.org/10.3923/jest.2011.465.479

Gude, V. G. (2017). Desalination and water reuse to address global water scarcity. *Reviews in Environmental Science and Biotechnology*. Springer Netherlands. https://doi.org/10.1007/s11157-017-9449-7

Gude, V. G. (2018a). *Renewable Energy Powered Desalination Handbook: Application and Thermodynamics*. *Renewable Energy Powered Desalination Handbook: Application and Thermodynamics*. Elsevier Inc. https://doi.org/10.1016/C2017-0-02851-3

Gude, V. G. (2018b). *Sustainable Desalination Handbook: Plant Selection, Design and Implementation*. *Sustainable Desalination Handbook: Plant Selection, Design and Implementation*. Elsevier. https://doi.org/10.1016/C2015-0-04758-X

Guhathakurta, P., & Saji, E. (2013). Detecting changes in rainfall pattern and seasonality index vis-` a-vis increasing water scarcity in Maharashtra. *Springer*. Retrieved from https://idp.springer.com

Harb, R. (2015). *Assessing the potential of rainwater harvesting system at the Middle East Technical University–Northern Cyprus campus*. *etd.lib.metu.edu.tr*. Retrieved from http://etd.lib.metu.edu.tr/upload/12619225/index.pdf

Huang, B., Pu, K., Wu, P., Wu, D., & Leng, J. (2020). Design, Selection and Application of Energy Recovery Device in Seawater Desalination: A Review.

Energies, *13*(16), 4150. https://doi.org/10.3390/en13164150

Husak, G. J., Michaelsen, J., & Funk, C. (2007). Use of the gamma distribution to represent monthly rainfall in Africa for drought monitoring applications. *International Journal of Climatology*, *27*(7), 935–944. https://doi.org/10.1002/joc.1441

Isidoro, D., Quílez, D., & Aragüés, R. (2004). Water balance and irrigation performance analysis: La Violada irrigation district (Spain) as a case study. *Agricultural Water Management*, *64*(2), 123–142. https://doi.org/10.1016/S0378-3774(03)00196-3

Ison, N. T., Feyerherm, A. M., Bark, L. D., Ison, N. T., Feyerherm, A. M., & Bark, L. D. (1971). Wet Period Precipitation and the Gamma Distribution. *Journal of Applied Meteorology*, *10*(4), 658–665. https://doi.org/10.1175/1520-0450(1971)010<0658:WPPATG>2.0.CO;2

IUCN, UNEP, F. (2000). Council Directive 75/440/EEC concerning the quality required of surface water intended for the abstraction of drinking water in the Member States. Retrieved October 16, 2019, from https://www.ecolex.org/details/legislation/council-directive-75440eec-concerning-the-quality-required-of-surface-water-intended-for-the-abstraction-of-drinking-water-in-the-member-states-lex-faoc019244/

Jasrotia, A. S., Majhi, A., & Singh, S. (2009). Water balance approach for rainwater harvesting using remote sensing and GIS techniques, Jammu Himalaya, India. *Water Resources Management*, *23*(14), 3035–3055. https://doi.org/10.1007/s11269-009-9422-5

Jones, E., Qadir, M., van Vliet, M. T. H., Smakhtin, V., & Kang, S. mu. (2019, March 20). The state of desalination and brine production: A global outlook. *Science of the Total Environment*. Elsevier B.V. https://doi.org/10.1016/j.scitotenv.2018.12.076

Kalogirou, S. (1997). Economic analysis of a solar assisted desalination system. *Renewable Energy*, *12*(4), 351–367. https://doi.org/10.1016/S0960-1481(97)00063-3

Kalogirou, S. (1998). Use of parabolic trough solar energy collectors for sea-water desalination. *Applied Energy*, *60*(2), 65–88. https://doi.org/10.1016/S0306-2619(98)00018-X

Kalogirou, S. A. (2001). Effect of fuel cost on the price of desalination water: A case for renewables. *Desalination*, *138*(1–3), 137–144. https://doi.org/10.1016/S0011-9164(01)00255-7

Kampata, J. M., Parida, B. P., & Moalafhi, D. B. (2008). Trend analysis of rainfall in the headstreams of the Zambezi River Basin in Zambia. *Physics and Chemistry of the Earth*, *33*(8–13), 621–625.

https://doi.org/10.1016/j.pce.2008.06.012

Kanellopoulou, E. A. (2002). Spatial distribution of rainfall seasonality in Greece. *Weather*, *57*(6), 215–219. https://doi.org/10.1256/004316502760053576

Karl, T. (1998). Secular trends of precipitation amount, frequency, and intensity in the United States. *Journals.Ametsoc.Org*. Retrieved from https://journals.ametsoc.org/bams/article/79/2/231/55906

Katz, R. W., & Brown, B. G. (1992). Extreme events in a changing climate: Variability is more important than averages. *Climatic Change*, *21*(3), 289–302. https://doi.org/10.1007/BF00139728

Kendall, A. M. (2015). The Kendall Package. *Http://Www Uni-Bayreuth.De*.

Kenway, S., Gregory, A., & McMahon, J. (2011). Urban Water Mass Balance Analysis. *Journal of Industrial Ecology*, *15*(5), 693–706. https://doi.org/10.1111/j.1530-9290.2011.00357.x

Khalaf, S., Al-Rimawi, F., Khamis, M., Nir, S., Bufo, S. A., Scrano, L., … Karaman, R. (2013). Efficiency of membrane technology, activated charcoal, and a micelle-clay complex for removal of the acidic pharmaceutical mefenamic acid. *Journal of Environmental Science and Health, Part A*, *48*(13), 1655–1662. https://doi.org/10.1080/10934529.2013.815475

Khan, S, Gabriel, H. F., & Rana, T. (2008). Standard precipitation index to track drought and assess impact of rainfall on watertables in irrigation areas. *Springer*, *22*, 159–177. https://doi.org/10.1007/s10795-008-9049-3

Khan, Sana. (2019). *Analysıs of Drought Events in North Cyprus*. Middle East Technical Unıversity.

Koyuncu, B. (2019). *Evapotranspiration Analysis of North Cyprus*. Mıddle East Technıcal Unıversıty. Retrieved from http://etd.lib.metu.edu.tr

Kummu, M., Tes, S., Yin, S., Adamson, P., Józsa, J., Koponen, J., … Sarkkula, J. (2014). Water balance analysis for the Tonle Sap Lake-floodplain system. *Hydrological Processes*, *28*(4), 1722–1733. https://doi.org/10.1002/hyp.9718

Lana, X., Serra, C., & Burgueño, A. (2001). Patterns of monthly rainfall shortage and excess in terms of the standardized precipitation index for Catalonia (NE Spain). *International Journal of Climatology*, *21*(13), 1669–1691. https://doi.org/10.1002/joc.697

Leta, O. T., El-Kadi, A. I., Dulai, H., & Ghazal, K. A. (2016). Assessment of climate change impacts on water balance components of Heeia watershed in Hawaii. *Journal of Hydrology: Regional Studies*, *8*, 182–197. https://doi.org/10.1016/j.ejrh.2016.09.006

Li, X. Y., Xu, H. Y., Sun, Y. L., Zhang, D. S., & Yang, Z. P. (2007). Lake-level change and water balance analysis at lake Qinghai, West China during recent

decades. *Water Resources Management*, *21*(9), 1505–1516. https://doi.org/10.1007/s11269-006-9096-1

Livada, I., & Asimakopoulos, D. (2005). Individual seasonality index of rainfall regimes in Greece. *Climate Research*, *28*(2), 155–161. https://doi.org/10.3354/cr028155

Loucks, D. P. (2000). Sustainable water resources management. *Water International*, *25*(1), 3–10. https://doi.org/10.1080/02508060008686793

Martin-Vide, J. (2004). Spatial distribution of a daily precipitation concentration index in peninsular Spain. *International Journal of Climatology*, *24*(8), 959–971. https://doi.org/10.1002/joc.1030

Mathbout, S., Lopez-Bustins, J. A., Royé, D., Martin-Vide, J., & Benhamrouche, A. (2020). Spatiotemporal variability of daily precipitation concentration and its relationship to teleconnection patterns over the Mediterranean during 1975–2015. *International Journal of Climatology*, *40*(3), 1435–1455. https://doi.org/10.1002/joc.6278

Mayor, B. (2020). Unraveling the Historical Economies of Scale and Learning Effects for Desalination Technologies. *Water Resources Research*, *56*(2). https://doi.org/10.1029/2019WR025841

Mccabe, G. J., & Markstrom, S. L. (2018). *A Monthly Water-Balance Model Driven By a Graphical User Interface Open-File Report 2007-1088*. Retrieved from http://www.usgs.gov/pubprod

Michaelides, S. C., Tymvios, F. S., & Michaelidou, T. (2009). Spatial and temporal characteristics of the annual rainfall frequency distribution in Cyprus. *Atmospheric Research*, *94*(4), 606–615. https://doi.org/10.1016/J.ATMOSRES.2009.04.008

Michiels, P., Gabriels, D., & Hartmann, R. (1992). Using the seasonal and temporal Precipitation concentration index for characterizing the monthly rainfall distribution in Spain. *CATENA*, *19*(1), 43–58. https://doi.org/10.1016/0341-8162(92)90016-5

Nachiappan, R. M. P., Kumar, B., & Manickavasagam, R. M. (2002). Estimation of subsurface components in the water balance of Lake Nainital (Kumaun Himalaya, India) using environmental isotopes. *Hydrological Sciences Journal*, *47*, S41–S54. https://doi.org/10.1080/02626660209493021

Ngongondo, C., Xu, C. Y., Gottschalk, L., & Alemaw, B. (2011). Evaluation of spatial and temporal characteristics of rainfall in Malawi: A case of data scarce region. *Theoretical and Applied Climatology*, *106*(1–2), 79–93. https://doi.org/10.1007/s00704-011-0413-0

Ngongondo, C., Xu, C. Y., Tallaksen, L. M., & Alemaw, B. (2015). Observed and simulated changes in the water balance components over Malawi, during 1971-

2000. *Quaternary International*, *369*, 7–16. https://doi.org/10.1016/j.quaint.2014.06.028

Nicholson, S. E., Davenport, M. L., & Malo, A. R. (1990). A comparison of the vegetation response to rainfall in the Sahel and East Africa, using normalized difference vegetation index. *Climatic Change*, *17*(2–3), 209–241. https://doi.org/10.1007/BF00138369

Nugroho, A. R., Tamagawa, I., Riandraswari, A., & Febrianti, T. (2019). Thornthwaite-Mather water balance analysis in Tambakbayan watershed, Yogyakarta, Indonesia. *MATEC Web of Conferences*, *280*, 05007. https://doi.org/10.1051/matecconf/201928005007

O Aybar, H., Egelio-lu, F., & Atikol, U. (2005). *An experimental study on an inclined solar water distillation system*. *Desalination* (Vol. 180).

Oner, H. (2019). *Economic Feasibility Assessment of Solar Powered Seawater Desalination Plants: Unconventional Freshwater Supply for Guzelyurt, Northern Cyprus*. Middle East Technical University .

Paraskeva, C. (2016). *A Digital Elevation Model for Cyprus based on the ALOS 2 W3D30 Digital Surface Model.* Retrieved from https://doi.org/10.6084/m9.figshare.3159991.v1

Phillips Agboola, O., & Egelioglu, F. (2012). Water scarcity in North Cyprus and solar desalination research: a review. *Desalination and Water Treatment*, *43*(1–3), 29–42. https://doi.org/10.1080/19443994.2012.672195

Poullikkas, A. (2010). An optimization model for the production of desalinated water using photovoltaic systems. *Desalination*, *258*(1–3), 100–105. https://doi.org/10.1016/j.desal.2010.03.036

Queluz, J. T. G., & Klar, A. E. (2013). Spatial distribution of climatic water balance in different rainfall regimes in the State of Pernambuco. *Applied Research & Agrotechnology*, *6*(1), 7–19. https://doi.org/10.5777/PAET.V6I1.2091

Salvati, L., Petitta, M., Ceccarelli, T., Perini, L., Di Battista, F., & Scarascia, M. E. V. (2008). Italy's renewable water resources as estimated on the basis of the monthly water balance. *Irrigation and Drainage*, *57*(5), 507–515. https://doi.org/10.1002/ird.380

Seyhun, R., & Akıntuğ, B. (2013). Trend Analysis of Rainfall in North Cyprus. In *Causes, Impacts and Solutions to Global Warming* (pp. 169–181). New York, NY: Springer New York. https://doi.org/10.1007/978-1-4614-7588-0_10

Stern, R. D., & Coe, R. (1984). A Model Fitting Analysis of Daily Rainfall Data. *Journal of the Royal Statistical Society. Series A (General)*, *147*(1), 1. https://doi.org/10.2307/2981736

Suhaila, J., & Jemain, A. A. (2012). Spatial analysis of daily rainfall intensity and

concentration index in Peninsular Malaysia. *Theoretical and Applied Climatology*, *108*(1–2), 235–245. https://doi.org/10.1007/s00704-011-0529-2

Tao, Y., Wang, W., Song, S., Ma, J., Tao, Y., Wang, W., … Ma, J. (2018). Spatial and Temporal Variations of Precipitation Extremes and Seasonality over China from 1961~2013. *Water*, *10*(6), 719. https://doi.org/10.3390/w10060719

Tsiourtis, N. X. (2001). Seawater desalination projects. The Cyprus experience. *Desalination*, *139*(1–3), 139–147. https://doi.org/10.1016/S0011-9164(01)00303-4

UNESCO. (2020). IHP-VIII: water security: responses to regional and global challenges (2014-2021) - UNESCO Digital Library. Retrieved October 5, 2020, from https://unesdoc.unesco.org/ark:/48223/pf0000225103

USGS. (2007). Thornthwaite. Retrieved December 8, 2020, from https://wwwbrr.cr.usgs.gov/projects/SW_MoWS/Thornthwaite.html

Vedavyasan, C. V. (2007). Pretreatment trends - an overview. *Desalination*, *203*(1–3), 296–299. https://doi.org/10.1016/j.desal.2006.04.012

Vehbi, B. O., & Doratli, N. (2010). Assessing the Impact of Tourism on the Physical Environment of a Small Coastal Town: Girne, Northern Cyprus. *European Planning Studies*, *18*(9), 1485–1505. https://doi.org/10.1080/09654313.2010.492587

WHO. (2004). *Guidelines for Third Edition Drinking-water Quality*.

WHO. (2006). Guidelines for Drinking-water Quality, *3*. Retrieved from http://oceanusgt.com/uploads/research/1850339455_20130525_Guidlines.pdf

Widén-Nilsson, E., Halldin, S., & Xu, C. yu. (2007). Global water-balance modelling with WASMOD-M: Parameter estimation and regionalisation. *Journal of Hydrology*, *340*(1–2), 105–118. https://doi.org/10.1016/j.jhydrol.2007.04.002

Wilks, D. S., & Wilks, D. S. (1990). Maximum Likelihood Estimation for the Gamma Distribution Using Data Containing Zeros. *Journal of Climate*, *3*(12), 1495–1501. https://doi.org/10.1175/1520-0442(1990)003<1495:MLEFTG>2.0.CO;2

Withers, A. (2005). Options for recarbonation, remineralisation and disinfection for desalination plants. *Desalination*, *179*(1-3 SPEC. ISS.), 11–24. https://doi.org/10.1016/j.desal.2004.11.051

Wolf, P. H., Siverns, S., & Monti, S. (2005). UF membranes for RO desalination pretreatment. *Desalination*, *182*(1–3), 293–300. https://doi.org/10.1016/j.desal.2005.05.006

Xu, P., Cath, T. Y., Robertson, A. P., Reinhard, M., Leckie, J. O., & Drewes, J. E. (2013, August 1). Critical review of desalination concentrate management, treatment and beneficial use. *Environmental Engineering Science*. Mary Ann

Liebert, Inc. 140 Huguenot Street, 3rd Floor New Rochelle, NY 10801 USA . https://doi.org/10.1089/ees.2012.0348

Zaifoğlu, H., Akıntuğ, B., & Yanmaz, A. M. (2017). Quality Control, Homogeneity Analysis, and Trends of Extreme Precipitation Indices in Northern Cyprus. *Journal of Hydrologic Engineering*, *22*(12), 05017024. https://doi.org/10.1061/(ASCE)HE.1943-5584.0001589

Zhang, Q., Xu, C.-Y., Zhang, Z., Chen, Y. D., Liu, C., & Lin, H. (2008). Spatial and temporal variability of precipitation maxima during 1960–2005 in the Yangtze River basin and possible association with large-scale circulation. *Journal of Hydrology*, *353*(3–4), 215–227. https://doi.org/10.1016/J.JHYDROL.2007.11.023

Zhang, Q., Xu, C., Gemmer, M., Chen, Y. D., & Liu, C. (2009). Changing properties of precipitation concentration in the Pearl River basin, China. *Stochastic Environmental Research and Risk Assessment*, *23*(3), 377–385. https://doi.org/10.1007/s00477-008-0225-7

APPENDICES

A. Annual CI, PCI and SI value for each station

Table A.1. Akdeniz station

Year	*CI*	*PCI*	*SI*
1978 -79	0.45	20.82	0.98
1979 - 80	0.41	17.65	1.00
1980 - 81	0.46	17.14	0.88
1981 - 82	0.54	22.27	1.13
1982 - 83	0.56	15.93	0.83
1983 - 84	0.49	17.99	0.96
1984 - 85	0.52	21.87	1.10
1985 - 86	0.62	23.77	0.98
1986 - 87	0.61	24.93	1.11
1987 - 88	0.53	20.19	1.01
1988 - 89	0.53	22.07	1.12
1989 -90	0.55	20.60	0.99
1990 - 91	0.51	19.18	0.90
1991 - 92	0.51	22.83	0.96
1992 - 93	0.52	21.39	1.08
1993 - 94	0.60	20.03	1.02
1994 - 95	0.67	24.04	1.01
1995 - 96	0.59	16.43	0.88
1996 - 97	0.56	19.00	0.96
1997 - 98	0.58	14.47	0.72
1998 - 99	0.33	28.44	1.22
1999 - 2000	0.39	17.14	0.94
2000 - 01	0.46	20.06	0.98
2001 - 02	0.42	19.40	0.88
2002 - 03	0.51	20.63	1.09
2003 - 04	0.55	26.54	1.30
2004 - 05	0.48	17.61	0.99
2005 - 06	0.69	22.42	1.01
2006 - 07	0.61	16.41	0.86
2007 - 08	0.60	24.14	1.06
2008 - 09	0.61	20.57	1.05
2009 - 10	0.59	21.41	1.05
2010 - 11	0.50	15.74	0.90
2011 - 12	0.51	18.84	0.89

2012 -13	0.64	23.81	1.08
2013 - 14	0.65	18.86	0.99
2014 - 15	0.56	15.62	0.79

Table A.2. Alaykoy station

Year	*CI*	*PCI*	*SI*
1978 -79	0.59	17.14	0.82
1979 - 80	0.52	20.66	0.97
1980 - 81	0.50	18.95	0.92
1981 - 82	0.59	15.63	0.84
1982 - 83	0.47	13.24	0.64
1983 - 84	0.55	14.37	0.73
1984 - 85	0.44	20.15	1.01
1985 - 86	0.52	16.49	0.83
1986 - 87	0.73	26.72	1.07
1987 - 88	0.58	16.36	0.91
1988 - 89	0.51	25.28	1.14
1989 -90	0.55	21.06	0.94
1990 - 91	0.48	20.47	1.06
1991 - 92	0.53	18.18	0.77
1992 - 93	0.52	17.86	0.91
1993 - 94	0.50	24.02	1.07
1994 - 95	0.60	20.67	0.86
1995 - 96	0.56	17.94	0.98
1996 - 97	0.58	13.76	0.75
1997 - 98	0.53	14.18	0.72
1998 - 99	0.48	16.94	0.79
1999 - 2000	0.57	15.25	0.71
2000 - 01	0.49	20.80	0.92
2001 - 02	0.60	13.57	0.63
2002 - 03	0.60	20.26	1.04
2003 - 04	0.55	27.72	1.18
2004 - 05	0.49	16.13	0.82
2005 - 06	0.53	19.19	0.94
2006 - 07	0.58	15.33	0.84
2007 - 08	0.63	20.44	1.03
2008 - 09	0.60	15.75	0.80
2009 - 10	0.61	22.01	1.06
2010 - 11	0.44	21.90	1.07
2011 - 12	0.57	20.24	0.94
2012 -13	0.53	17.91	0.98
2013 - 14	0.53	20.08	0.92

2014 - 15	0.63	15.71	0.83

Table A.3. Alevkaya station

Year	*CI*	*PCI*	*SI*
1978 -79	0.49	14.27	0.82
1979 - 80	0.56	18.71	0.90
1980 - 81	0.45	16.74	0.80
1981 - 82	0.56	16.18	0.85
1982 - 83	0.50	14.25	0.70
1983 - 84	0.57	17.26	0.95
1984 - 85	0.49	24.42	0.99
1985 - 86	0.49	16.42	0.79
1986 - 87	0.42	18.35	0.89
1987 - 88	0.50	18.55	1.00
1988 - 89	0.50	21.60	1.04
1989 -90	0.53	20.76	0.97
1990 - 91	0.56	26.19	1.21
1991 - 92	0.69	32.53	1.10
1992 - 93	0.57	19.82	0.96
1993 - 94	0.37	21.86	1.07
1994 - 95	0.58	28.55	0.94
1995 - 96	0.53	20.74	0.95
1996 - 97	0.49	14.74	0.78
1997 - 98	0.59	13.48	0.64
1998 - 99	0.55	16.61	0.81
1999 - 2000	0.51	17.14	0.85
2000 - 01	0.48	18.25	0.93
2001 - 02	0.55	20.32	0.87
2002 - 03	0.58	22.05	1.03
2003 - 04	0.51	24.98	1.16
2004 - 05	0.50	17.40	0.88
2005 - 06	0.59	25.81	1.07
2006 - 07	0.68	20.66	0.91
2007 - 08	0.54	20.26	0.97
2008 - 09	0.61	12.88	0.63
2009 - 10	0.62	19.80	0.94
2010 - 11	0.69	18.48	0.94
2011 - 12	0.65	17.51	0.99
2012 -13	0.74	20.36	1.06
2013 - 14	0.79	29.05	1.12

2014 - 15	0.69	14.43	0.63

Table A.4. Beyarmudu station

Year	*CI*	*PCI*	*SI*
1978 -79	0.54	28.09	0.93
1979 - 80	0.55	26.13	1.00
1980 - 81	0.50	19.97	0.90
1981 - 82	0.54	17.39	0.89
1982 - 83	0.61	19.71	0.94
1983 - 84	0.64	22.31	1.01
1984 - 85	0.65	38.35	1.26
1985 - 86	0.53	15.47	0.85
1986 - 87	0.63	26.43	1.04
1987 - 88	0.58	20.68	1.04
1988 - 89	0.55	21.53	0.99
1989 -90	0.57	18.97	0.83
1990 - 91	0.56	22.83	1.08
1991 - 92	0.63	28.01	1.03
1992 - 93	0.55	17.97	0.92
1993 - 94	0.59	22.88	1.06
1994 - 95	0.67	26.89	0.96
1995 - 96	0.63	27.84	1.09
1996 - 97	0.57	15.49	0.84
1997 - 98	0.62	14.21	0.76
1998 - 99	0.55	22.95	1.17
1999 - 2000	0.50	19.56	0.93
2000 - 01	0.62	26.10	1.04
2001 - 02	0.48	21.47	0.99
2002 - 03	0.54	19.89	1.08
2003 - 04	0.60	35.14	1.43
2004 - 05	0.63	20.71	0.94
2005 - 06	0.64	23.42	1.17
2006 - 07	0.65	20.39	0.95
2007 - 08	0.65	16.12	0.88
2008 - 09	0.63	14.72	0.74
2009 - 10	0.62	20.86	1.02
2010 - 11	0.67	14.62	0.74

2011 - 12	0.69	19.83	0.92
2012 -13	0.62	23.08	1.00
2013 - 14	0.71	24.07	0.99
2014 - 15	0.67	16.85	0.87

Table A.5. Beylerbeyi station

Year	*CI*	*PCI*	*SI*
1978 -79	0.67	18.04	0.97
1979 - 80	0.57	23.27	1.04
1980 - 81	0.52	16.71	0.75
1981 - 82	0.54	16.22	0.91
1982 - 83	0.49	14.91	0.74
1983 - 84	0.52	17.29	0.81
1984 - 85	0.69	27.01	1.25
1985 - 86	0.60	15.60	0.77
1986 - 87	0.56	23.81	1.15
1987 - 88	0.50	22.07	1.02
1988 - 89	0.50	20.87	1.11
1989 -90	0.54	33.17	1.19
1990 - 91	0.52	25.23	1.20
1991 - 92	0.54	24.95	1.04
1992 - 93	0.60	21.03	0.99
1993 - 94	0.62	23.47	1.12
1994 - 95	0.60	25.32	0.91
1995 - 96	0.58	20.36	1.03
1996 - 97	0.56	18.63	0.82
1997 - 98	0.61	16.25	0.85
1998 - 99	0.63	20.43	0.96
1999 - 2000	0.55	21.96	1.04
2000 - 01	0.56	18.86	0.81
2001 - 02	0.68	32.02	1.06
2002 - 03	0.61	26.39	1.19
2003 - 04	0.57	27.09	1.25
2004 - 05	0.55	17.00	0.87
2005 - 06	0.58	25.51	1.01
2006 - 07	0.62	19.08	0.85
2007 - 08	0.57	20.21	1.08
2008 - 09	0.51	15.95	0.85
2009 - 10	0.64	20.12	0.91
2010 - 11	0.63	28.58	1.00
2011 - 12	0.62	26.16	1.09
2012 -13	0.63	19.34	0.96

2013 - 14	0.58	19.90	1.03
2014 - 15	0.65	19.73	0.91

Table A.6. Bogaz station

Year	*CI*	*PCI*	*SI*
1978 -79	0.55	15.80	1.03
1979 - 80	0.53	21.92	0.91
1980 - 81	0.50	16.39	0.99
1981 - 82	0.53	17.63	1.03
1982 - 83	0.42	14.20	1.02
1983 - 84	0.40	17.40	0.85
1984 - 85	0.51	26.21	1.19
1985 - 86	0.53	17.81	0.83
1986 - 87	0.54	23.79	0.93
1987 - 88	0.46	19.41	1.03
1988 - 89	0.67	26.96	1.12
1989 -90	0.51	27.08	1.05
1990 - 91	0.59	23.81	1.12
1991 - 92	0.59	27.15	1.10
1992 - 93	0.61	19.65	1.13
1993 - 94	0.55	22.97	1.02
1994 - 95	0.55	26.41	0.70
1995 - 96	0.55	18.47	1.25
1996 - 97	0.56	16.95	1.06
1997 - 98	0.52	20.41	0.83
1998 - 99	0.59	19.52	1.04
1999 - 2000	0.50	16.68	0.78
2000 - 01	0.51	21.70	0.84
2001 - 02	0.59	21.08	0.95
2002 - 03	0.57	20.96	1.02
2003 - 04	0.58	28.54	1.28
2004 - 05	0.51	15.05	0.99
2005 - 06	0.51	21.56	1.02
2006 - 07	0.60	15.74	0.84
2007 - 08	0.55	19.61	1.13
2008 - 09	0.54	20.35	0.95
2009 - 10	0.64	22.40	1.15
2010 - 11	0.73	30.97	1.04
2011 - 12	0.68	23.64	0.75
2012 -13	0.71	27.10	0.93
2013 - 14	0.64	17.24	0.88
2014 - 15	0.63	18.44	0.67

Table A.7. Camlıbel station

Year	*CI*	*PCI*	*SI*
1978 -79	0.55	15.80	1.03
1979 - 80	0.53	21.92	0.91
1980 - 81	0.50	16.39	0.99
1981 - 82	0.53	17.63	1.03
1982 - 83	0.42	14.20	1.02
1983 - 84	0.40	17.40	0.85
1984 - 85	0.51	26.21	1.19
1985 - 86	0.53	17.81	0.83
1986 - 87	0.54	23.79	0.93
1987 - 88	0.46	19.41	1.03
1988 - 89	0.67	26.96	1.12
1989 -90	0.51	27.08	1.05
1990 - 91	0.59	23.81	1.12
1991 - 92	0.59	27.15	1.10
1992 - 93	0.61	19.65	1.13
1993 - 94	0.55	22.97	1.02
1994 - 95	0.55	26.41	0.70
1995 - 96	0.55	18.47	1.25
1996 - 97	0.56	16.95	1.06
1997 - 98	0.52	20.41	0.83
1998 - 99	0.59	19.52	1.04
1999 - 2000	0.50	16.68	0.78
2000 - 01	0.51	21.70	0.84
2001 - 02	0.59	21.08	0.95
2002 - 03	0.57	20.96	1.02
2003 - 04	0.58	28.54	1.28
2004 - 05	0.51	15.05	0.99
2005 - 06	0.51	21.56	1.02
2006 - 07	0.60	15.74	0.84
2007 - 08	0.55	19.61	1.13
2008 - 09	0.54	20.35	0.95
2009 - 10	0.64	22.40	1.15
2010 - 11	0.73	30.97	1.04
2011 - 12	0.68	23.64	0.75
2012 -13	0.71	27.10	0.93
2013 - 14	0.64	17.24	0.88
2014 - 15	0.63	18.44	0.67

Table A.8. Cayırova station

Year	*CI*	*PCI*	*SI*
1978 -79	0.60	20.85	1.03
1979 - 80	0.65	21.42	0.91
1980 - 81	0.53	17.27	0.78
1981 - 82	0.62	21.09	0.87
1982 - 83	0.60	19.00	0.85
1983 - 84	0.63	18.84	0.90
1984 - 85	0.66	40.94	1.18
1985 - 86	0.63	18.91	0.84
1986 - 87	0.60	21.30	1.02
1987 - 88	0.59	22.78	1.09
1988 - 89	0.50	24.57	1.11
1989 -90	0.50	22.10	0.99
1990 - 91	0.56	26.68	1.13
1991 - 92	0.46	25.18	0.97
1992 - 93	0.54	22.45	1.03
1993 - 94	0.50	22.20	1.16
1994 - 95	0.52	14.66	0.68
1995 - 96	0.59	29.96	1.07
1996 - 97	0.44	17.02	0.87
1997 - 98	0.60	14.67	0.75
1998 - 99	0.60	20.06	0.96
1999 - 2000	0.53	15.51	0.83
2000 - 01	0.63	18.35	0.95
2001 - 02	0.63	32.20	1.07
2002 - 03	0.58	23.79	1.06
2003 - 04	0.61	41.48	1.32
2004 - 05	0.58	21.41	0.99
2005 - 06	0.66	29.91	1.23
2006 - 07	0.60	18.78	0.90
2007 - 08	0.53	19.17	0.88
2008 - 09	0.68	23.18	1.04
2009 - 10	0.58	21.59	1.00
2010 - 11	0.63	18.24	0.84
2011 - 12	0.62	17.53	0.89
2012 -13	0.65	15.85	0.86
2013 - 14	0.61	19.48	0.95
2014 - 15	0.61	15.70	0.75

Table A.9. Degirmenlik station

Year	*CI*	*PCI*	*SI*
1978 -79	0.61	15.94	1.03
1979 - 80	0.58	20.34	1.02
1980 - 81	0.40	18.08	0.84
1981 - 82	0.53	17.34	0.88
1982 - 83	0.54	13.74	0.65
1983 - 84	0.60	18.01	0.91
1984 - 85	0.54	27.46	1.06
1985 - 86	0.54	17.74	0.81
1986 - 87	0.52	24.75	1.09
1987 - 88	0.49	17.82	1.00
1988 - 89	0.63	34.56	1.33
1989 -90	0.50	20.72	0.98
1990 - 91	0.43	25.97	1.16
1991 - 92	0.49	25.07	0.90
1992 - 93	0.52	18.67	1.01
1993 - 94	0.49	27.63	1.17
1994 - 95	0.60	33.50	1.07
1995 - 96	0.54	22.66	0.92
1996 - 97	0.33	14.85	0.76
1997 - 98	0.62	15.09	0.77
1998 - 99	0.45	17.35	0.86
1999 - 2000	0.63	21.37	0.94
2000 - 01	0.51	23.24	0.94
2001 - 02	0.55	19.29	0.90
2002 - 03	0.55	22.22	1.07
2003 - 04	0.53	26.74	1.13
2004 - 05	0.51	13.87	0.75
2005 - 06	0.64	28.29	1.02
2006 - 07	0.60	16.32	0.82
2007 - 08	0.44	16.89	0.88
2008 - 09	0.47	14.38	0.79
2009 - 10	0.60	16.18	0.82
2010 - 11	0.56	18.06	0.97
2011 - 12	0.58	18.69	0.90
2012 -13	0.58	17.45	0.89
2013 - 14	0.45	27.67	1.12
2014 - 15	0.52	14.67	0.75

Table A.10. Dipkarpaz station

Year	*CI*	*PCI*	*SI*
1978 -79	0.58	23.89	1.03
1979 - 80	0.53	18.86	0.91
1980 - 81	0.48	22.67	0.99
1981 - 82	0.57	18.77	1.03
1982 - 83	0.47	19.50	1.02
1983 - 84	0.55	15.17	0.85
1984 - 85	0.62	28.32	1.19
1985 - 86	0.58	22.33	0.83
1986 - 87	0.64	20.24	0.93
1987 - 88	0.57	24.49	1.03
1988 - 89	0.60	24.32	1.12
1989 -90	0.61	20.11	1.05
1990 - 91	0.59	23.77	1.12
1991 - 92	0.61	25.33	1.10
1992 - 93	0.65	33.79	1.13
1993 - 94	0.52	18.42	1.02
1994 - 95	0.56	17.95	0.70
1995 - 96	0.65	31.69	1.25
1996 - 97	0.56	21.11	1.06
1997 - 98	0.54	16.43	0.83
1998 - 99	0.55	24.06	1.04
1999 - 2000	0.53	14.36	0.78
2000 - 01	0.48	17.02	0.84
2001 - 02	0.65	23.37	0.95
2002 - 03	0.55	20.94	1.02
2003 - 04	0.62	32.56	1.28
2004 - 05	0.55	24.08	0.99
2005 - 06	0.37	21.06	1.02
2006 - 07	0.55	16.49	0.84
2007 - 08	0.64	30.82	1.13
2008 - 09	0.61	19.39	0.95
2009 - 10	0.64	33.35	1.15
2010 - 11	0.63	23.81	1.04
2011 - 12	0.60	26.75	0.75
2012 -13	0.53	15.17	0.93
2013 - 14	0.59	18.30	0.88
2014 - 15	0.59	14.36	0.67

Table A.11. Dortyol station

Year	*CI*	*PCI*	*SI*
1978 -79	0.55	19.19	0.97
1979 - 80	0.52	21.28	0.93
1980 - 81	0.51	15.66	0.78
1981 - 82	0.56	16.93	0.84
1982 - 83	0.50	13.50	0.72
1983 - 84	0.41	17.82	0.90
1984 - 85	0.53	27.49	1.03
1985 - 86	0.47	15.29	0.78
1986 - 87	0.53	22.37	0.95
1987 - 88	0.55	15.82	0.80
1988 - 89	0.52	20.04	1.03
1989 -90	0.52	18.90	0.96
1990 - 91	0.55	24.98	1.18
1991 - 92	0.51	23.67	0.92
1992 - 93	0.58	19.39	0.81
1993 - 94	0.44	21.38	1.14
1994 - 95	0.51	28.90	0.93
1995 - 96	0.55	36.25	1.16
1996 - 97	0.60	21.69	1.00
1997 - 98	0.52	13.03	0.64
1998 - 99	0.52	23.06	1.02
1999 - 2000	0.46	14.53	0.62
2000 - 01	0.49	21.89	1.05
2001 - 02	0.58	17.33	0.77
2002 - 03	0.54	19.43	0.95
2003 - 04	0.53	34.84	1.31
2004 - 05	0.54	17.94	0.91
2005 - 06	0.55	19.05	0.91
2006 - 07	0.44	19.01	0.97
2007 - 08	0.54	23.14	1.08
2008 - 09	0.47	19.53	1.02
2009 - 10	0.46	23.31	1.05
2010 - 11	0.65	20.69	1.08
2011 - 12	0.55	19.54	0.94
2012 -13	0.59	19.22	0.85
2013 - 14	0.49	18.61	0.97
2014 - 15	0.53	20.54	0.96

Table A.12. Ercan station

Year	*CI*	*PCI*	*SI*
1978 -79	0.73	18.20	0.95
1979 - 80	0.64	20.91	1.02
1980 - 81	0.47	16.92	0.86
1981 - 82	0.63	18.59	0.92
1982 - 83	0.61	14.05	0.75
1983 - 84	0.54	15.83	0.77
1984 - 85	0.63	23.43	0.91
1985 - 86	0.57	14.36	0.68
1986 - 87	0.67	20.68	0.91
1987 - 88	0.62	18.17	1.04
1988 - 89	0.61	24.23	1.10
1989 -90	0.63	23.51	1.00
1990 - 91	0.56	21.24	1.10
1991 - 92	0.65	18.74	0.82
1992 - 93	0.65	17.36	0.93
1993 - 94	0.58	25.07	1.03
1994 - 95	0.53	39.94	1.07
1995 - 96	0.63	24.17	1.12
1996 - 97	0.63	18.19	0.93
1997 - 98	0.67	16.09	0.81
1998 - 99	0.58	18.42	0.91
1999 - 2000	0.62	24.09	1.00
2000 - 01	0.58	14.76	0.70
2001 - 02	0.60	15.66	0.70
2002 - 03	0.69	18.61	0.92
2003 - 04	0.66	34.27	1.28
2004 - 05	0.60	15.93	0.78
2005 - 06	0.62	19.29	0.94
2006 - 07	0.76	17.31	0.83
2007 - 08	0.61	16.09	0.84
2008 - 09	0.63	13.32	0.69
2009 - 10	0.64	18.56	0.93
2010 - 11	0.67	18.67	0.90
2011 - 12	0.62	17.24	0.78
2012 -13	0.59	17.24	0.89
2013 - 14	0.69	18.54	0.84
2014 - 15	0.66	14.75	0.74

Table A.13. Esentepe station

Year	*CI*	*PCI*	*SI*
1978 -79	0.66	20.36	0.83
1979 - 80	0.51	19.63	0.96
1980 - 81	0.44	19.05	0.81
1981 - 82	0.52	13.82	0.70
1982 - 83	0.44	15.32	0.74
1983 - 84	0.48	17.03	0.84
1984 - 85	0.53	23.85	1.07
1985 - 86	0.50	20.59	0.98
1986 - 87	0.63	26.34	1.01
1987 - 88	0.52	18.13	0.98
1988 - 89	0.55	21.85	1.15
1989 -90	0.56	17.65	0.82
1990 - 91	0.48	25.97	1.19
1991 - 92	0.54	26.74	1.02
1992 - 93	0.58	17.00	0.90
1993 - 94	0.54	19.57	1.09
1994 - 95	0.57	20.32	0.93
1995 - 96	0.53	18.54	0.95
1996 - 97	0.49	16.79	0.79
1997 - 98	0.59	15.21	0.65
1998 - 99	0.51	20.94	1.03
1999 - 2000	0.62	13.92	0.72
2000 - 01	0.54	17.48	0.84
2001 - 02	0.61	23.64	0.92
2002 - 03	0.60	21.93	1.05
2003 - 04	0.49	26.27	1.18
2004 - 05	0.52	18.07	0.93
2005 - 06	0.56	17.61	0.83
2006 - 07	0.62	21.89	1.04
2007 - 08	0.52	20.90	0.96
2008 - 09	0.58	15.62	0.83
2009 - 10	0.59	18.76	0.94
2010 - 11	0.65	19.75	0.91
2011 - 12	0.63	16.68	0.85
2012 -13	0.66	18.30	0.94
2013 - 14	0.75	25.01	1.09
2014 - 15	0.58	13.10	0.68

Table A.14. Gaziveren station

Year	*CI*	*PCI*	*SI*
1978 -79	0.49	18.05	0.93
1979 - 80	0.51	17.65	0.94
1980 - 81	0.43	17.70	0.91
1981 - 82	0.60	18.01	1.00
1982 - 83	0.55	21.03	0.87
1983 - 84	0.34	16.26	0.92
1984 - 85	0.47	20.39	1.16
1985 - 86	0.47	16.29	0.77
1986 - 87	0.58	24.77	1.15
1987 - 88	0.53	22.57	1.08
1988 - 89	0.53	30.32	1.13
1989 -90	0.45	24.23	1.15
1990 - 91	0.38	19.40	0.97
1991 - 92	0.46	26.33	1.07
1992 - 93	0.56	19.67	1.10
1993 - 94	0.52	20.18	0.97
1994 - 95	0.64	16.19	0.82
1995 - 96	0.54	18.87	0.89
1996 - 97	0.42	18.36	0.95
1997 - 98	0.49	18.08	0.93
1998 - 99	0.55	20.76	0.99
1999 - 2000	0.43	18.93	1.04
2000 - 01	0.63	16.59	0.83
2001 - 02	0.55	18.47	0.94
2002 - 03	0.58	21.65	0.95
2003 - 04	0.54	27.78	1.22
2004 - 05	0.55	13.95	0.74
2005 - 06	0.60	19.68	0.96
2006 - 07	0.61	17.03	0.91
2007 - 08	0.54	22.33	1.13
2008 - 09	0.65	20.67	1.09
2009 - 10	0.64	24.41	1.17
2010 - 11	0.50	19.63	1.06
2011 - 12	0.53	20.80	0.89
2012 -13	0.59	18.01	0.95
2013 - 14	0.55	15.20	0.75
2014 - 15	0.51	14.17	0.69

Table A.15. Gecitkale station

Year	*CI*	*PCI*	*SI*
1978 -79	0.68	15.74	0.81
1979 - 80	0.67	20.23	0.90
1980 - 81	0.52	15.03	0.69
1981 - 82	0.55	15.03	0.70
1982 - 83	0.56	15.97	0.80
1983 - 84	0.61	19.97	0.96
1984 - 85	0.60	20.11	0.86
1985 - 86	0.56	17.57	0.93
1986 - 87	0.62	20.64	0.83
1987 - 88	0.63	20.30	1.04
1988 - 89	0.55	17.32	0.82
1989 -90	0.54	22.65	0.96
1990 - 91	0.49	33.98	1.25
1991 - 92	0.49	28.82	0.99
1992 - 93	0.63	20.55	0.89
1993 - 94	0.50	22.65	1.13
1994 - 95	0.55	28.09	0.95
1995 - 96	0.54	34.31	1.30
1996 - 97	0.54	18.65	0.85
1997 - 98	0.55	14.96	0.82
1998 - 99	0.48	19.76	0.99
1999 - 2000	0.55	18.22	0.97
2000 - 01	0.52	19.50	0.78
2001 - 02	0.47	18.34	0.82
2002 - 03	0.59	21.29	1.04
2003 - 04	0.51	29.87	1.11
2004 - 05	0.48	15.04	0.77
2005 - 06	0.63	23.22	1.13
2006 - 07	0.63	21.78	0.96
2007 - 08	0.60	16.31	0.88
2008 - 09	0.62	11.69	0.57
2009 - 10	0.65	21.69	1.05
2010 - 11	0.71	17.97	0.92
2011 - 12	0.64	20.20	1.03
2012 -13	0.64	14.78	0.71
2013 - 14	0.65	21.50	1.06
2014 - 15	0.71	15.78	0.80

Table A.16. Girne station

Year	*CI*	*PCI*	*SI*
1978 -79	0.68	19.36	1.02
1979 - 80	0.62	22.85	1.01
1980 - 81	0.50	16.95	0.76
1981 - 82	0.60	17.85	0.96
1982 - 83	0.54	14.16	0.66
1983 - 84	0.60	18.55	0.89
1984 - 85	0.71	29.06	1.16
1985 - 86	0.63	24.15	1.04
1986 - 87	0.63	22.56	1.10
1987 - 88	0.63	22.97	1.08
1988 - 89	0.66	22.05	1.13
1989 -90	0.61	27.92	1.16
1990 - 91	0.52	27.34	1.18
1991 - 92	0.59	21.79	1.06
1992 - 93	0.61	19.20	0.90
1993 - 94	0.62	23.78	1.11
1994 - 95	0.66	24.34	1.03
1995 - 96	0.56	21.88	1.03
1996 - 97	0.56	18.46	0.88
1997 - 98	0.61	17.61	0.93
1998 - 99	0.64	20.74	0.99
1999 - 2000	0.59	18.89	0.93
2000 - 01	0.62	22.65	0.98
2001 - 02	0.68	21.72	1.04
2002 - 03	0.64	23.09	1.19
2003 - 04	0.61	31.25	1.35
2004 - 05	0.62	18.99	0.87
2005 - 06	0.63	28.24	1.03
2006 - 07	0.69	25.02	1.00
2007 - 08	0.73	28.94	1.23
2008 - 09	0.68	20.12	1.03
2009 - 10	0.69	23.13	1.08
2010 - 11	0.66	25.32	0.97
2011 - 12	0.63	23.77	1.05
2012 -13	0.64	18.16	0.94
2013 - 14	0.64	16.55	0.84
2014 - 15	0.64	21.54	0.99

Table A.17. Gonendere station

Year	*CI*	*PCI*	*SI*
1978 -79	0.56	20.79	1.00
1979 - 80	0.62	20.22	0.97
1980 - 81	0.53	16.84	0.77
1981 - 82	0.61	14.69	0.76
1982 - 83	0.43	17.03	0.79
1983 - 84	0.51	17.98	0.99
1984 - 85	0.54	31.11	1.02
1985 - 86	0.58	20.36	0.88
1986 - 87	0.60	18.28	0.83
1987 - 88	0.56	18.70	0.90
1988 - 89	0.43	21.40	0.99
1989 -90	0.48	17.52	0.78
1990 - 91	0.49	29.94	1.25
1991 - 92	0.45	23.59	0.87
1992 - 93	0.57	21.27	0.95
1993 - 94	0.52	23.86	1.25
1994 - 95	0.69	28.74	0.94
1995 - 96	0.55	27.22	0.98
1996 - 97	0.41	15.74	0.68
1997 - 98	0.44	16.88	0.93
1998 - 99	0.51	18.13	0.91
1999 - 2000	0.52	16.22	0.86
2000 - 01	0.48	17.51	0.76
2001 - 02	0.47	21.62	0.88
2002 - 03	0.57	20.00	1.06
2003 - 04	0.41	23.20	1.06
2004 - 05	0.48	16.60	0.89
2005 - 06	0.65	28.81	1.25
2006 - 07	0.65	20.39	0.97
2007 - 08	0.69	17.68	0.89
2008 - 09	0.57	14.80	0.79
2009 - 10	0.64	23.64	1.11
2010 - 11	0.60	17.44	0.91
2011 - 12	0.54	18.14	0.92
2012 -13	0.53	20.81	0.93
2013 - 14	0.64	27.40	1.14
2014 - 15	0.62	15.88	0.78

Table A.18. Guzelyurt station

Year	*CI*	*PCI*	*SI*
1978 -79	0.50	21.31	0.91
1979 - 80	0.56	16.81	0.94
1980 - 81	0.54	18.10	0.90
1981 - 82	0.69	17.23	0.92
1982 - 83	0.55	16.16	0.71
1983 - 84	0.57	16.35	0.88
1984 - 85	0.58	20.99	1.10
1985 - 86	0.54	14.33	0.70
1986 - 87	0.60	25.57	1.13
1987 - 88	0.58	18.57	0.96
1988 - 89	0.57	26.39	1.14
1989 -90	0.54	22.78	0.96
1990 - 91	0.47	21.08	1.00
1991 - 92	0.55	24.30	1.05
1992 - 93	0.43	19.20	1.05
1993 - 94	0.51	20.03	1.00
1994 - 95	0.65	16.95	0.83
1995 - 96	0.59	15.65	0.84
1996 - 97	0.53	18.79	0.92
1997 - 98	0.62	18.07	0.88
1998 - 99	0.62	21.50	0.99
1999 - 2000	0.38	19.15	0.94
2000 - 01	0.67	17.95	0.96
2001 - 02	0.57	18.03	0.92
2002 - 03	0.60	20.36	1.02
2003 - 04	0.56	27.09	1.09
2004 - 05	0.57	14.76	0.82
2005 - 06	0.62	18.13	0.89
2006 - 07	0.70	19.67	0.98
2007 - 08	0.60	22.89	1.15
2008 - 09	0.64	20.10	1.05
2009 - 10	0.69	23.34	1.11
2010 - 11	0.59	16.31	0.91
2011 - 12	0.53	20.73	0.93
2012 -13	0.62	17.54	0.91
2013 - 14	0.61	17.62	0.88
2014 - 15	0.60	14.87	0.77

Table A.19. Iskele station

Year	*CI*	*PCI*	*SI*
1978 -79	0.60	24.65	1.06
1979 - 80	0.61	19.29	0.97
1980 - 81	0.43	20.46	0.91
1981 - 82	0.61	26.59	1.08
1982 - 83	0.51	15.02	0.84
1983 - 84	0.54	17.26	0.90
1984 - 85	0.57	31.99	1.13
1985 - 86	0.56	19.66	1.03
1986 - 87	0.53	19.92	0.92
1987 - 88	0.54	22.16	1.09
1988 - 89	0.45	18.04	0.90
1989 -90	0.53	31.82	1.06
1990 - 91	0.46	29.03	1.21
1991 - 92	0.47	32.00	1.07
1992 - 93	0.53	16.38	0.81
1993 - 94	0.48	20.09	0.99
1994 - 95	0.52	19.71	0.88
1995 - 96	0.53	28.93	1.20
1996 - 97	0.53	17.17	0.96
1997 - 98	0.54	13.89	0.73
1998 - 99	0.38	24.80	0.97
1999 - 2000	0.61	17.11	0.74
2000 - 01	0.59	24.99	1.06
2001 - 02	0.59	25.42	0.99
2002 - 03	0.55	16.72	0.70
2003 - 04	0.59	44.14	1.39
2004 - 05	0.68	24.18	1.05
2005 - 06	0.56	24.12	1.03
2006 - 07	0.63	27.24	0.95
2007 - 08	0.54	17.28	0.90
2008 - 09	0.59	17.22	0.87
2009 - 10	0.61	21.63	1.08
2010 - 11	0.62	16.64	0.94
2011 - 12	0.62	15.86	0.83
2012 -13	0.63	17.59	0.93
2013 - 14	0.60	18.33	0.97
2014 - 15	0.60	14.36	0.69

Table A.20. Kantara station

Year	*CI*	*PCI*	*SI*
1978 -79	0.60	24.65	1.06
1979 - 80	0.61	19.29	0.97
1980 - 81	0.43	20.46	0.91
1981 - 82	0.61	26.59	1.08
1982 - 83	0.51	15.02	0.84
1983 - 84	0.54	17.26	0.90
1984 - 85	0.57	31.99	1.13
1985 - 86	0.56	19.66	1.03
1986 - 87	0.53	19.92	0.92
1987 - 88	0.54	22.16	1.09
1988 - 89	0.45	18.04	0.90
1989 -90	0.53	31.82	1.06
1990 - 91	0.46	29.03	1.21
1991 - 92	0.47	32.00	1.07
1992 - 93	0.53	16.38	0.81
1993 - 94	0.48	20.09	0.99
1994 - 95	0.52	19.71	0.88
1995 - 96	0.53	28.93	1.20
1996 - 97	0.53	17.17	0.96
1997 - 98	0.54	13.89	0.73
1998 - 99	0.38	24.80	0.97
1999 - 2000	0.61	17.11	0.74
2000 - 01	0.59	24.99	1.06
2001 - 02	0.59	25.42	0.99
2002 - 03	0.55	16.72	0.70
2003 - 04	0.59	44.14	1.39
2004 - 05	0.68	24.18	1.05
2005 - 06	0.56	24.12	1.03
2006 - 07	0.63	27.24	0.95
2007 - 08	0.54	17.28	0.90
2008 - 09	0.59	17.22	0.87
2009 - 10	0.61	21.63	1.08
2010 - 11	0.62	16.64	0.94
2011 - 12	0.62	15.86	0.83
2012 -13	0.63	17.59	0.93
2013 - 14	0.60	18.33	0.97
2014 - 15	0.60	14.36	0.69

Table A.21. Lapta station

Year	*CI*	*PCI*	*SI*
1978 -79	0.64	18.19	0.76
1979 - 80	0.55	24.70	1.07
1980 - 81	0.48	20.00	1.04
1981 - 82	0.53	16.03	0.88
1982 - 83	0.49	21.99	0.93
1983 - 84	0.48	23.49	1.03
1984 - 85	0.63	23.82	1.14
1985 - 86	0.56	19.39	0.93
1986 - 87	0.57	24.24	1.12
1987 - 88	0.52	20.15	0.79
1988 - 89	0.51	37.51	1.16
1989 -90	0.57	23.40	0.98
1990 - 91	0.55	22.85	1.06
1991 - 92	0.54	24.69	1.17
1992 - 93	0.53	26.25	1.13
1993 - 94	0.57	18.56	1.02
1994 - 95	0.65	16.88	0.90
1995 - 96	0.47	16.96	0.90
1996 - 97	0.46	27.93	1.12
1997 - 98	0.55	19.94	0.95
1998 - 99	0.61	16.41	0.81
1999 - 2000	0.46	33.29	1.00
2000 - 01	0.51	27.36	1.25
2001 - 02	0.67	22.38	1.12
2002 - 03	0.67	19.75	0.97
2003 - 04	0.58	21.47	0.94
2004 - 05	0.53	17.93	0.89
2005 - 06	0.52	21.44	1.09
2006 - 07	0.56	22.54	1.08
2007 - 08	0.58	25.96	1.18
2008 - 09	0.64	21.90	0.95
2009 - 10	0.67	23.21	1.04
2010 - 11	0.63	16.43	0.80
2011 - 12	0.66	14.57	0.77
2012 -13	0.64	20.31	0.93
2013 - 14	0.59	21.92	1.01
2014 - 15	0.64	21.46	0.99

Table A.22. Lefke station

Year	*CI*	*PCI*	*SI*
1978 -79	0.58	22.34	0.98
1979 - 80	0.48	16.22	0.92
1980 - 81	0.46	20.46	0.91
1981 - 82	0.58	17.05	0.87
1982 - 83	0.54	15.58	0.79
1983 - 84	0.52	15.60	0.87
1984 - 85	0.50	20.38	1.11
1985 - 86	0.52	13.90	0.68
1986 - 87	0.47	18.86	0.95
1987 - 88	0.42	17.97	0.93
1988 - 89	0.56	28.25	1.18
1989 -90	0.57	24.24	1.10
1990 - 91	0.38	21.00	1.01
1991 - 92	0.37	27.97	1.09
1992 - 93	0.61	19.61	0.98
1993 - 94	0.48	23.41	1.09
1994 - 95	0.53	22.60	0.94
1995 - 96	0.49	16.91	0.90
1996 - 97	0.55	18.15	0.92
1997 - 98	0.48	18.47	0.96
1998 - 99	0.47	20.19	0.95
1999 - 2000	0.43	19.38	1.07
2000 - 01	0.49	17.65	0.85
2001 - 02	0.55	18.71	0.91
2002 - 03	0.56	20.47	0.98
2003 - 04	0.50	32.09	1.30
2004 - 05	0.50	19.06	0.91
2005 - 06	0.63	19.69	0.99
2006 - 07	0.69	17.17	0.84
2007 - 08	0.50	17.18	0.85
2008 - 09	0.58	16.99	0.88
2009 - 10	0.64	24.66	1.11
2010 - 11	0.51	19.25	0.98
2011 - 12	0.49	18.59	0.87
2012 -13	0.60	16.32	0.78
2013 - 14	0.63	19.15	0.78
2014 - 15	0.58	14.53	0.76

Table A.23. Lefkosa station

Year	*CI*	*PCI*	*SI*
1978 -79	0.67	22.21	1.02
1979 - 80	0.57	21.14	0.99
1980 - 81	0.56	18.84	0.96
1981 - 82	0.67	21.60	1.01
1982 - 83	0.59	14.98	0.74
1983 - 84	0.61	16.68	0.77
1984 - 85	0.63	21.52	1.01
1985 - 86	0.61	16.71	0.81
1986 - 87	0.69	23.36	1.03
1987 - 88	0.63	18.26	1.04
1988 - 89	0.63	24.41	1.07
1989 -90	0.60	16.48	0.83
1990 - 91	0.47	24.66	1.21
1991 - 92	0.61	20.69	0.83
1992 - 93	0.59	18.47	0.93
1993 - 94	0.58	23.64	1.05
1994 - 95	0.72	21.86	0.98
1995 - 96	0.60	20.76	0.97
1996 - 97	0.60	14.15	0.73
1997 - 98	0.60	15.29	0.78
1998 - 99	0.58	15.78	0.84
1999 - 2000	0.66	20.69	0.96
2000 - 01	0.67	15.01	0.74
2001 - 02	0.66	13.66	0.55
2002 - 03	0.66	18.35	0.83
2003 - 04	0.60	27.20	1.04
2004 - 05	0.65	13.95	0.69
2005 - 06	0.58	15.72	0.77
2006 - 07	0.63	15.25	0.81
2007 - 08	0.64	27.44	1.06
2008 - 09	0.61	16.58	0.92
2009 - 10	0.67	20.11	1.02
2010 - 11	0.55	19.37	0.99
2011 - 12	0.66	18.35	0.93
2012 -13	0.71	18.57	1.00
2013 - 14	0.79	24.74	0.98
2014 - 15	0.71	14.00	0.70

Table A.24. Magusa station

Year	*CI*	*PCI*	*SI*
1978 -79	0.58	32.36	1.13
1979 - 80	0.45	23.45	0.98
1980 - 81	0.51	18.33	0.98
1981 - 82	0.58	19.00	0.99
1982 - 83	0.64	17.69	0.85
1983 - 84	0.62	17.05	0.92
1984 - 85	0.66	25.37	1.10
1985 - 86	0.66	21.59	0.99
1986 - 87	0.62	23.42	0.95
1987 - 88	0.64	18.96	0.97
1988 - 89	0.59	19.11	0.96
1989 -90	0.68	27.59	0.98
1990 - 91	0.58	25.42	1.20
1991 - 92	0.63	34.64	1.17
1992 - 93	0.65	17.23	0.94
1993 - 94	0.58	21.13	0.97
1994 - 95	0.58	25.04	0.98
1995 - 96	0.61	28.30	1.07
1996 - 97	0.56	16.15	0.90
1997 - 98	0.69	15.62	0.81
1998 - 99	0.64	22.58	1.02
1999 - 2000	0.65	15.92	0.89
2000 - 01	0.67	17.56	0.88
2001 - 02	0.61	20.90	0.92
2002 - 03	0.60	18.98	0.95
2003 - 04	0.65	34.82	1.34
2004 - 05	0.66	19.88	0.99
2005 - 06	0.68	29.12	1.25
2006 - 07	0.71	27.42	0.89
2007 - 08	0.63	35.07	1.20
2008 - 09	0.54	16.75	0.86
2009 - 10	0.66	26.28	1.22
2010 - 11	0.65	20.77	0.90
2011 - 12	0.70	18.48	0.83
2012 -13	0.63	26.64	0.97
2013 - 14	0.62	16.69	0.77
2014 - 15	0.69	15.73	0.86

Table A.25. Mehmetcik station

Year	*CI*	*PCI*	*SI*
1978 -79	0.58	32.36	1.13
1979 - 80	0.45	23.45	0.98
1980 - 81	0.51	18.33	0.98
1981 - 82	0.58	19.00	0.99
1982 - 83	0.64	17.69	0.85
1983 - 84	0.62	17.05	0.92
1984 - 85	0.66	25.37	1.10
1985 - 86	0.66	21.59	0.99
1986 - 87	0.62	23.42	0.95
1987 - 88	0.64	18.96	0.97
1988 - 89	0.59	19.11	0.96
1989 -90	0.68	27.59	0.98
1990 - 91	0.58	25.42	1.20
1991 - 92	0.63	34.64	1.17
1992 - 93	0.65	17.23	0.94
1993 - 94	0.58	21.13	0.97
1994 - 95	0.58	25.04	0.98
1995 - 96	0.61	28.30	1.07
1996 - 97	0.56	16.15	0.90
1997 - 98	0.69	15.62	0.81
1998 - 99	0.64	22.58	1.02
1999 - 2000	0.65	15.92	0.89
2000 - 01	0.67	17.56	0.88
2001 - 02	0.61	20.90	0.92
2002 - 03	0.60	18.98	0.95
2003 - 04	0.65	34.82	1.34
2004 - 05	0.66	19.88	0.99
2005 - 06	0.68	29.12	1.25
2006 - 07	0.71	27.42	0.89
2007 - 08	0.63	35.07	1.20
2008 - 09	0.54	16.75	0.86
2009 - 10	0.66	26.28	1.22
2010 - 11	0.65	20.77	0.90
2011 - 12	0.70	18.48	0.83
2012 -13	0.63	26.64	0.97
2013 - 14	0.62	16.69	0.77
2014 - 15	0.69	15.73	0.86

Table A.26. Salamis station

Year	*CI*	*PCI*	*SI*
1978 -79	0.50	29.89	0.96
1979 - 80	0.45	24.24	1.00
1980 - 81	0.49	21.86	0.96
1981 - 82	0.49	16.44	0.90
1982 - 83	0.51	16.95	0.92
1983 - 84	0.53	16.74	0.88
1984 - 85	0.62	34.14	1.20
1985 - 86	0.63	19.13	0.96
1986 - 87	0.58	24.33	0.97
1987 - 88	0.63	17.60	0.96
1988 - 89	0.56	18.50	0.97
1989 -90	0.49	25.80	0.96
1990 - 91	0.54	25.14	1.16
1991 - 92	0.58	28.21	0.97
1992 - 93	0.55	19.83	0.87
1993 - 94	0.48	24.93	1.17
1994 - 95	0.63	26.34	1.14
1995 - 96	0.55	29.05	1.08
1996 - 97	0.55	18.35	1.04
1997 - 98	0.57	14.23	0.74
1998 - 99	0.49	19.26	0.91
1999 - 2000	0.52	19.12	0.90
2000 - 01	0.61	17.83	0.92
2001 - 02	0.62	29.47	1.11
2002 - 03	0.48	17.29	0.94
2003 - 04	0.62	33.49	1.26
2004 - 05	0.67	18.83	0.93
2005 - 06	0.69	20.02	0.96
2006 - 07	0.64	24.53	0.90
2007 - 08	0.60	19.13	0.96
2008 - 09	0.57	14.28	0.76
2009 - 10	0.66	27.61	1.20
2010 - 11	0.62	24.40	0.99
2011 - 12	0.66	17.70	0.83
2012 -13	0.56	17.96	0.84
2013 - 14	0.64	19.77	0.97
2014 - 15	0.65	15.22	0.81

Table A.27. Serdarli station

Year	*CI*	*PCI*	*SI*
1978 -79	0.54	16.23	0.86
1979 - 80	0.56	22.61	0.97
1980 - 81	0.47	15.63	0.72
1981 - 82	0.50	16.60	0.92
1982 - 83	0.48	14.09	0.73
1983 - 84	0.54	16.20	0.82
1984 - 85	0.58	25.27	0.95
1985 - 86	0.48	24.07	0.95
1986 - 87	0.48	20.50	0.75
1987 - 88	0.56	19.42	1.04
1988 - 89	0.51	30.19	1.21
1989 -90	0.49	20.92	0.89
1990 - 91	0.34	24.25	1.14
1991 - 92	0.52	25.40	0.97
1992 - 93	0.54	18.28	0.90
1993 - 94	0.50	23.11	1.20
1994 - 95	0.64	32.31	1.03
1995 - 96	0.64	22.64	1.00
1996 - 97	0.49	14.55	0.73
1997 - 98	0.63	16.55	0.82
1998 - 99	0.52	18.12	0.92
1999 - 2000	0.65	17.37	0.92
2000 - 01	0.56	14.75	0.67
2001 - 02	0.51	13.90	0.65
2002 - 03	0.60	20.84	0.98
2003 - 04	0.56	26.37	1.10
2004 - 05	0.53	16.18	0.86
2005 - 06	0.57	17.62	0.81
2006 - 07	0.63	15.03	0.76
2007 - 08	0.57	14.47	0.74
2008 - 09	0.57	16.56	0.87
2009 - 10	0.68	19.75	0.95
2010 - 11	0.65	18.11	0.90
2011 - 12	0.61	16.77	0.81
2012 -13	0.58	14.65	0.83
2013 - 14	0.68	31.29	1.16
2014 - 15	0.61	15.15	0.71

Table A.28. Tatlisu station

Year	*CI*	*PCI*	*SI*
1978 -79	0.70	17.39	0.90
1979 - 80	0.64	19.91	0.93
1980 - 81	0.52	19.89	0.78
1981 - 82	0.64	16.39	0.90
1982 - 83	0.53	17.65	0.90
1983 - 84	0.58	17.37	0.83
1984 - 85	0.67	25.60	1.07
1985 - 86	0.64	16.63	0.91
1986 - 87	0.65	18.94	0.86
1987 - 88	0.59	20.39	1.03
1988 - 89	0.54	20.90	1.09
1989 -90	0.78	28.65	1.01
1990 - 91	0.44	23.03	1.08
1991 - 92	0.54	24.52	1.03
1992 - 93	0.53	18.09	0.90
1993 - 94	0.42	20.16	1.06
1994 - 95	0.56	21.09	1.00
1995 - 96	0.49	20.30	0.99
1996 - 97	0.55	15.16	0.77
1997 - 98	0.65	13.89	0.74
1998 - 99	0.53	17.55	0.84
1999 - 2000	0.55	19.39	0.88
2000 - 01	0.50	15.76	0.76
2001 - 02	0.61	25.28	1.02
2002 - 03	0.47	17.36	0.86
2003 - 04	0.44	26.95	1.20
2004 - 05	0.49	18.59	0.96
2005 - 06	0.64	25.13	1.03
2006 - 07	0.56	19.60	0.91
2007 - 08	0.56	17.53	0.99
2008 - 09	0.47	19.00	0.97
2009 - 10	0.53	19.42	0.95
2010 - 11	0.65	17.36	0.87
2011 - 12	0.66	21.44	1.00
2012 -13	0.62	16.40	0.92
2013 - 14	0.64	21.01	0.95
2014 - 15	0.64	12.70	0.57

Table A.29. Vadili station

Year	*CI*	*PCI*	*SI*
1978 -79	0.63	26.01	0.91
1979 - 80	0.47	22.42	0.91
1980 - 81	0.44	17.75	0.99
1981 - 82	0.52	21.74	1.03
1982 - 83	0.44	20.75	1.02
1983 - 84	0.53	14.67	0.85
1984 - 85	0.57	28.40	1.19
1985 - 86	0.47	14.31	0.83
1986 - 87	0.56	27.88	0.93
1987 - 88	0.44	16.12	1.03
1988 - 89	0.46	22.61	1.12
1989 -90	0.60	27.77	1.05
1990 - 91	0.54	24.11	1.12
1991 - 92	0.53	33.08	1.10
1992 - 93	0.54	18.92	1.13
1993 - 94	0.48	22.67	1.02
1994 - 95	0.53	41.36	0.70
1995 - 96	0.58	33.63	1.25
1996 - 97	0.54	17.53	1.06
1997 - 98	0.56	16.34	0.83
1998 - 99	0.53	18.12	1.04
1999 - 2000	0.46	16.66	0.78
2000 - 01	0.55	21.84	0.84
2001 - 02	0.58	21.41	0.95
2002 - 03	0.58	18.22	1.02
2003 - 04	0.57	36.18	1.28
2004 - 05	0.53	22.07	0.99
2005 - 06	0.50	17.54	1.02
2006 - 07	0.67	20.28	0.84
2007 - 08	0.64	15.04	1.13
2008 - 09	0.59	14.16	0.95
2009 - 10	0.62	18.14	1.15
2010 - 11	0.72	18.23	1.04
2011 - 12	0.67	16.44	0.75
2012 -13	0.55	17.94	0.93
2013 - 14	0.67	20.61	0.88
2014 - 15	0.64	13.89	0.67

Table A.30. Yeni Erenkoy station

Year	*CI*	*PCI*	*SI*
1978 -79	0.58	19.69	1.01
1979 - 80	0.48	16.07	0.82
1980 - 81	0.51	23.01	0.89
1981 - 82	0.64	21.82	0.98
1982 - 83	0.53	16.19	0.81
1983 - 84	0.59	14.13	0.72
1984 - 85	0.52	21.02	0.95
1985 - 86	0.58	21.26	0.90
1986 - 87	0.56	16.52	0.88
1987 - 88	0.58	21.95	1.00
1988 - 89	0.59	19.51	1.08
1989 -90	0.47	21.19	1.05
1990 - 91	0.41	20.87	1.02
1991 - 92	0.52	23.91	0.97
1992 - 93	0.60	30.70	1.17
1993 - 94	0.50	21.00	1.12
1994 - 95	0.51	21.59	0.91
1995 - 96	0.51	27.66	1.10
1996 - 97	0.52	18.57	0.81
1997 - 98	0.59	15.37	0.79
1998 - 99	0.56	25.32	1.05
1999 - 2000	0.56	17.34	0.93
2000 - 01	0.60	18.53	0.92
2001 - 02	0.61	25.06	0.97
2002 - 03	0.61	20.56	0.99
2003 - 04	0.61	40.08	1.42
2004 - 05	0.63	26.71	1.09
2005 - 06	0.69	22.91	1.08
2006 - 07	0.51	16.59	0.84
2007 - 08	0.60	18.68	0.81
2008 - 09	0.62	20.06	1.05
2009 - 10	0.61	29.96	1.17
2010 - 11	0.60	19.77	0.95
2011 - 12	0.57	19.72	0.94
2012 -13	0.63	17.00	0.94
2013 - 14	0.62	18.01	1.02
2014 - 15	0.60	13.02	0.58

Table A.31. Yesilırmak station

Year	*CI*	*PCI*	*SI*
1978 -79	0.55	19.64	0.93
1979 - 80	0.52	18.26	0.91
1980 - 81	0.51	18.19	0.85
1981 - 82	0.56	16.54	0.95
1982 - 83	0.61	15.90	0.83
1983 - 84	0.41	18.67	0.99
1984 - 85	0.46	22.88	1.20
1985 - 86	0.50	16.16	0.89
1986 - 87	0.47	21.12	0.93
1987 - 88	0.48	19.15	0.92
1988 - 89	0.52	27.86	1.16
1989 -90	0.50	26.13	1.05
1990 - 91	0.41	18.36	0.90
1991 - 92	0.49	31.27	1.14
1992 - 93	0.53	20.16	0.96
1993 - 94	0.45	22.75	1.09
1994 - 95	0.65	20.51	0.94
1995 - 96	0.58	16.47	0.85
1996 - 97	0.57	17.39	0.89
1997 - 98	0.56	20.45	0.98
1998 - 99	0.66	22.38	1.05
1999 - 2000	0.33	21.83	1.14
2000 - 01	0.53	19.49	0.86
2001 - 02	0.36	18.27	0.88
2002 - 03	0.48	23.83	1.13
2003 - 04	0.31	32.04	1.30
2004 - 05	0.34	16.18	0.87
2005 - 06	0.40	17.38	0.86
2006 - 07	0.46	22.31	0.99
2007 - 08	0.56	17.40	0.91
2008 - 09	0.59	18.81	0.95
2009 - 10	0.55	18.26	0.90
2010 - 11	0.55	16.32	0.87
2011 - 12	0.57	18.68	0.89
2012 -13	0.57	16.73	0.79
2013 - 14	0.61	16.51	0.80
2014 - 15	0.58	14.89	0.78

Table A.32. Ziyamet station

Year	*CI*	*PCI*	*SI*
1978 -79	0.67	25.20	1.12
1979 - 80	0.55	15.44	0.78
1980 - 81	0.35	17.66	0.76
1981 - 82	0.60	24.34	0.98
1982 - 83	0.51	14.70	0.75
1983 - 84	0.56	17.68	0.87
1984 - 85	0.60	23.48	1.01
1985 - 86	0.84	21.01	0.87
1986 - 87	0.63	19.02	0.96
1987 - 88	0.70	35.19	1.10
1988 - 89	0.54	21.76	1.06
1989 -90	0.58	22.82	1.02
1990 - 91	0.53	21.84	1.08
1991 - 92	0.65	22.89	1.04
1992 - 93	0.59	18.83	0.88
1993 - 94	0.45	20.29	1.04
1994 - 95	0.59	18.66	0.84
1995 - 96	0.60	29.88	1.15
1996 - 97	0.60	13.58	0.72
1997 - 98	0.63	14.99	0.76
1998 - 99	0.51	26.42	1.09
1999 - 2000	0.47	16.20	0.91
2000 - 01	0.57	16.51	0.82
2001 - 02	0.62	22.64	0.90
2002 - 03	0.61	24.86	1.17
2003 - 04	0.61	45.33	1.36
2004 - 05	0.53	22.13	0.95
2005 - 06	0.65	25.67	1.05
2006 - 07	0.59	21.39	0.96
2007 - 08	0.58	27.14	0.98
2008 - 09	0.60	18.01	0.85
2009 - 10	0.54	23.12	1.03
2010 - 11	0.51	13.60	0.66
2011 - 12	0.50	20.21	0.93
2012 -13	0.54	17.45	0.93
2013 - 14	0.55	31.57	1.11
2014 - 15	0.55	16.74	0.76

Table A.33. Zumrutkoy station

Year	*CI*	*PCI*	*SI*
1978 -79	0.51	19.24	0.91
1979 - 80	0.56	18.23	1.02
1980 - 81	0.46	21.57	1.01
1981 - 82	0.61	16.32	0.95
1982 - 83	0.46	15.54	0.67
1983 - 84	0.41	15.30	0.83
1984 - 85	0.42	19.66	1.05
1985 - 86	0.48	15.94	0.73
1986 - 87	0.54	26.70	1.15
1987 - 88	0.39	19.85	0.97
1988 - 89	0.42	25.75	1.13
1989 -90	0.46	24.93	1.04
1990 - 91	0.47	21.11	0.97
1991 - 92	0.50	26.49	1.05
1992 - 93	0.54	17.81	0.97
1993 - 94	0.30	22.34	1.04
1994 - 95	0.52	19.43	0.87
1995 - 96	0.53	17.17	0.98
1996 - 97	0.55	21.29	0.93
1997 - 98	0.54	17.46	0.90
1998 - 99	0.51	21.47	1.04
1999 - 2000	0.64	15.91	0.86
2000 - 01	0.59	19.30	0.88
2001 - 02	0.56	18.03	0.90
2002 - 03	0.57	19.66	0.99
2003 - 04	0.41	28.92	1.19
2004 - 05	0.56	16.87	0.88
2005 - 06	0.61	20.81	1.04
2006 - 07	0.59	18.10	0.86
2007 - 08	0.54	22.73	1.18
2008 - 09	0.58	20.39	1.09
2009 - 10	0.70	24.55	1.07
2010 - 11	0.50	16.88	0.97
2011 - 12	0.51	18.39	0.83
2012 -13	0.61	16.75	0.90
2013 - 14	0.64	22.65	1.07
2014 - 15	0.53	16.19	0.78

B. Quality of The Desalinated Water

Table B.1. Quality of the desalinated water using three stages one pass

Water quality parameter	*Permeate from the 1st stage*	*Permeate from the 2nd stage*	*Permeate from the 3rd stage*	*Final permeate*
pH	6	5.8	5.7	5.8
Ca^{2+} (mg/L)	1.56	2.67	0.02	1.48
Mg^{2+} (mg/L)	9.57	5.97	5.65	7.22
Na^{+} (mg/L)	339.7	212.3	200.4	259.4
K^{+} (mg/L)	15.46	9.63	9.07	11.65
CO_3^{2-} (mg/L)	0.01	0.01	0.01	0.01
HCO_3^{-} (mg/L)	5.41	3.46	3.29	4.13
SO_4^{2-} (mg/L)	8.71	5.44	5.15	6.58
Cl^{-} (mg/L)	561.3	350.8	331	423.6
F^{-} (mg/L)	0.07	0.04	0.04	0.05
Boron (mg/L)	1.69	1.33	1.34	1.46
TDS (mg/L)	952	597.1	594	720

Table B.2. Quality of the concentrate using three stages one pass

Water quality parameter	*Concentrate from the 1st stage*	*Concentrate from the 2nd stage*	*Concentrate from the 3rd stage*
pH	7	7.1	7.1
Ca^{2+} (mg/L)	5334	694.8	855.8
Mg^{2+} (mg/L)	1731	2255	2778

Na^+ (mg/L)	13498	17532	21559
K^+ (mg/L)	530.6	688.8	846.7
CO_3^{2-} (mg/L)	2.98	5.05	7.43
HCO_3^- (mg/L)	177.6	228.1	277.8
SO_4^{2-} (mg/L)	3855	5024	6190
Cl^- (mg/L)	24334	31617	38886
F^- (mg/L)	2.04	2.65	3.25
Boron (mg/L)	3.45	4.09	4.73
TDS (mg/L)	44685	58070	71431

Table B.3. Quality of the desalinated water using three stages two passes

Water quality parameter	*1st pass*			*Permeate from 2nd pass*	*Final permeate*
	Permeate from the 1st stage	*Permeate from the 2nd stage*	*Permeate from the 3rd stage*		
pH	5.2	4.9	5.0	7.8	5.1
Ca^{2+} (mg/L)	4.5	1.49	1.85	0.02	1.48
Mg^{2+} (mg/L)	14.67	4.87	6.04	0.08	4.84
Na^+ (mg/L)	581.2	173.6	214.7	5.34	172.5
K^+ (mg/L)	23.61	7.87	9.72	0.34	7.86
CO_3^{2-} (mg/L)	0.0	0.0	0.0	0.1	0.0
HCO_3^- (mg/L)	6.27	2.74	3.14	2.08	3.13
SO_4^{2-} (mg/L)	13.36	4.43	5.5	0.04	4.39
Cl^- (mg/L)	857.9	287.2	355.2	7.47	285.1
F^- (mg/L)	0.1	0.03	0.04	0.0	0.03

Boron (mg/L)	2.1	1.24	1.43	0.62	1.2
TDS (mg/L)	1451	489.4	604.4	18.93	486.2

Table B.4. Quality of the concentrate using three stages two passes

Water quality parameter	*1st pass*			*Concentrate from 2nd pass*
	Concentrate from the 1st stage	*Concentrate from the 2nd stage*	*Concentrate from the 3rd stage*	
pH	6.1	6.2	6.4	8.9
Ca^{2+} (mg/L)	451.7	600.3	806	7.13
Mg^{2+} (mg/L)	1466	1948	2616	23.29
Na^{+} (mg/L)	11488	15222	20382	906.1
K^{+} (mg/L)	451.8	598.3	800.6	37.04
CO_3^{2-} (mg/L)	0.19	0.39	0.79	18.82
HCO_3^{-} (mg/L)	111.6	147.5	196.7	184.4
SO_4^{2-} (mg/L)	3262	4337	5827	21.29
Cl^{-} (mg/L)	20725	27471	36794	1362
F^{-} (mg/L)	1.74	2.30	3.08	0.16
Boron (mg/L)	6.1	6.3	7	3.43
TDS (mg/L)	41010	51350	68435	2579

C. Aquifers, Dams and Wastewater Treatments Plants in Northern Cyprus

Table C.1. Aquifers in Northern Cyprus (Phillips Agboola & Egelioglu, 2012)

Aquifer name	*Recharging rate ($10^6 m^3$)*	*Sustainable discharging rate ($10^6 m^3$)*	*Discharge rate ($10^6 m^3$)*
Guzelyurt	37	37	57
Akdeniz	1.5	1.5	1.5
Lefke-G. Konagi Y.dalga	15.5	6	6
Girne- coast	5	5	5
Gazimagusa	2	2	8.5
Beyarmudu	0.5	0.5	0.5
Cayoun- Guvericinlik-Turkmenkoy	2	2	2
Lefkosa- serdarli	0.5	0.5	0.5
Yesilkoy	1.6	1.6	3
Yedikonuk-Buyukkonuk	0.3	0.3	0.3
Diipkarpaz	1.5	1.5	1.5
Korucam	1.2	1.2	1.2
Girne mountains	11.5	11.5	11.5
Others	2	2	2

Table C.2. Dams in Northern Cyprus (Phillips Agboola & Egelioglu, 2012)

Dam		*Construction year*	*Capacity (10^3)*
District	Name		
Gazimagusa	Gonendere	1987	940
	Gecitkale	1989	1360
	Mersinlik	1989	1140
	Tatlisu	1989	156
	Ergazi	1989	400
Guzelyurt	Akdeniz	1988	1470
	Gemikonagi	1988	4120
Girne	Gecitkoy	1989	1800
	Zeytinlik	1989	50
	Karsiyaka	1989	25
	Arapkoy 1	1990	440
	Arapkoy 2	1990	600
	Besparmak	1992	775
	Dagyolu	1994	392
Lefkosa	Dgirmenlik	1990	297
	Hamitkoy	1992	529
	Serdali	1992	391
	Lefosa	1994	517

Table C.3. Wastewater treatment plants in Northern Cyprus (Phillips Agboola & Egelioglu, 2012)

City	*Plant name*	*Capcity*
Gazimagusa	Gazimagusa Belediyesi Atik Suaritna Tesisi	4100 m^3/ day
Girne	Atik su Aritma Tesisi	-
Guzelyurt	ODTU plant	-
	Guzelyurt Belediyesi Atik su Tesisi	1200 ton/day
Lefkusa	Haspolat Atik Su Artima Tesisi	30000 m^3/day
Lefke	Hospital water treatment plant-Cengiz topel hastanesi atik su tesisi	30 m^3/day

D. WAVE Software and RO Modules Data Sheets

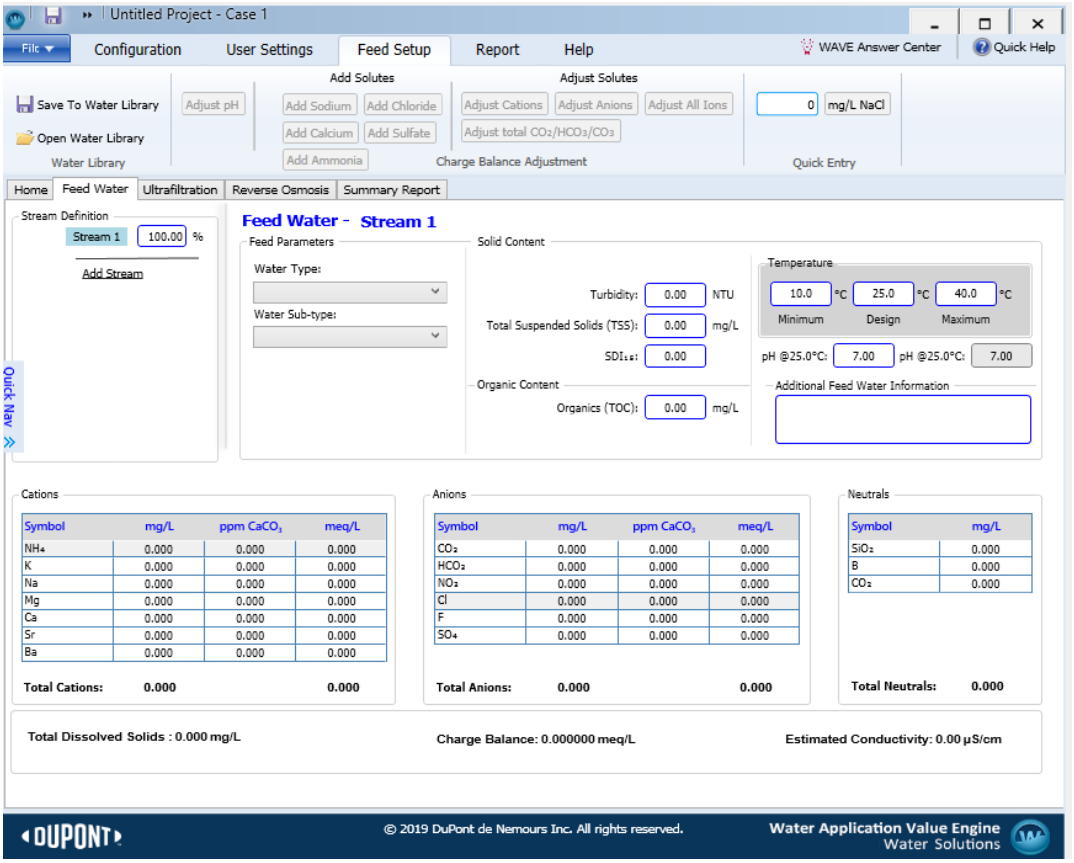

Figure D.1. Feedwater quality input page of WAVE software

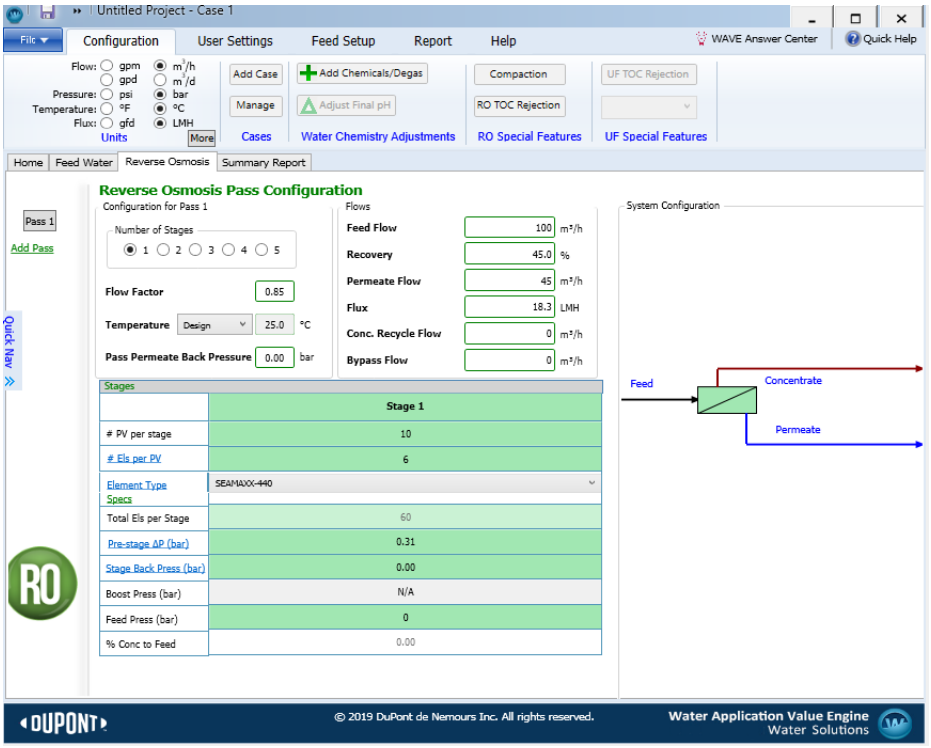

Figure D.2. System configurations input page of WAVE software

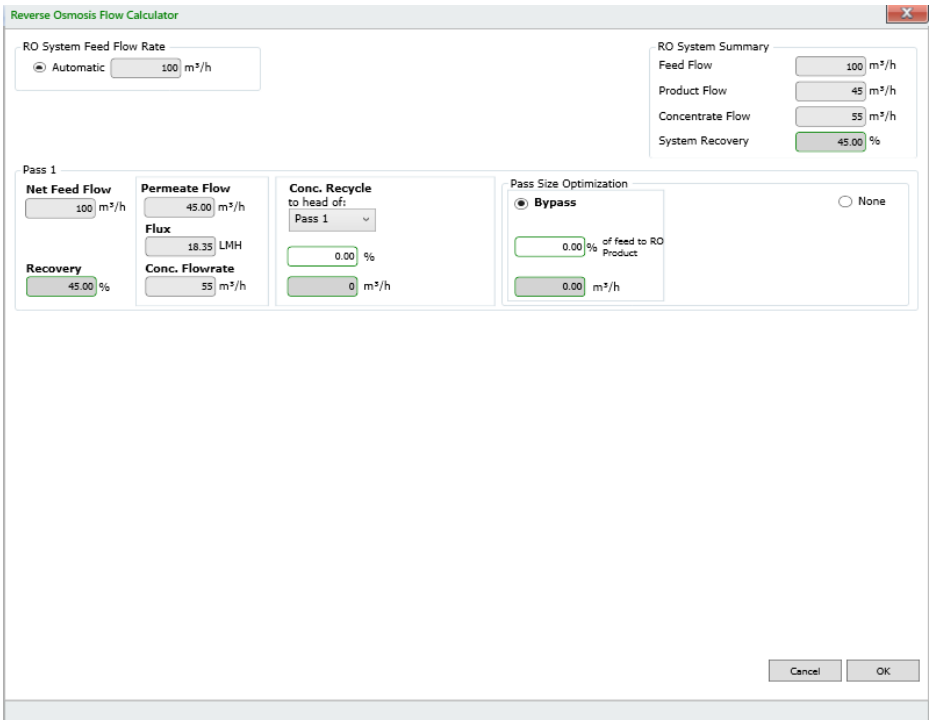

Figure D.3. System configurations input page for bypass and recycling in WAVE software

Typical Properties of Standard Test performed at 600 psi (4.1 MPa)

FilmTec™ Element	Active Area (ft^2)	Active Area (m^2)	Feed Spacer Thickness (mil)	Permeate Flowrate (gpd)	Permeate Flowrate (m^3/d)	Stabilized Boron Rejection	Stabilized Salt Rejection (%)
Seamaxx™-440	440	41	28	9,050	34.2	81.8	99.47

1. The above values are based on the following test conditions: 32,000 ppm NaCl, 600 psi (4.1 MPa), 77°F (25°C), pH 8, 8% recovery.
2. Permeate flows for individual elements may vary ± 15%.
3. Minimum Salt Rejection is 99.25%.
4. Stabilized salt rejection is generally achieved within 24 – 48 hours of continuous use; depending upon feedwater characteristics and operating conditions.
5. Product specifications may vary slightly as improvements are implemented.
6. Specific boron stabilized rejection based on the following test conditions: 32,000 ppm NaCl, 5 ppm boron, 600 psi (4.1 MPa), 77°F (25°C), pH 8, 8% recovery.
7. Active area guaranteed ± 5%. Active area as stated by DuPont Water Solutions is not comparable to the nominal membrane area figure often stated by some element suppliers.

Expected Properties and Performance at Common Standard Test Conditions: 800 psi (5.5 MPa)

FilmTec™ Element	Active Area (ft^2)	Active Area (m^2)	Feed Spacer Thickness (mil)	Permeate Flowrate (gpd)	Permeate Flowrate (m^3/d)	Stabilized Boron Rejection (%)	Stabilized Salt Rejection (%)
Seamaxx™-440	440	41	28	17,000	64.4	89	99.70

Figure D.4. Seamax -440 seawater RO modules datasheet

Product Type Spiral-wound element with polyamide thin-film composite membrane

Typical Properties

FilmTec™ Element	Active Area (ft^2)	Active Area (m^2)	Feed Spacer Thickness (mil)	Permeate Flow Rate (GPD)	Permeate Flow Rate (m^3/d)	Typical Stabilized Salt Rejection (%)	Minimum Salt Rejection (%)
BW30HRLE-440i	440	41	28	12,650	48	99.3	99.1

a. Permeate flow and salt (NaCl) rejection based on the following standard test conditions: 2,000 ppm NaCl, 150 psi (10.3 bar), 77°F (25°C), pH 8, 15% recovery.
b. Flow rates for individual elements may vary but will be no more than ± 15%.
c. Stabilized salt rejection is generally achieved within 24-48 hours of continuous use; depending upon feedwater characteristics and operating conditions.
d. Sales specifications may vary as design revisions take place.
e. Active area guaranteed ± 3%. Active area as stated by DuPont Water Solutions is not comparable to nominal membrane area often stated by some manufacturers.

Figure D.5. BW30HRLE -440 brackish water RO modules datasheet

ORTA DOĞU TEKNİK ÜNİVERSİTESİ
FEN BİLİMLERİ ENSTİTÜSÜ MÜDÜRLÜĞÜ

TEZ İZİN FORMU / THESIS PERMISSION FORM

PROGRAM / PROGRAM

Sürdürülebilir Çevre ve Enerji Sistemleri / Sustainable Environment and Energy Systems ☑

Siyaset Bilimi ve Uluslararası İlişkiler / Political Science and International Relations ☐

İngilizce Öğretmenliği / English Language Teaching ☐

Elektrik Elektronik Mühendisliği / Electrical and Electronics Engineering ☐

Bilgisayar Mühendisliği / Computer Engineering ☐

Makina Mühendisliği / Mechanical Engineering ☐

YAZARIN / AUTHOR
Soyadı / Surname : Hilal
Adı / Name : Adnan Yaser Adnan
Programı / Program : Sustainable Environment and Energy Systems

TEZİN ADI / TITLE OF THE THESIS (**İngilizce** / English) : WATER RESOURCES ASSESSMENT OF NORTHERN CYPRUS FOR A SUSTAINABLE MANAGEMENT

TEZİN TÜRÜ / DEGREE: **Yüksek Lisans** / Master ☑ **Doktora** / PhD ☐

1. **Tezin tamamı dünya çapında erişime açılacaktır.** / Release the entire work immediately for access worldwide. ☐

2. **Tez iki yıl süreyle erişime kapalı olacaktır.** / Secure the entire work for patent and/or proprietary purposes for a period of **two years.** * ☑

3. **Tez altı ay süreyle erişime kapalı olacaktır.** / Secure the entire work for period of **six months.** * ☐

Yazarın imzası / Author Signature ..... **Tarih** / Date .....

Tez Danışmanı / Thesis Advisor Full Name: Asst. Prof. Dr. Bengü Bozkaya Schrotter

Tez Danışmanı İmzası / Thesis Advisor Signature: .....

Eş Danışmanı / Co-Advisor Full Name: Asst. Prof. Dr. Bertuğ Akıntuğ

Eş Danışmanı İmzası / Co-Advisor Signature: .....

Program Koordinatörü / Program Coordinator Full Name: Assoc. Prof. Dr. Ceren İnce Derogar

Program Koordinatörü İmzası / Program Coordinator Signature: .....